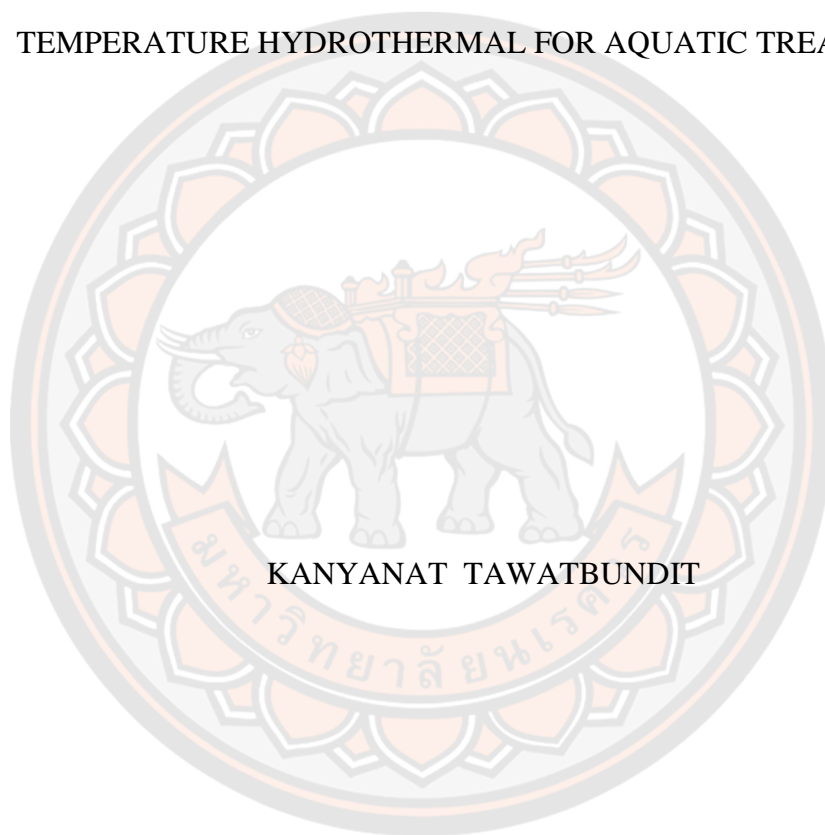




ACTIVATED CARBON PREPARATION FROM SUGARCANE LEAF VIA LOW
TEMPERATURE HYDROTHERMAL FOR AQUATIC TREATMENT



KANYANAT TAWATBUNDIT

A Thesis Submitted to the Graduate School of Naresuan University
in Partial Fulfillment of the Requirements
for the Doctor of Philosophy in Chemistry

2022

Copyright by Naresuan University

ACTIVATED CARBON PREPARATION FROM SUGARCANE LEAF VIA LOW
TEMPERATURE HYDROTHERMAL FOR AQUATIC TREATMENT



A Thesis Submitted to the Graduate School of Naresuan University
in Partial Fulfillment of the Requirements
for the Doctor of Philosophy in Chemistry
2022

Copyright by Naresuan University

Thesis entitled "ACTIVATED CARBON PREPARATION FROM SUGARCANE
LEAF VIA LOW TEMPERATURE HYDROTHERMAL FOR AQUATIC
TREATMENT"

By Kanyanat Tawatbundit

has been approved by the Graduate School as partial fulfillment of the requirements
for the Doctor of Philosophy in Chemistry of Naresuan University

Oral Defense Committee

..... Chair
(Associate Professor Preecha Panya, Ph.D.)

..... Advisor
(Associate Professor Sumrit Mopoung, Ph.D.)

..... Internal Examiner
(Assistant Professor Anchalee Sirikulajorn, Ph.D.)

..... Internal Examiner
(Nimit Sriprang, Ph.D.)

..... Internal Examiner
(Assistant Professor Nonglak Yimtragool, Ph.D.)

..... External Examiner
(Associate Professor Preecha Panya, Ph.D.)

Approved

.....
(Associate Professor Krongkarn Chootip, Ph.D.)
Dean of the Graduate School

Title ACTIVATED CARBON PREPARATION FROM SUGARCANE LEAF VIA LOW TEMPERATURE HYDROTHERMAL FOR AQUATIC TREATMENT

Author Kanyanat Tawatbundit

Advisor Associate Professor Sumrit Mopoung, Ph.D.

Academic Paper Ph.D. Dissertation in Chemistry, Naresuan University, 2022

Keywords Activated carbon, hydrothermal, aquatic treatment, sugarcane leaf

ABSTRACT

This research studied the effects of hydrothermal pretreatment process, concentration of KMnO_4 (0%, 1%, 3%, and 5%wt), and the activation temperature (300, 350, and 400°C) on the production activated carbon samples from sugarcane leaves used as the starting material. The preparation of activated carbon samples made without the hydrothermal pretreatment process showed decreasing percentage yields of 36.5000, 23.4667, and 16.4000 with increasing activation temperature of 300, 350 and 400°C, respectively. In the case of the hydrochar activated carbon (activated carbon samples made with the hydrothermal pretreatment process), the results showed that decreasing percentage yields of 36.2333, 23.3669, and 20.3286 with increasing activation temperature. Increasing KMnO_4 concentration showed the same trend for percentage yield as increasing activation temperature for all conditions. In the case of the ash percentage content, the same trend has been observed for all conditions. The volatile matter percentage content decreased with increasing activation temperature and KMnO_4 concentration, that relates to higher fixed carbon percentage. However, at the activation temperature of 300°C the results obtained with 3% and 5%wt of KMnO_4 showed opposite results. Furthermore, the moisture percent content showed increasing values with increasing activation temperature and increasing KMnO_4 concentration, up to 3% wt. However, the moisture percentage has decreased when 5%wt of KMnO_4 was used for all of the activation temperatures. This can be due to excessive amount of KMnO_4 occluding the surface area of the activated

carbon product and possibly producing oxide compounds of Mn and K, which are resistant to decomposition by heat treatment. In terms of elemental analysis, the hydrochar activated carbon products obtained at increasing activation temperatures showed increasing carbon content. In addition, the O/C ratio of the hydrochar activated carbon samples increased with increasing of KMnO_4 concentration. The hydrothermal pretreatment process and activation temperature showed the effect of the increasing content of aromatic compounds in the products. The addition of KMnO_4 into the activated carbon resulted in the formation of functional groups such as C-O, Mn-OH, O-Mn-O, and Mn-O on the surface of activated carbon samples. The addition of KMnO_4 caused increases of negative zeta potential values in the pH range from 3 to 11. The surface area and porous structure of the hydrochar activated carbon samples showed increasing values with increasing activation temperature for all conditions. Moreover, increasing KMnO_4 concentration resulted in increasing of the surface area. However, the values decreased when 5%wt of KMnO_4 was used. This is because the excessive amount of KMnO_4 occluded the surface of the product materials and damaged the porous structure of the activated carbon samples. The use of the hydrochar activated carbon sample made with 3% of KMnO_4 at the activation temperature of 350 °C as a filter in an aquaponics system demonstrated that the quality of water was improved with pH rising from 7.2 to 7.4, DO rising from 9.6 to 13.3 mg/L, and turbidity decreasing from 2.90 to 2.54 NTU. Furthermore, the decrease of ammonia, nitrite, and orthophosphate concentrations with relative removal rates of 86.84%, 73.17%, and 53.33%, respectively, was obtained. These water quality improvements resulted in better growth of catfish and red oak lettuce because the plant root absorbed the nitrite and orthophosphate needed for their growth. In addition, the activated carbon powders that were used as the filter could adsorb and filter the suspended materials, which led to better water quality.

ACKNOWLEDGEMENTS

First and foremost, I would like to thank my advisor, Associate Professor Dr. Sumrit Mopoung for his support in my dissertation, beneficial advice, good guidance and knowledge of chemistry.

I also appreciate the committee member, Assistant Professor Dr. Anchalee Sirikulajorn, Dr. Nimit Sriprang, Assistant Professor Dr. Nonglak Yimtragool and Associate Professor Dr. Preecha Panya for suggestion and criticism as the external examiner.

I also appreciate the Science Achievement Scholarship of Thailand (SAST) for financial support.

I also acknowledge the science lab center and department of chemistry, faculty of science, Naresuan University for supplying all laboratory facilities and all the analysis.

I would like to thank my family who were always beside me and supporting me. Thank you for being a part of my life.

Kanyanat Tawatbundit

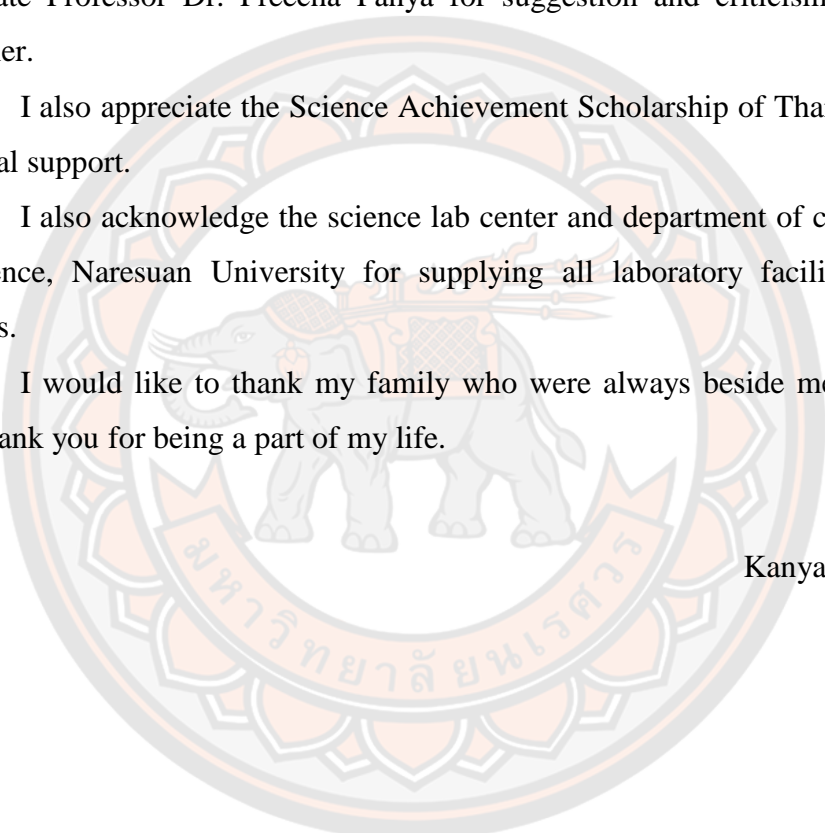
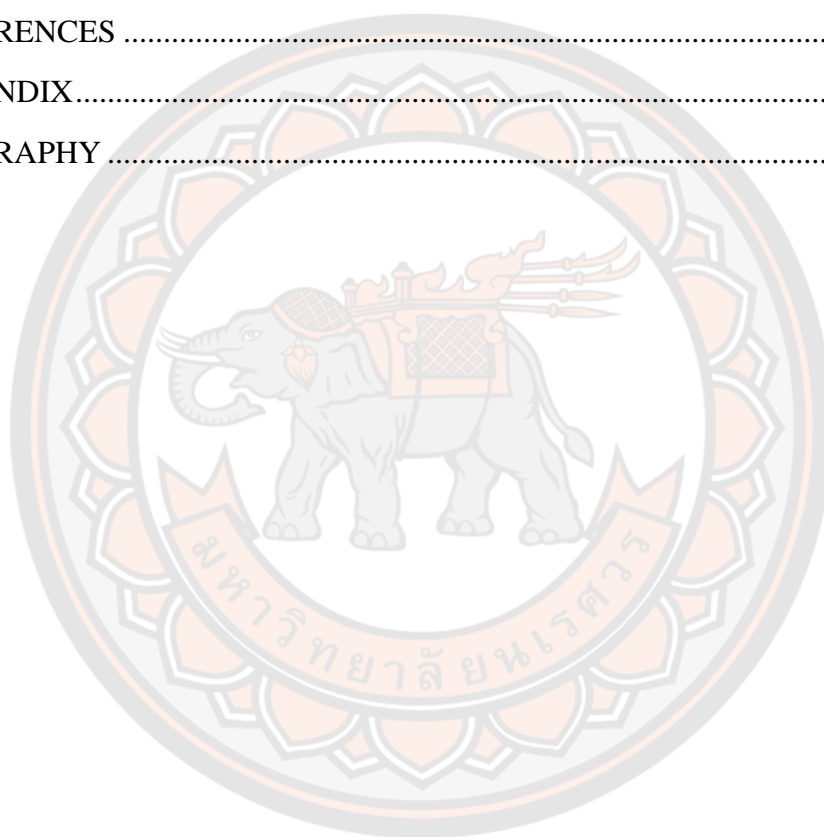


TABLE OF CONTENTS

	Page
ABSTRACT.....	C
ACKNOWLEDGEMENTS.....	E
TABLE OF CONTENTS.....	F
LIST OF TABLES.....	I
LIST OF FIGURES.....	N
ABBREVIATION.....	Q
CHAPTER I INTRODUCTION.....	1
Rationale for the study.....	1
Purposes of the study.....	3
Significance of the study.....	3
Scope of the study.....	3
CHAPTER II LITERATURE REVIEW.....	4
1. Activation process for producing activated carbons.....	5
2. The preparation of activated carbons via hydrothermal pretreatment method.....	8
3. Activated carbons modified with potassium permanganate (KMnO ₄).....	12
4. Activated carbons prepared from sugarcane.....	16
5. The use of activated carbons in aquatic treatment.....	18
6. Role of nutrients in plant growth.....	23
7. Catfish.....	25
8. Red oak lettuce.....	25
CHAPTER III THE PREPARATION OF SUGARCANE LEAF ACTIVATED CARBON AND THEIR CHARACTERISTIC.....	27
Equipment and tools.....	27
Materials and Chemicals.....	27
Experimental.....	28
1. The producing of sugarcane leaves activated carbon.....	28

2. Proximate analysis.....	29
2.1 Moisture content (M).....	29
2.2 Ash content (ASH)	30
2.3 Volatile matter content (VM).....	30
2.4 Fixed carbon content (FC).....	31
3. The preparation for zeta potential analysis.....	31
4. Characterization.....	31
Results and Discussion	32
1. Proximate analysis and yield percentage of sugarcane leaf activated carbon	32
2. Morphologies and elemental composition of sugarcane leaf activated carbon by SEM-EDS	36
3. FTIR spectrum of activated carbon of sugarcane leaf activated carbon	42
4. XRD patterns of activated carbon of sugarcane leaf activated carbon.....	46
5. Surface area and porous structure of sugarcane leaf activated carbon.....	49
6. Zeta potential of the hydrochar activated carbon sample with addition 0% wt and 1% wt of KMnO_4 at 350°C	51
CHAPTER IV THE USING OF SUGARCANE LEAF ACTIVATED CARBON FOR AQUATIC TREATMENT.....	53
Equipment.....	53
Apparatus	53
Materials and Reagents.....	53
Experimental.....	54
1. The construction of an aquaponics system.....	54
2. Water analysis	56
2.1 Dissolved oxygen (DO) by Winkler titration method	56
2.2 Ammonium ion (NH_3^+) by indophenol reaction	57
2.3 Nitrite ion (NO_2^-) by diazo-azo colorimetric method.....	58
2.4 Orthophosphate ion (PO_4^{3-}) by ascorbic acid method	59
2.5 Turbidity and pH	61

Results and Discussion	61
1. The pH values of water	61
2. The dissolved oxygen (DO) values of water	62
3. The turbidity of water	64
4. The measurement of ammonia, nitrite and orthophosphate	65
5. The growth of catfish and red oak lettuce	67
CHAPTER V CONCLUSION.....	69
REFERENCES	71
APPENDIX.....	83
BIOGRAPHY	139



LIST OF TABLES

	Page
Table 1 Proximate analysis and %yield of sugarcane leaf activated carbon products.	34
Table 2 Elemental composition of activated carbon products from EDS.....	37
Table 3 Surface area and porosity of sugarcane leaf activated carbon by BET	50
Table 4 The removal and percent relative removal rate of NH ₃ , NO ₂ ⁻ and orthophosphate.....	67
Table 5 The growth parameters of red oak at 4 th week.....	68
Table 6 The %moisture calculation of sugarcane leaf.....	84
Table 7 The %ash calculation of sugarcane leaf.....	84
Table 8 The %volatile matter calculation of sugarcane leaf.....	85
Table 9 The %moisture calculation of SLAC without hydrothermal pretreatment at 300°C activation temperature	85
Table 10 The %ash calculation of SLAC without hydrothermal pretreatment at 300°C activation temperature.....	86
Table 11 The %volatile mater calculation of SLAC without hydrothermal pretreatment at 300°C activation temperature	86
Table 12 The %yield calculation of SLAC without hydrothermal pretreatment at 300°C activation temperature	87
Table 13 The %moisture calculation of SLAC 0%KMnO ₄ with hydrothermal pretreatment at 300°C activation temperature	87
Table 14 The %ash calculation of SLAC 0%KMnO ₄ with hydrothermal pretreatment at 300°C activation temperature	88
Table 15 The %volatile matter calculation of SLAC 0%KMnO ₄ with hydrothermal pretreatment at 300°C activation temperature	88
Table 16 The %yield calculation of SLAC 0%KMnO ₄ with hydrothermal pretreatment at 300°C activation temperature	89
Table 17 The %moisture calculation of SLAC 1%KMnO ₄ with hydrothermal pretreatment at 300°C activation temperature	89

Table 18 The %ash calculation of SLAC 1%KMnO ₄ with hydrothermal pretreatment at 300°C activation temperature	90
Table 19 The %volatile matter calculation of SLAC 1%KMnO ₄ with hydrothermal pretreatment at 300°C activation temperature	90
Table 20 The %yield calculation of SLAC 1%KMnO ₄ with hydrothermal pretreatment at 300°C activation temperature	91
Table 21 The %moisture calculation of SLAC 3%KMnO ₄ with hydrothermal pretreatment at 300°C activation temperature	91
Table 22 The %ash calculation of SLAC 3%KMnO ₄ with hydrothermal pretreatment at 300°C activation temperature	92
Table 23 The %volatile matter calculation of SLAC 3%KMnO ₄ with hydrothermal pretreatment at 300°C activation temperature	92
Table 24 The %yield calculation of SLAC 3%KMnO ₄ with hydrothermal pretreatment at 300°C activation temperature	93
Table 25 The %moisture calculation of SLAC 5%KMnO ₄ with hydrothermal pretreatment at 300°C activation temperature	93
Table 26 The %ash calculation of SLAC 5%KMnO ₄ with hydrothermal pretreatment at 300°C activation temperature	94
Table 27 The %volatile matter calculation of SLAC 5%KMnO ₄ with hydrothermal pretreatment at 300°C activation temperature	94
Table 28 The %yield calculation of SLAC 5%KMnO ₄ with hydrothermal pretreatment at 300°C activation temperature	95
Table 29 The %moisture calculation of SLAC without hydrothermal pretreatment at 350°C activation temperature	95
Table 30 The %ash calculation of SLAC without hydrothermal pretreatment at 350°C activation temperature.....	96
Table 31 The %volatile matter calculation of SLAC without hydrothermal pretreatment at 350°C activation temperature	96
Table 32 The %yield calculation of SLAC without hydrothermal pretreatment at 350°C activation temperature	97
Table 33 The %moisture calculation of SLAC 0%KMnO ₄ with hydrothermal pretreatment at 350°C activation temperature	97

Table 34 The %ash calculation of SLAC 0% KMnO ₄ with hydrothermal pretreatment at 350°C activation temperature	98
Table 35 The %volatile matter calculation of SLAC 0% KMnO ₄ with hydrothermal pretreatment at 350°C activation temperature	98
Table 36 The %yield calculation of SLAC 0% KMnO ₄ with hydrothermal pretreatment at 350°C activation temperature	99
Table 37 The %moisture calculation of SLAC 1% KMnO ₄ with hydrothermal pretreatment at 350°C activation temperature	99
Table 38 The %ash calculation of SLAC 1% KMnO ₄ with hydrothermal pretreatment at 350°C activation temperature	100
Table 39 The %volatile matter calculation of SLAC 1% KMnO ₄ with hydrothermal pretreatment at 350°C activation temperature	100
Table 40 The %yield calculation of SLAC 1% KMnO ₄ with hydrothermal pretreatment at 350°C activation temperature	101
Table 41 The %moisture calculation of SLAC 3% KMnO ₄ with hydrothermal pretreatment at 350°C activation temperature	101
Table 42 The %ash calculation of SLAC 3% KMnO ₄ with hydrothermal pretreatment at 350°C activation temperature	102
Table 43 The %volatile matter calculation of SLAC 3% KMnO ₄ with hydrothermal pretreatment at 350°C activation temperature	102
Table 44 The %yield calculation of SLAC 3% KMnO ₄ with hydrothermal pretreatment at 350°C activation temperature	103
Table 45 The %moisture calculation of SLAC 5% KMnO ₄ with hydrothermal pretreatment at 350°C activation temperature	103
Table 46 The %ash calculation of SLAC 5% KMnO ₄ with hydrothermal pretreatment at 350°C activation temperature	104
Table 47 The %volatile matter calculation of SLAC 5% KMnO ₄ with hydrothermal pretreatment at 350°C activation temperature	104
Table 48 The %yield calculation of SLAC 5% KMnO ₄ with hydrothermal pretreatment at 350°C activation temperature	105
Table 49 The %moisture calculation of SLAC without hydrothermal pretreatment at 400°C activation temperature	105

Table 50 The %ash calculation of SLAC without hydrothermal pretreatment at 400°C activation temperature.....	106
Table 51 The %volatile matter calculation of SLAC without hydrothermal pretreatment at 400°C activation temperature	106
Table 52 The %yield calculation of SLAC without hydrothermal pretreatment at 400°C activation temperature	107
Table 53 The %moisture calculation of SLAC 0%KMnO ₄ with hydrothermal pretreatment at 400°C activation temperature	107
Table 54 The %ash calculation of SLAC 0%KMnO ₄ with hydrothermal pretreatment at 400°C activation temperature	108
Table 55 The %volatile matter calculation of SLAC 0%KMnO ₄ with hydrothermal pretreatment at 400°C activation temperature	108
Table 56 The %yield calculation of SLAC 0%KMnO ₄ with hydrothermal pretreatment at 400°C activation temperature	109
Table 57 The %moisture calculation of SLAC 1%KMnO ₄ with hydrothermal pretreatment at 400°C activation temperature	109
Table 58 The %ash calculation of SLAC 1%KMnO ₄ with hydrothermal pretreatment at 400°C activation temperature	110
Table 59 The %volatile matter calculation of SLAC 1%KMnO ₄ with hydrothermal pretreatment at 400°C activation temperature	110
Table 60 The %yield calculation of SLAC 1%KMnO ₄ with hydrothermal pretreatment at 400°C activation temperature	111
Table 61 The %moisture calculation of SLAC 3%KMnO ₄ with hydrothermal pretreatment at 400°C activation temperature	111
Table 62 The %ash calculation of SLAC 3%KMnO ₄ with hydrothermal pretreatment at 400°C activation temperature	112
Table 63 The %volatile matter calculation of SLAC 3%KMnO ₄ with hydrothermal pretreatment at 400°C activation temperature	112
Table 64 The %yield calculation of SLAC 3%KMnO ₄ with hydrothermal pretreatment at 400°C activation temperature	113
Table 65 The %moisture calculation of SLAC 5%KMnO ₄ with hydrothermal pretreatment at 400°C activation temperature	113

Table 66 The %ash calculation of SLAC 5%KMnO ₄ with hydrothermal pretreatment at 400°C activation temperature	114
Table 67 The %volatile matter calculation of SLAC 5%KMnO ₄ with hydrothermal pretreatment at 400°C activation temperature	114
Table 68 The %yield calculation of SLAC 5%KMnO ₄ with hydrothermal pretreatment at 400°C activation temperature	115



LIST OF FIGURES

	Page
Figure 1 The producing steps of activated carbon	5
Figure 2 SEM images of char (a), AC at 400°C (b) and 600°C (c) with IR 3.0 [6]	7
Figure 3 Effects of microwave power (a) and radiation time on AC (b) [14].....	8
Figure 4 (top) SEM images of CS (a), CHCS (b) and AC2_CHCS (c), (bottom) FTIR spectra of CS (d) and CHCS and AC2_CHCS before and after MB adsorption (e) [16]	9
Figure 5 Schematic illustrations of hemicellulose after hydrothermal pretreatment Process	11
Figure 6 SEM of raw hydrochar (a), ACHC-KOH 1:1 (b) and ACHC-KOH 1M (c) [19]....	12
Figure 7 The granules potassium permanganate.....	13
Figure 8 The SEM images of raw pistachio nut shell (a), AC with 0%wt of KMnO ₄ (b) and AC with 9.9%wt of KMnO ₄ (c) [25]	15
Figure 9 Schematic illustrations of aquaponics process	20
Figure 10 Suggested placement of biochar filter in aquaponics for removal of particulate matter and turbidity [51]	22
Figure 11 Clarias macrocephalus.....	25
Figure 12 the red oak lettuce (left) and the green oak lettuce (right)	26
Figure 13 Schematic illustrations of the producing activated carbon process.....	28
Figure 14 Proximate analysis % yield (a), %moisture content (b), %ash content (c), %volatile matter content (d) and fixed carbon content (e) of SLAC with and without hydrothermal pretreatment process and addition of 0 to 5% of KMnO ₄ at 300°C (blue), 350°C (red) and 400°C (green)	35
Figure 15 SEM images of the hydrochar activated carbon sample at 300°C (left) addition with 0% wt (a), 1% wt (b), 3% wt (c) and 5% wt (d) of KMnO ₄ , 350°C (center) addition with 0% wt (e), 1% wt (f), 3% wt (g) and 5% wt (h) of KMnO ₄ and 400°C (right) addition with 0% wt (i), 1% wt (j), 3% wt (k) and 5% wt (l) of KMnO ₄ and activated carbon sample without hydrothermal pretreatment process at 350°C (m) ...	38

Figure 16 SEM images of the activated carbon without hydrothermal pretreatment process at 350°C (a) and hydrochar activated carbon sample at 350°C addition with 0% wt (b).....	39
Figure 17 SEM images of the hydrochar activated carbon sample at 350°C addition with 0% wt (a), 1% wt (b), 3% wt (c) and 5% wt (d) of KMnO ₄	40
Figure 18 SEM images of the hydrochar activated carbon sample with addition 1% wt of KMnO ₄ at 300°C (a), 350°C (b), 400°C (c) and 5% wt of KMnO ₄ at 300°C (d), 350°C (e) and 400°C (f).....	41
Figure 19 FTIR spectra of the without hydrothermal pretreatment process activated carbon sample 300°C (a), 350°C (b) and 400°C (c), the hydrochar activated carbon sample with 0%wt of KMnO ₄ at 300°C (d), 350°C (e) and 400°C (f), 1% wt of KMnO ₄ at 300°C (g), 350°C (h) and 400°C (i), 3%wt of KMnO ₄ at 300°C (j), 350°C (k) and 400°C (l) and 5% wt of KMnO ₄ at 300°C (m), 350°C (n) and 400°C (o)	42
Figure 20 FTIR spectra of the without hydrothermal pretreatment process activated carbon sample at 300°C (a), 350°C (b) and 400°C (c) and the hydrochar activated carbon sample addition with 0% wt of KMnO ₄ at 300°C (d), 350°C (e) and 400°C (f)	43
Figure 21 FTIR spectra of the hydrochar activated carbon sample at 350°C addition with 0% wt (a), 1% wt (b), 3% wt (c) and 5% wt (d) of KMnO ₄	44
Figure 22 FTIR spectra of the hydrochar activated carbon sample with addition 1% wt of KMnO ₄ at (a) 300°C, (b) 350°C and (c) 400°C, 5% wt of KMnO ₄ at 300°C (d), 350°C (e) and 400°C (f).....	45
Figure 23 XRD patterns of the without hydrothermal pretreatment process activated carbon sample 300°C (a), 350°C (b) and 400°C (c), the hydrochar activated carbon sample with 0%wt of KMnO ₄ at 300°C (d), 350°C (e) and 400°C (f), 1% wt of KMnO ₄ at 300°C (g), 350°C (h) and 400°C (i), 3%wt of KMnO ₄ at 300°C (j), 350°C (k) and 400°C (l) and 5% wt of KMnO ₄ at 300°C (m), 350°C (n) and 400°C (o)	46
Figure 24 XRD patterns of the hydrochar activated carbon sample with addition 1% wt of KMnO ₄ at (a) 300°C, (b) 350°C and (c) 400°C, 5% wt of KMnO ₄ at 300°C (d), 350°C (e) and 400°C (f).....	47
Figure 25 XRD patterns of the without hydrothermal pretreatment process activated carbon sample at 300°C (a), 350°C (b) and 400°C (c) and the hydrochar activated carbon sample addition with 0% wt of KMnO ₄ at 300°C (d), 350°C (e) and 400°C (f)	48

Figure 26 XRD patterns of the hydrochar activated carbon sample at 350°C addition with 0% wt (a), 1% wt (b), 3% wt (c) and 5% wt (d) of KMnO_4	49
Figure 27 The surface area (a) and micropore volume (b) of activated carbon sample	51
Figure 28 Zeta Potential of the hydrochar activated carbon sample at 350°C with addition 0% wt (blue) and 1% wt (red) of KMnO_4	52
Figure 29 aquaculture system (a), hydroponic system (b), aquaponics system (c) and aquaponics system with activated carbon powders filter (d)	55
Figure 30 pH values of water of pond No.1 (a), pond No.2 (b), pond No.3 (c) and pond No.4 (d)	62
Figure 31 DO values of water of pond No.1 (a), pond No.2 (b), pond No.3 (c) and pond No.4 (d)	63
Figure 32 Turbidity values of water of pond No.1 (a), pond No.2 (b), pond No.3 (c) and pond No.4 (d)	64
Figure 33 Nitrogen cycle in aquaponic system.....	65
Figure 34 The catfish growth of pond No.1 (a), pond No.3 (b) and pond No.4 (c).....	68
Figure 35 Red oak lettuce (a) and catfish (b).....	116
Figure 36 3 kg of sugarcane leaf activated carbon powders	116
Figure 37 The fishponds were built by using interlocking bricks with 2 m of width, 2 m of length and 70 cm of height	117
Figure 38 The PVC tube was used to hydroponic system	117
Figure 39 The hydroponic system without connecting to aquaculture systems with sugarcane leaf activated carbon powders filter	118
Figure 40 The calibration curve for determination the nitrites concentration in aquaponics system by spectrophotometer at the wavelength 540 nm	118
Figure 41 The calibration curve for determination the orthophosphate concentration in aquaponics system by spectrophotometer at the wavelength 880 nm	119

ABBREVIATION

% wt	=	Percent weight by weight
°C	=	Degree Celsius
Å	=	Angstrom
a.m.	=	Ante Meridiem
AC	=	Activated carbon
ASH	=	Ash content
BET	=	Surface area and porosity analyzer
BOD	=	Biochemical oxygen demand
cm	=	Centimeter
cm ⁻¹	=	Reciprocal centimeter
cm ³ /g	=	Cubic centimeter per gram
CO ₂	=	Carbon dioxide
DI	=	Deionized water
DO	=	Dissolved oxygen
DW	=	Distilled water
EDX	=	Energy Dispersive X-Ray Spectroscopy
FC	=	fixed carbon content
FTIR	=	Fourier-transform infrared spectroscopy
g	=	Gram
g/stem	=	Gram per stem
H ⁺	=	Protons
HS	=	Hydrochar sample
kg	=	Kilogram
l	=	Wavelength
LHW	=	Liquid hot water
m	=	Meter
M	=	Moisture content
m ² /g	=	Square meters per gram
mg/L	=	Milligram per liter

mL	=	milliliter
N ₂	=	Nitrogen
nm	=	nanometer
NO ₂ ⁻	=	Nitrite
NTU	=	Nephelometric Turbidity unit
O ₂	=	Oxygen
OFG	=	Oxygenated functional group
pH	=	Positive potential of the hydrogen ions
PO ₄ ³⁻	=	orthophosphate
ppm	=	Part per million
Psi	=	Pound per Square Inch
rt	=	Room temperature
SEM	=	Scanning electron microscopy
SLAC	=	Sugarcane leaf activated carbon
UV-Vis	=	Ultraviolet-visible spectrophotometry
VM	=	Volatile matter content
w/t HPT	=	Without hydrothermal pretreatment
XRD	=	X-ray Diffraction
ZS	=	Nanoparticle sizing and zeta potential analyzer

CHAPTER I

INTRODUCTION

Rationale for the study

Activated carbon (AC), sometimes, it was called “activated charcoal”, is a functional carbon material. It is well known as a highly porous carbon material with a wide specific surface area. Carbon is the major element, that contains in activated carbon about 87-99%, but it still has other elements, is also composed of oxygen, hydrogen, sulfur and nitrogen. Including, other compounds existing in the precursor, that was used for the activated carbon producing process or the additives during production (0.1 to 0.2% of activated carbon is a useless element that cannot removed after the activation process and remains in the form of ash) [1-4]. Currently, activated carbon is an attractive topic due to its characterized, low-cost precursor material, including reducing agricultural wastes. That causes natural pollution. The various types of agriculture waste usually use as precursor materials, including wood, coal, some polymer and so on. [5]. The numerous advantage industrial applications such as gas storage – storage for natural gas, adsorption capacity – activated carbon is an extensively used as adsorbent in the treatment of drinking water and wastewater or adsorb color and odor, electrochemistry – electrode materials in electrochemical device, effective capture, hold material and separation, including supporting material for catalysis in various reaction. However, these commercial productions are not effective enough, leading to the producing activated carbon from newly precursor materials that much attention. The producing of activated carbon comprises of two stages, carbonizing and activating. Activated carbon can basically be produced by two processes: physical and chemical activation (single step process) [6]. Nevertheless, one of the assisting methods for producing activated carbon is hydrothermal pretreatment (HTP). Hydrothermal pretreatment process is commonly known as autohydrolysis or liquid hot water (LHW) pretreatment that uses hot water for carbonaceous precursor pretreatment with no chemicals must be added. In short, hydrothermal pretreatment process is the most effective process, low-cost and eco-friendly. Their production procedure can be adjusted to modify the chemical

characteristics of precursor material, that leads the formation of the activated carbon to give a better porous structure. That was very significant to their application. Because of precursor material structure changes by chemical reactions such as recondensation, hydrolysis, dehydration, decarboxylation, aromatization, and polymerization, which occur by water at mild temperature and under the pressure that water still in liquid stage [7]. The hydrochar character has more benefits than its original. There is high carbon content, energy density, heating value and low aromatization degree, including higher oxygenated functional group (OFG) at the surface. Because of its unique characteristics, it is a good fuel, a good raw material for digestion process, and a perfect choice of a functional carbon-rich material. All the above-mentioned, hydrothermal pretreatment is a thermochemical conversion method that a very effective for producing activated carbon or functional precursor materials. Many period studies indicate the better porous structure, quality and yield of activated carbon after using hydrothermal pretreatment assisting method. Increasing the world's population has resulted in a huge increase in basic needs for food, water, land and other natural resources. And fish and fish products are one of the foods that are popular all over the world. Leading to aquaculture will require more input. especially food causing more waste from production system. The waste from aquaculture has made a public concern. For example, fish biogas – methane (CH_4), carbon dioxide (CO_2), hydrogen sulfide (H_2S) and hydrogen (H_2), fish biofertilizer – nitrogen, phosphorous and potassium, fish bio-oil or biodiesel, fish protein hydrolysate, fish collagen, natural pigment and chitosan. In the future, the aquaculture sector will need to produce more with less. This means increasing input, pollution and waste production. Activated carbon is an effective adsorbent. One of many applications is water purification. The suitability of source water in freshwater aquaculture for increasing production as temperature: 25 to 32°C (tropical), turbidity: 25 to 80 ppm, salinity: 0.5 to 1.0 ppt, alkalinity: 50 to 300 ppm, hardness: 50 ppm (CaCO_3 : >100 ppm), pH: 6.5 to 9.0, dissolved oxygen (DO): 4.0 to 5.0 ppm, carbon dioxide (CO_2): < 10 ppm, nitrogen gas: 10 to 20 ppm, ammonia: < 0.1 ppm, nitrile (NO_2^-): < 1 ppm, nitrate (NO_3^-): < 3 ppm, chlorine (Cl): < 0.02 ppm [8-11]

Purposes of the study

- 1) In the first approve, sugarcane leaf activated carbons were prepared by using the hydrothermal low temperature.
- 2) In the second approve, sugarcane leaf activated carbons were used as adsorption filter for aquaponic system.

Significance of the study

This dissertation focuses on the producing of activated carbon via hydrothermal pretreatment process low temperature that was used as an assisted activated method using sugarcane leaf as the carbon precursor. The application of the sugarcane leaf activated carbon was used for aquatic treatment.

Scope of the study

- 1) The preparation of sugarcane leaf activated carbon via hydrothermal pretreatment followed by physical activation.
- 2) The stainless-steel autoclave (XFS-280B) was used in the hydrothermal pretreatment process of sugarcane leaf for 2 hours.
- 3) The sugarcane leaf activated carbon will be characterized via Fourier-transform infrared spectrometer (FT-IR), scanning electron microscopy and energy dispersive X-ray Spectrometer (SEM-EDS), X-ray Diffraction (XRD), surface area and porosity analyzer by gas adsorption (BET) and nanoparticle sizing and zeta potential analyzer (ZS).
- 4) The sugarcane leaf activated carbon will be used for aquatic treatment.

CHAPTER II

LITERATURE REVIEW

Nowadays, there are many processes to produce activated carbon. Carbonization and activation are two main processes. However, the starting or raw material preparation was one of the most essential processes for producing of the activated carbon. Because the producing of powdered or granular activated carbon, the precursor material was essentially crushed to suitable size. If the precursor material has an unsuitable size cause the mesopore and macropore does not generate enough in the carbonization process. The activated reagent was distributed less on the material surface in the activation process. Carbonization was the most important process because micropore structure would be generated in this process. Although micropore structures were formed after the carbonization process, these micropore structures were not good enough for the uses as sorbent yet. Therefore, the increasing of the porous structure of the carbonized material by activation process was very necessary.

This dissertation focuses on the production of activated carbon from sugarcane leaf for use as the water filter for aquaponics system. The sugarcane leaf activated carbon is prepared via low temperature hydrothermal pretreatment process with the difference KMnO_4 concentration (0%, 1%, 3% and 5%wt). The purpose of this chapter is to review the preparation of sugarcane leaf activated carbon (SLAC) and their application. This literature review contained the following:

1. Activation process for producing activated carbons
2. The preparation of activated carbons via hydrothermal pretreatment method
3. Activated carbons modified with potassium permanganate (KMnO_4)
4. Activated carbons prepared from sugarcane
5. The use of activated carbons in aquatic treatment
6. Role of nutrients in plant growth
7. Catfish
8. Red oak lettuce

1. Activation process for producing activated carbons

The activation process was the most important process for the increasing micropore structure because diluted substance will remove from carbonized materials surface. Activated carbon could basically be produced by two processes: physical and chemical activation (Figure 1). Physical or thermal activation consists of carbon dioxide (CO₂), oxygen (O₂), air and steam activation. Normally, the producing of activated carbon by using physical or thermal activation has two steps – one is thermal carbonization under inert gas such as nitrogen (N₂), argon (Ar) and helium (He) [5, 6]. And the other is activation in high temperature oven to obtain the high surface area and micropore structure of activated carbon. In 2002 J. Pastor-Villegas and C. J. Duran-Valle presented the porous structure of the granular rockrose activated carbon. The preparation was carbonized under N₂ atmosphere at 600°C and activated by CO₂ and steam at the difference temperature at 700 to 950°C. The results showed that the temperature shows little effect of a pore volume in two conditions of activated carbons. The comparison at the higher temperature, both conditions of activated carbons show the similar volume of micropore because of increasing temperature lead to fast reaction that use only the most accessible part of the porous structure [12].

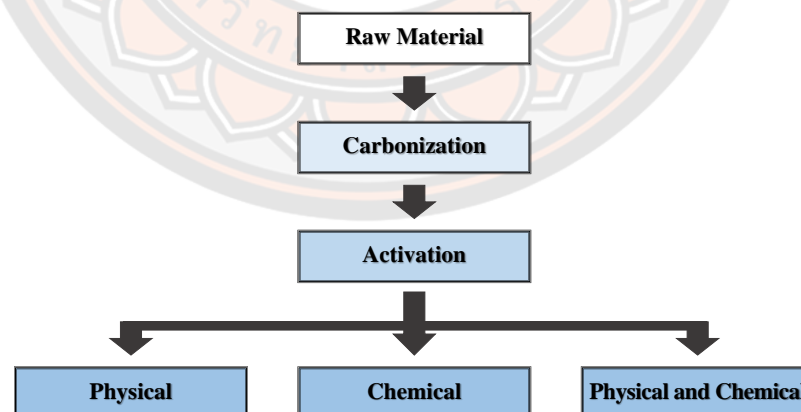


Figure 1 The producing steps of activated carbon

Chemical activation was known as the single step process of producing activated carbons. In comparison, chemical activation normally used lower temperature and shorter time than the physical activation. In addition, the number of porous structures and carbon yields are better than physical activation. The popular chemical agents are alkali and alkaline earth metal that contained substance and some acid such as sodium hydroxide (NaOH), sodium carbonate (Na₂CO₃), potassium hydroxide (KOH), potassium carbonate (K₂CO₃), zinc chloride (ZnCl₂), magnesium chloride (MgCl₂), aluminium chloride (AlCl₃), ammonium chloride (NH₄Cl), nitric acid (HNO₃), phosphoric acid (H₃PO₄) and sulfuric acid (H₂SO₄) [6].

L. Muniandy et al. presented the producing activated carbon from rice husk, which has a high porous structure. NaOH and KOH were used as chemical activation. The AC samples which prepared under a difference activating agent, but the same conditions – impregnation ratio was 1:2, activation temperature at 750°C, 60 minute of activation time under N₂ flow indicated that the BET surface area of 682.6 and 594.9 m²/g and total pore volume of 0.401 and 0.340 cm³/g for KOH and NaOH, respectively [6]. In the same way, Hakan Demiral and Isil Uzun presented the poplar wood activated carbons by using Na₂CO₃ and K₂CO₃ as activating agent under the same condition – impregnation ratio was 1:3, activation temperature at 900°C under N₂ flow showed that the BET surface area of 1596 and 1579 m²/g and total pore volume of 0.8796 and 0.8559 cm³/g for KOH and NaOH, respectively [13]. From these results, potassium ion acts as an activating agent better than sodium ion. Because potassium metal was more reactive than sodium metal. Moreover, the activated carbon that activated with potassium ion responded at high temperature (≥ 750°C). This is because most C=C aromatic bonds are always thermally stable compounds [5].

Furthermore, zinc chloride was extensively used as activating agent in the activation process. Because the activated carbon products had a highly porous structure and surface area (≥ 2400 m²/g). S.Yorgun et al. presented a high surface area of Paulownia wood activated carbon sample by using ZnCl₂ as activating agent. The activation temperatures were selected in the range of 400°C to 700°C. The suitable condition was found that the activation temperature at 400°C with the impregnant

ratio of 4.0 provided the highest total pore volume and surface area about $0.69 \text{ cm}^3/\text{g}$ and $2736 \text{ m}^2/\text{g}$, respectively. Below 500°C , ZnCl_2 acted as dehydration reagent and inhibited the formation of the tar, including promoted burning of carbon. On the other hand, the results at the highest activation temperature showed the lowest total pore volume and surface area. Above 500°C , ZnCl_2 does not act as an activating agent because of pore collapsing and heat shrinkage. According to SEM images (Figure 2), activated carbon at 400°C showed pore structure like honeycomb voids. While 600°C is irregular shapes [5].

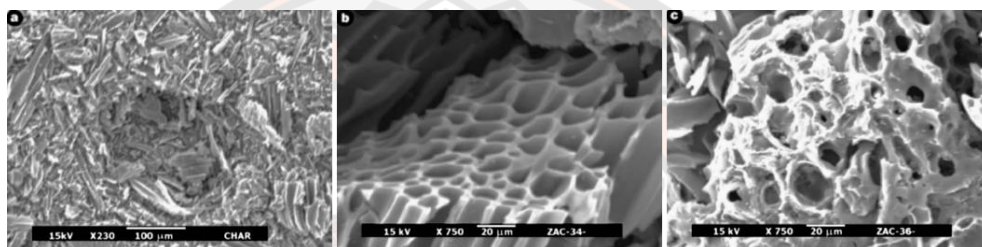


Figure 2 SEM images of char (a), AC at 400°C (b) and 600°C (c) with IR 3.0 [6]

As mentioned before, some acid was used as activating agents. Q-S. Liu et al. prepared bamboo activated carbon. Phosphoric acid acted as an activating agent with a microwave induced. This work studied the effects of microwave power, radiation time and impregnant ratio. The results showed that microwave power by 350W, radiation time 20 minutes and impregnated ratio was 1:1 showed the surface area and carbon yield about $1432 \text{ m}^2/\text{g}$ and 48%, respectively. As can be seen in Figure 3, at low microwave power, the porous structure developed not enough because of strong reaction between precursor material and phosphoric acid. Furthermore, radiation time played a vital role in the development of pore structure. In the beginning, the total pore structure significantly increases. As the activation time continues, the increasing of the pore structure becomes a slow and little drop at 30 minutes. This is because the porous structure can be ruined, if exposure to microwave radiation for a long time [14].

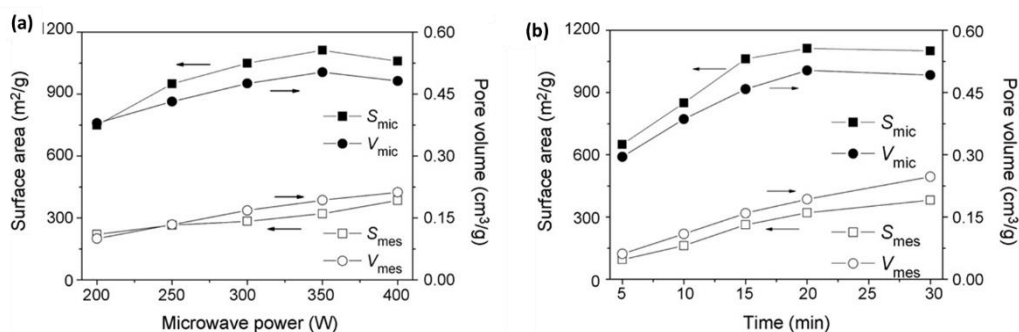


Figure 3 Effects of microwave power (a) and radiation time on AC (b) [14]

2. The preparation of activated carbons via hydrothermal pretreatment method

In addition, the use of carbonization and activation are the two direct processes for producing activated carbon. Nevertheless, the hydrothermal-base process is another method that was used to assist at producing activated carbon. Hydrothermal-base process, also commonly known as autohydrolysis or liquid hot water (LHW) pretreatment that uses hot water for biomass pretreatment with no chemical addition [15]. This process was applied to a wide variety of biomass material. This process can be combined with other processes; some used this method in carbonization process and others used to assisted in activation process. Because hydrothermal pretreatment is efficient and environmentally friendly. It is used to modify the porous structure of activated carbon products. Besides, the original structure of precursor material was changed by hydrothermal pretreatment, which occurred by water at a mild temperature (180 to 250°C) and under the pressure that water still in liquid stage (10 to 40 bar) [7].

F. Mbarki el al. showed the study of activated carbon performances using hydrothermal carbonization (HTC) pre-treatment. This work used corn stigmata (CS) as carbon precursor. Before carbonization at 900°C for one hour, the temperature was used in hydrothermal carbonization pre-treatment step at 180°C. Besides, some resultant carbons hydrochar corn stigmata (CHCS) were activated at 900°C during 0.5, 1, 2 or 3 hours again that were labelled ACT_CHCS (t means activation time (h)). SEM images (Figure 4) showed the comparison of CHCS and CS between

AC2_CHCS, indicating CS showed a rough and non-porous structure surface. CHCS presented a more porous structure with a rough surface with the BET surface area of $188 \text{ m}^2/\text{g}$. While AC2_CHCS showed several microspheres (small spherical particles) with the highest BET surface area of $1111 \text{ m}^2/\text{g}$ lead to AC2_CHCS was used as methylene blue adsorption. After methylene blue adsorption, AC2_CHCS showed slight changes of FT-IR spectra in comparison to AC2_CHCS before adsorption. The decrease of a band at 1551 cm^{-1} is π - π interaction between methylene blue adsorption and activated carbon surface, the band appearance at 1383 cm^{-1} of aromatic amine. And overall, activated carbons showed the intensity decrease with respect to their carbonaceous and increase of aromaticity after carbonization at 900°C [16].

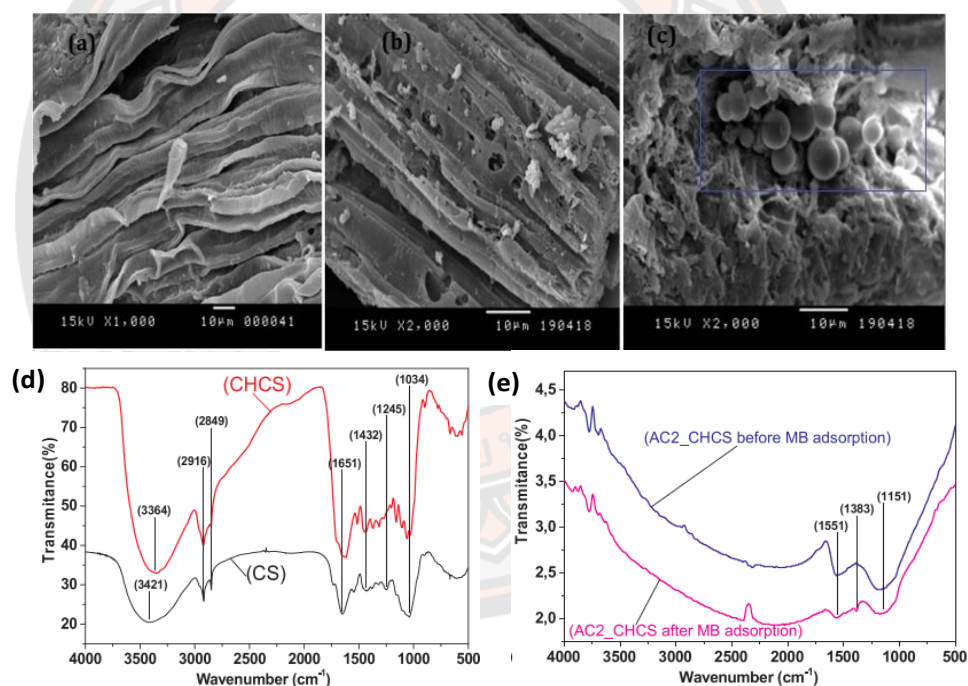


Figure 4 (top) SEM images of CS (a), CHCS (b) and AC2_CHCS (c), (bottom) FTIR spectra of CS (d) and CHCS and AC2_CHCS before and after MB adsorption (e) [16]

E. Yagmar et al. presented the preparation of raw mixed southern hardwood (MSH) activated carbon sample via autohydrolysis pretreatment process. The autohydrolysis pretreatment process temperature was used from 130 to 170°C for 100 minutes. From all results, the autohydrolysis pretreatment process activated carbon

product at 150°C with activation at 450°C for 1 hour under an inert nitrogen atmosphere. That gave a higher BET surface area of 2143 m²/g and total pore volume of 1.474 cm³/g than the activated carbon sample without autohydrolysis pretreatment process. (BET surface area of 1799 m²/g and pore volume of 1.284 cm³/g) [17].

G. Sun et al. presented the preparation of *Eucommia ulmoides* Oliver (EUC) wood activated carbon sample via hydrothermal pretreatment process. The following of increasing hydrothermal temperature from 150 to 200°C, the results indicated the hydrothermal temperature of 170°C was observed the highest surface area of 1534.06 m²/g and the total pore volume of 1.79 cm³/g. The activated carbon sample without hydrothermal pretreatment process showed the surface area of 1405.43 m²/g and the total pore volume 1.31 cm³/g. In contrast, the increasing of temperature during hydrothermal pretreatment process to 200°C, the surface area decreases to 1284.69 m²/g with 1.51 cm³/g of the total pore volume. These results can be explained that at low temperature (less than 170°C), hemicelluloses were removed while linins did not damage. And they created a pore to support the wide access of activating agent to the surface substrate led to increasing the surface area. In the order hand, at high temperature (more than 170°C) caused the collapse of surface area and prevented the activated agent from access to the surface [15].

It was found that the hydrothermal pretreatment process improves activated carbon products were higher yield, carbon content and better porous structure than the activated carbon sample without hydrothermal pretreatment process. Because hydrothermal pretreatment process was useful to extract and convert the component of solid samples in activated carbon producing process. Moreover, hydrothermal temperature strongly influenced the quantity of extraction. As mentioned above, many works clearly reported that hemicelluloses in raw material can be removed by high temperature water, while the element composition of samples did not significantly change. Zerriouh and Belbirl reported decompositions of hemicellulose in the range of 180-240°C, while cellulose and lignin decomposed in the range of 230 to 310°C and 300 to 400°C, respectively [18].

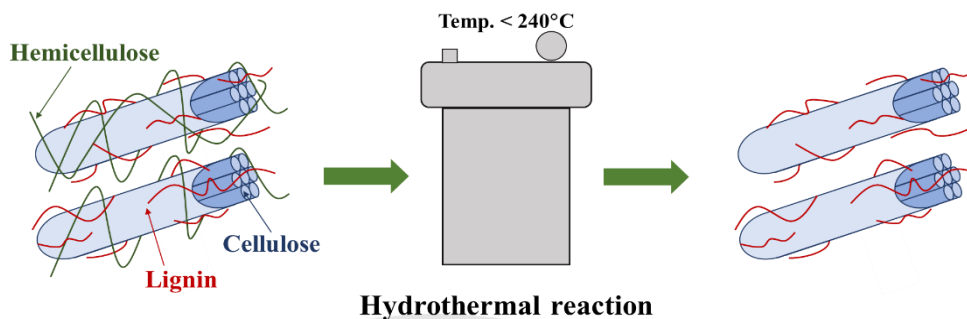


Figure 5 Schematic illustrations of hemicellulose after hydrothermal pretreatment Process

T.H. Tran et al. presented the study of methylene blue adsorption of coffee husk activated carbon, that comparison of two methods – hydrothermal and soaking method. Raw coffee husk hydrochar samples were prepared via hydrothermal pretreatment process at 180°C for 6 hours, it was call “raw hydrochar”. ACHC–KOH 1M was prepared by activating the 10 g of raw hydrochar sample with the aid of 200 mL of KOH solution 1.0 mol/L, stirred for 30 minutes and then put to hydrothermal pretreatment process at 130°C for 2 hours. ACHC–KOH 1:1 was prepared by soaking with KOH solution in the ratio of 1:1 for 36 hours. Both of condition was pyrolyzed in a tubular furnace in a stream of pure nitrogen at 700°C for 2 hours. The SEM morphologies were shown in Figure 6. The surface area of the raw hydrochar sample was formless, uneven and tight with a little pore. While the others showed layered uneven surfaces with different pore sizes. ACHC–KOH 1M activated carbon indicated more functional groups on the surface than ACHC–KOH 1:1 activated carbon. The surface functional groups played a vital role in the adsorption capacity of the sample. Three samples could be more adsorbed methylene blue when the initial concentration of its increased (50 to 500 mg/L), the raw hydrochar sample, ACHC–KOH 1:1 and ACHC–KOH 1M showed the highest adsorption capacities of 103.62, 314.05 and 357.38 mg/L, respectively. ACHC–KOH 1M showed the best methylene

blue adsorption capacity. This is because of the hydrothermal pretreatment process that favorable functional groups on the surface [19].

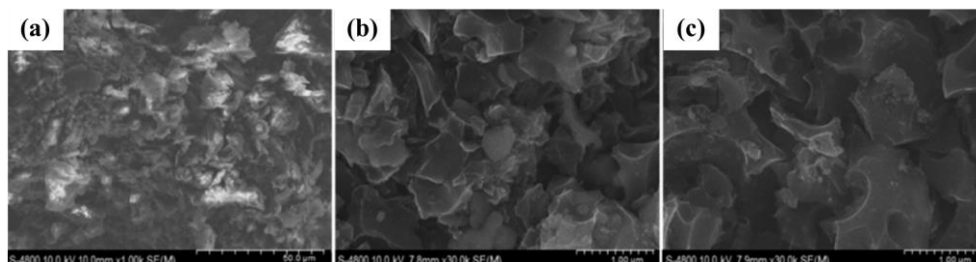
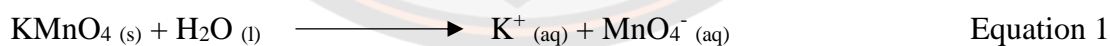


Figure 6 SEM of raw hydrochar (a), ACHC-KOH 1:1 (b) and ACHC-KOH 1M (c) [19]

3. Activated carbons modified with potassium permanganate (KMnO₄)

Potassium permanganate was an inorganic compound with the chemical formula KMnO₄. It was a hot pink to purple solution or almost black crystal (Figure 7), that could be dissolved in water as K⁺ and MnO₄⁻ (Equation 1), That was a well-known oxidizing agent, and its byproducts did not show poisonous. Therefore, the most popular applications of KMnO₄ take advantage of its oxidizing properties, including low cost, dissolvable in water, eco-friendly oxidant, and it could be used in various conditions. In addition, it has been over 50 years for pollutants treatment in drinking water and waste-water applications [20].



KMnO₄ was often used in well water to control odor and taste, removal of manganese, removal of iron and color. This substance was most often used to treat water before it was filtered. It also showed the better for removing sulfide odors than chlorine [21].



Figure 7 The granules potassium permanganate

Water for life, water was a necessary component of all living on earth, that unable to live without water. The human body is made up of 70% water, because water performs many functions such as digestion, dissolves nutrients and oxygen, regulates temperature, circulates blood, dissolves toxins. to expel from the body and so on. Water was used in every activity, that was always chemically treated to remove harmful substances and bacteria until clean and then returned to the water supply. There are many chemicals that could be used to treat water. Past work has shown that the water treatment system has been validated by pretreatment of KMnO_4 sand-filtered wastewater in combination with ultrafiltration (UF). The ultrafiltration process was widely used in the treatment of drinking water and removal of bacteria and turbidity. However, UF membrane fouling problems resulted in a reduction in membrane permeation and increase in the applied pressure required, which led to decrease filtration efficiency. It was found that the KMnO_4 concentration showed significant developments to eliminate the effectiveness of natural organic matter, which was also known as foulant removal. This is because of the changed organic pollutants characteristics by the KMnO_4 oxidation. Leading to this, total membrane resistance of the KMnO_4 using was lower than without using of KMnO_4 . KMnO_4 oxidized Fe to metal oxide particles, leading to disappearing during the EDS analysis. Because natural organic matter was absorbed by metal oxide particles. Metal oxide particles on the membrane surface effect on the better permeation. KMnO_4 converted hydrous manganese dioxide and metal ions oxidized metal oxide particles. It could be adsorbed organics and better stuck to the membrane surface. This is because its pore

volume was larger than the membrane pores. SEM showed that a significant fouling that had clogged the membrane was very loose and easy to be removed by water washing [22].

Currently, the water pollution problem increases from community and industrial wastewater sources. There are many ways to improve water quality. The use of chemicals is one of the most widely used methods. Because it is convenient and gives good results to removal pollutants in wastewater. Later, it is developed wastewater treatment by using activated carbon due to its good absorbent properties. This is commonly known as activated carbon filters. It actually adsorbs contaminants to an activated carbon filter. It is used to remove unwanted tastes, odors, and some volatile organic contaminants from drinking water. The activated carbon filter capability depends on the specific type and concentration of the contaminant. Activated carbon filter does not adsorb every type of contaminant such as some heavy metal, microbes, hardness and so on [23].

Activated carbon can remove organic compounds from air and water by being a good adsorbent or filter. G. Zhang et al showed the study of modified activated carbon by different concentrations of KMnO_4 . It was found that activity of activated carbon gradually increased with the KMnO_4 concentration increase. When the KMnO_4 concentration reached 0.06 mol/L, the activity of activated carbon was the best. While the KMnO_4 concentration was more than 0.06 mol/L, the activity of activated carbon slightly decreases. Because of its chemical properties and specific surface area. At first, the activated carbon sample modified by KMnO_4 showed improved specific surface area and pore diameter, including active oxygen groups on surface and alkaline or acidity would change. When the KMnO_4 concentration was too high, it showed the strong oxidizing property. Which not only destroys the porous structure but also clogs the pores and reduces the specific surface area. In addition, at high concentrations of KMnO_4 , the difference oxygen functional groups was reduced. [24].

F. Tavakoli Foroushani et al. investigated the pore characteristics of pistachio nut shell activated carbon on the use of KMnO_4 . The pistachio nut shell were soaked in the bath with the different concentration of KMnO_4 before they were put in furnace. The comparison of two samples with the same condition, but different

concentrations of KMnO_4 . The surface of the precursor material was quite rough. But it appears fully rigidified with a few shallow gaps. All activated carbon samples showed the same rather complex pattern of pores (Figure 8). While two different KMnO_4 concentration samples showed differences in the porous structure. KMnO_4 pretreatment leads the surface area to lower but mesopores size was bigger. That was very important in the application of filtering. Therefore, the role of KMnO_4 could be summarized as an oxidizing agent. Not only increased the mesopore size, but also decreased the specific surface area [25].

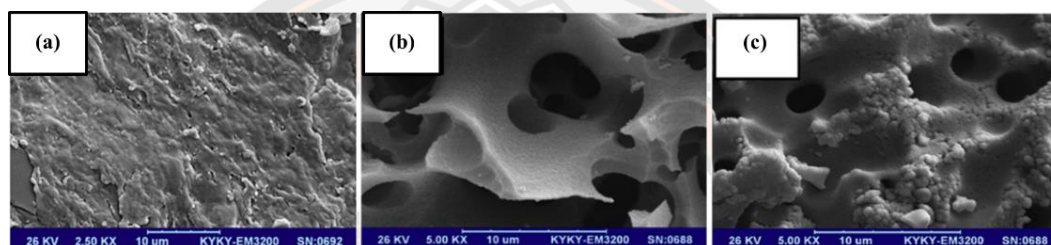


Figure 8 The SEM images of raw pistachio nut shell (a), AC with 0%wt of KMnO_4 (b) and AC with 9.9%wt of KMnO_4 (c) [25]

Y. Zhang et. al reported the influence of KMnO_4 on the adsorption of activated carbon powder by two different processes. The first process, organic matter was oxidized by KMnO_4 , before absorbed onto powder activated carbon. And the other, activated carbon powder was oxidized by KMnO_4 , before the organic matter was absorbed onto activated carbon powder in raw water.

Process 1: The reduction of COD_{Mn} and UV_{254} slightly decreased when the only used activated carbon powder to adsorb, but the concentration of activated carbon powder was more than 45 mg/L. COD_{Mn} removal and UV_{254} reduction increased with the increasing KMnO_4 concentration. At 2 mg/L of KMnO_4 and 30 mg/L of powder activated carbon showed COD_{Mn} removal rate reached 29%. This is because most KMnO_4 reacts with organic matter in water, and some were reduced to products – other hydrated oxide or MnO_2 . MnO_2 , the cover on the surface area of powder activated carbon, leading its level to absorbed organic matter decrease.

However, MnO_2 had complex reactions with HA, specifically at high level of MnO_2 . HA defines a mixture of different functional groups organic matter, including various molecular weights. The combination between powder activated carbon and KMnO_4 (especially the high concentration of KMnO_4), leading to increase of organic matter reduction. It can be summarized that the KMnO_4 oxidation should be formed to MnO_2 , MnO_2 can have complex reaction with HA and some of HA could be react with organic matter, which results in the significant decreasing of UV_{254} . Therefore, with the increasing of KMnO_4 concentration, organic matter was adsorbed on the activated carbon powder surface area, including the forming with MnO_2 , that significant decreasing of UV_{254} .

Process 2: the results showed that the removal of organic matter does not significantly change, though the high concentration of powder activated carbon. At 2 mg/L of KMnO_4 and 30 mg/L of powder activated carbon showed slightly lower CODMn removal rate than Process 1 (18%). Compared to process 1, some KMnO_4 was used after the addition of activated carbon powder and some activated carbon powder lost its ability to adsorb organic matter. This results in lower organic removal rates compared to KMnO_4 only. During process 2, after activated carbon powder was oxidized by KMnO_4 , small floccules was observed. The floccule adsorption could be adsorb organic matter and the oxidation of KMnO_4 together, not only the adsorption of activated carbon powder [26].

4. Activated carbons prepared from sugarcane

Agriculture has been main occupation of the Thai population for a long time. Since many areas in the country are suitable for agriculture, such as low-lying areas suitable for rice farming, plentifully areas suitable for gardening or farming and arid climates such as grasslands suitable for raising animals, and so on. Since agriculture is the main occupation of the Thai people, there are many agricultural products such as twigs, leaves, stems, etc., which must be destroyed by dumping or burning, causing air pollution, including the amount of waste left to destination. It is a burden to removal.

T. Adinaveen et al. studied the properties of sugarcane bagasse activated carbon. The sugarcane bagasse activated carbon showed specific capacitance of 92 to 340 F/g as well as good electrochemical property. X-ray diffraction during higher activation temperature showed crystallites structure of silica and carbon, FTIR spectrum showed silica in carbon composite. The surface area of pre-carbonized carbon (without activation), SC600 (activation at 600°C), SC700°C and SC800°C showed the value of 169.60, 676.95, 666.87 and 549.78 m²/g, respectively. Their pore volume showed 0.246, 0.424, 0.387 and 0.338 cm³/g, respectively. SEM morphology of SC600 showed the many microporous structures in the surface as well as deep pits and many folds. Because the evaporation of organic matter results in increased structural destruction, including the increasing of the surface area and the total pore volume [27].

Sugarcane molasses were a low-cost by-product from the sugar industry. J. Srenscek-Nazzal et al. studied the production of sugarcane molasses activated carbon, characterization and methane storage potential. At 780°C of carbonized temperature, the microporous materials showed the highest surface area of 2202 m²/g. The methane adsorption capacities showed maximum value of 197.23 mg/g (12.33 mmol/g) at 50 bar and 20°C [28].

Activated carbon or biochar are one concept of reducing post-harvest and increasing value to agriculture waste materials such as fluoride and bacterial removal from drinking water by sugarcane bagasse, wheat straw or sawdust activated carbon [29], water purification by bamboo charcoal [30], carbon dioxide capture by argan fruit shell [31] or mombin fruit stones activated carbon [32], manganese and iron removal by rice husk or sugarcane bagasse activated carbon [33], chromium removal from wastewater by coconut shell [34], chestnut oak [35], lead removal [36] or supercapacitor from sugarcane bagasse activated carbon [37] and so on.

The waste material from the sugar production process was one of the most productive crop wastes. Sugarcane bagasse has many advantages, including low cost, stable and high yield, which were advantageous for industrial production. The sugarcane bagasse structure consists of 38 to 59% cellulose, 18 to 26% hemicellulose, and 16 to 25% lignin. It showed that sugarcane bagasse contains more hemicellulose than the other precursor material as well as its structure is loose. This is suitable for

the ethanol industry and extract fermentation sugar. However, each year, more than 20 million tons of sugarcane bagasse are used as fuel to produce electricity. Nonetheless, there are still 2.14 hundred thousand tons of bagasse left over. Therefore, the production of activated carbon from bagasse was an innovation to reduce agricultural waste and can also be used to treat or eliminate pollutants contaminated in wastewater. Moreover, sugarcane bagasse had a lot of oxygen and carbon elements. Including, ash content is lower than other agricultural wastes, leading to the great precursor material in activated carbon preparation process. The activated carbon has high adsorption capacity because of their porous structure, leading to can adsorb various types of heavy metal from wastewater for industrial sectors before discarding. Activated carbon can also be used to adsorb color and adsorb odor.

Sugarcane was widely cultivated and used in industry in Thailand. Sugarcane leaf was a large amount of postharvest scrap produced during sugarcane harvesting. Sugarcane leaf was a source of lignocellulosic biomass and inexpensive abundant. That was agricultural waste, could be used as renewable energy. Sugarcane leaf was now used as raw materials in bioethanol products. But the process requires chemicals to break down cellulose and hemicellulose to form sugars. However, using as raw materials for activated carbon could be recycled excess energy due to producing lower pollutant as by-product.

5. The use of activated carbons in aquatic treatment

Activated carbon was a product that has a high carbon content from biomass such as agricultural waste, wood and animal manure. That were prepared by carbonization or pyrolysis process. Awad et al. reported that the biochar gave the plant growth ratio increases by improving physical, chemical and biological properties of soil, including the ability fixation of fertilizers and organic/inorganic contaminants [38]. Biochar had functional groups on the external surface and porous structure, which ability to bind metal ions - exchanging metal with cation on the surface (K^+ and Na^+), the internal complex with organic substances or oxide compounds of biochar, complex around the surface and functional groups and

precipitation in salt form. These are some reasons that activated carbon or biochar widely used for water treatment in aquatic environment [39].

Activated carbon was a great adsorbent due to the specific surface area and good total pore volume. Leading to the perfect removal of various types of dissolved heavy metals in aquatic environments. However, the modified activated carbon adsorption capacity was better than the original activated carbon. Humic acid is one of the organic compounds that can absorb Hg ions. Working with activated carbon that the way to increase the removal of Hg. G. Jin et al. reported that used the humic acid modified activated carbon sample for the removal of Hg (II) in an aquatic environment. Compared with the original activated carbon, activated carbon with humic acid can absorb Hg more than the original activated carbon. This is because of its large specific surface area, higher mesopore and micropore volume. The humic acid impregnation had no effect on the porous structure, but it changed the chemical functional groups on the surfaces of activated carbon. The adsorption capacity of Hg decreased with increasing impregnated time, temperature and pH due to a low free surface area [40].

Aquaponics as called from hydroponic and aquaculture, that work together with each other (Figure 9). It can be definition; This is a system that integrates fishponds with plants in a single system. Fish provide nutrients from the plant growth for decreasing nutrient concentration in the water. Currently, this system is very popular in a small area to maintain the balance of the environment. Physical and chemical properties of water depend on the kind and number of fish. Generally, the conductivity and pH should be in the range of 1 to 3 ds/m and 5.5 to 6, respectively. Because the changing of pH leads to nitrogen changing. Therefore, this system must control water quality [41]. The aquaponics system can reuse and treat water quality. The use of this system leads to lower costs for treating water and maintenance apparatus, including use less fertilizer. Aquaponics were considered a sustainable system with using the lower cost for increasing incomes [42]. In addition, the aquaponics system products were regarded as organic products that safe and good for health [43].

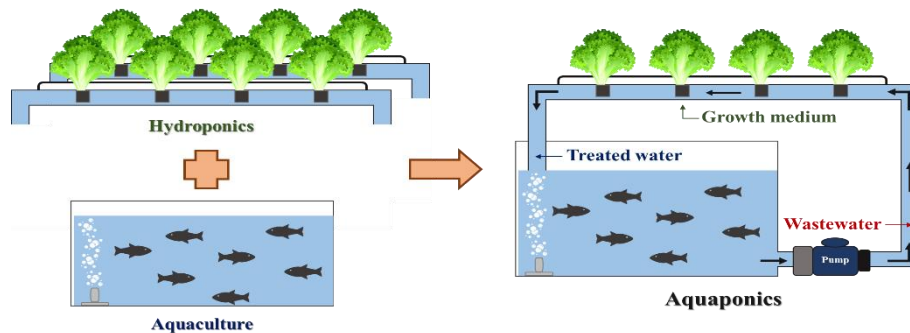


Figure 9 Schematic illustrations of aquaponics process

Hydroponic was a fast-developing eco-industrial technology to produce commercial harvest with high nutrient solutions. It was a method used to grow certain vegetables, mainly leafy vegetables, and herbs. They were grown sustainably with considerably less water, instead of soil. Which enables them to be of a higher quality and more nutritious. Hydroponic had many advantages such as good-quality and safe products, disease management and short planting periods and increased yields. Maintaining the optimal concentration of nutrient solutions around the roots that should be used inert surfaces such as coconut coir, peat, perlite, vermiculite (perlite and vermiculite were the popular material plant growing due to their good water adsorption properties) [38] and manure [44]. Moreover, plant root could be adsorbed macronutrient (N, P and K) and secondary nutrient (Ca, Mg, S, Mn, B, Zn and Mo) [45], including uptake soluble compound from polluted water that the source of nutrient for plants [46]. Yang et al. reported hydroponics could be removed nitrate of 91% within 3 days, nitrile of 97% within 2 days and nitrogen 71% within 1 day, including 17 to 47% of chemical oxygen demand (COD), 31 to 64% of total nitrogen, 8 to 15% of total phosphorus and dissolved oxygen (DO) concentration of 0.7 mg/L (the lowest), which played a vital role in the conversion and removal of $\text{NO}_x\text{-N}$ and $\text{NH}_3\text{-N}$ [47].

Hydroponic system was a simple and efficient technology for treating wastewater from aquaculture system. However, this system showed low qualities to remove suspended solids. Pan et al. reported the hydroponic system was improved for the great treatment from aquaculture system. The ryegrass was grown in perforated

plastic plates with many layers of unwoven cotton fabric. The different layers of fabric showed removing total, volatile solids and suspended solids. The vertical filtrations increasing improved the removal of solid. The 1-day treatment with 0.8 m² five cells showed the total solids removal of 66%, volatile solids of 71%, suspended solids of 91%, and adsorbed total nitrogen about 72%, total phosphorus of 80%, chemical oxygen demand of 63%, and total ammonia nitrogen of 85%. Therefore, this work showed the simple and efficient technology for treat wastewater from aquaculture system, by the connecting with hydroponic system which showed high relatively concentrations of suspended solids [46]. Moreover, Sikawa et al. explored the use of sand and gravel to treat water from catfish ponds used to grow lettuce as a hydroponics system. It was found to have a low ability to remove suspended solids as well [48].

Not only does growing plants in the hydroponics system has advantages, but it also has disadvantages. Organic plantings used in hydroponics system can change their characteristics due to the deterioration of organic matter during the growing season. Organic matter degradation influences plant growth: nitrogen fixation, the appearance of new organic compounds leads to plant toxicity. Changes in the ability to exchange cations or increased salinity in plant growth The loss of organic matter and structural changes in the substrate decreases aeration capacity. This causes the roots to lack oxygen. [49].

At the same time, the aquaculture system still has some disadvantages because of its fast-growing industries. When the fish meat in the market is less than the demand of consumers, resulting in the entrepreneurs needing to expand the fish farming area to be enough for the demand of the markets. One of some disadvantages is dropping polluted water that was rich in nitrogen and phosphorus from this system into the aquatic environment, maybe environmental pollution. Not only nitrogen is an important element for all living things, but also still toxic to fish in the form of ammonia. They were transformed to nitrite (NO₂⁻) by nitrifying bacteria, in the first step. After that, it were transformed to nitrate (NO₃⁻) and N₂ by nitrification and denitrification process, respectively [41]. Moreover, the study of growing plants by water from the aquaculture system showed that the average concentration of ammonia, NO₃⁻ and phosphate (PO₄³⁻) are 0.35, 0.34 and 0.19 mg/L. respectively. It

was found that the growing of lettuce, green vegetables, mustard, sage, garlic, celery, and herbs as well [42]. Some was used for fish anesthetics removal from water [50].

Currently, Biochar was offered as a low-cost medium-duty filter in aquaponics system. Z. Khiari et al. presented the bamboo biochar that was used as a filter into the aquaponics system. This work investigates the filtration process on a small- and large-scale. The small-scale resulted in two biochar media sizes (fine and coarse) on their particle size distribution and turbidity removal efficiency. Both sizes can be able to purify wastewater from aquaponics system, but fine biochar gave better filtration characteristics than coarse biochar. The large-scale experimental used mixture biochar media size revealed the high intensity removal of turbidity from the aquaponics system. The aquaponics system could be combined with the biochar filtration step before water returned to plant growth system [51].

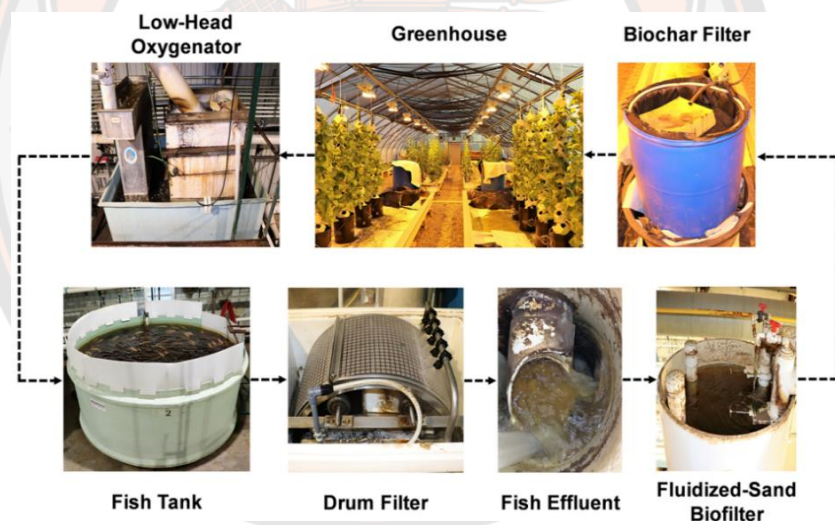


Figure 10 Suggested placement of biochar filter in aquaponics for removal of particulate matter and turbidity [51]

It was found that activated carbon is ideal for capturing suspended particles and removing turbidity from the aquatic environment. The quality of the filter plays a vital role in the treatment of wastewater before it sends the treated water into the plant growth system. Despite a lot of research but still it is necessary to confirm the advantages of activated carbon in water treatment.

6. Role of nutrients in plant growth

Plants were the only living things that could make their own food. Even so, plants need nutrients to use in their growth process and various activities within the cell, as well as humans and animals. Plants make food by bringing various elements that were contained in water, air and soil through the process of photosynthesis and other minerals are absorbed to create starch, proteins, fats, enzymes, hormones and so on. When the absorption of nutrients in the water, air and soil is analyzed. The nutrients are found 92 different elements, but only 17 elements are important and necessary to the growth of plants. The basic requirement of plants, nutrients are divided into two categories: macronutrients (plants would die without these) and micronutrients (plants need in very small amounts (parts per million)). Each plant's nutrients are important for different parts of plant growth when the plants are not getting enough nutrients. They often show symptoms or signs of a deficiency of these essential nutrients.

Macronutrients - plants required in larger amounts. That consists of primary nutrient elements and secondary nutrient elements.

1) Primary nutrient elements

1.1) Nitrogen (N)

Nitrogen was an essential element for plant growth. Especially, the production of amino acids, nucleic acids, proteins and hormones, as well as being directly involved in the photosynthesis process. Nitrogen is one of the main components of chlorophyll. that makes plants green. In shortage conditions, the color of the leaves turns yellow, smaller leaf size, stunted stem and low productivity. Nitrogen is utilized by plants through absorption by root plant in the form of nitrate salts (NO_3^-) and ammonium salts (NH_4^+). Plants also receive nitrogen from the decomposition of organic matter and transformation of organic matter by soil microorganisms. Including getting it from certain plants, such as the containing rhizobium to help fix nitrogen from the air. Ammonia, nitrite and nitrate are nitrogen compounds, which are very important for fish in the water.

1.2) Phosphorus (P)

Phosphorus is a nutrient that stimulates and accelerates plant root growth. It is an element that affects the control of flowering, fruiting and seeding, and is also important for processes such as photosynthesis, energy transfer and plant respiration. In shortage conditions, the roots of the plant cannot grow completely, the mature leaves change color from green to purple and brown and fall off, the stem is stunted, and neither flowering nor fruiting. Phosphorus is utilized by plants through absorption by root plant in the form of hydrogen phosphate ions (HPO_4^{2-}) and dihydrogen phosphate ions (H_2PO_4^-).

1.3) Potassium (K)

Potassium is a nutrient that contributes to the synthesis of sugars, starches and proteins, including the transport of sugars, starches and oils. It helps in resistance to certain diseases and insects. In shortage conditions, the stem is not strong, incomplete flower and fruit growth. Especially, the output is of low quality. Potassium is a water-soluble element. Potassium is adsorbed in the form of potassium ions.

2) Secondary nutrient elements

2.1) Calcium (Ca)

Calcium is an element that enhances the utilization of nitrogen. The amount of calcium found in plants is found mainly in growing areas such as leaflets, bud and roots.

2.2) Magnesium (Mg)

Magnesium is a component of the green parts of the leaves, stems, fruits and other parts, that plays a vital role in the formation of food and protein.

2.3) Sulfur (S)

Sulfur is an essential element to produce proteins. That is a constituent of proteins and some vitamins, such as vitamin B1. It also has an indirect effect on the creation of the green part, the process of respiration, food synthesis, and it is a component of volatile substances with a unique smell such as onions, garlic and so on.

Micronutrients, it also called “beneficial element”. Plants need to be used in small amounts. There are 8 elements - iron (Fe), manganese (Mn), boron (B), molybdenum (Mo), copper (Cu), zinc (Zn), chlorine (Cl), and nickel (Ni) [52-54].

7. Catfish

Clarias macrocephalus of broadhead catfish plays an important role as an economically aquaculture. That is a native of Southeast Asia. The use in human consumption in countries such as Thailand and Philippines. It is a fast growing and resistant to disease [55, 56].



Figure 11 *Clarias macrocephalus*

Kingdom	Animalia
Phylum	Chordata
Class	Actinopterygii
Order	Siluriformes
Family	Clariidae
Genus	Clarias
Species	<i>C. macrocephalus</i>

8. Red oak lettuce

Lettuce (*Lactuca sativa*) has been widely cultivated plant in hydroponic systems in Thailand. There are many types of lettuce that were widely cultivated in hydroponic systems such as Batavia, green oak and red oak. That can be eaten in a salad mix, sandwich, or as a side dish. One popular type of lettuce is red oak lettuce. It tastes crispy with a slightly sweet, buttery texture, incredibly mellow and nutty flavor. Nutty flavor was defined as the “nut-like fragrant (nonspecific)” [57]. The appearance of the leaves is curled and ruffled at the edges, which looks like green oak lettuce, as shown in Figure 12. However, the difference is that the leaves have a dark red color at the top, while the bottom from the stem blends into streaks of green. In addition, red oak lettuce is very nutritious.



Figure 12 the red oak lettuce (left) and the green oak lettuce (right)

Red oak lettuce was a plant that can grow well in almost any soil, clay, loam and sandy loam. However, it can be grown well in hydroponics system with a pH between 6.0 to 6.8 and temperatures between 21 to 26°C. The planting area should receive full light because it needs light all day. Red oak lettuce can be grown all year round. Red oak lettuce can take around 40 to 45 days to grow. Red oak lettuce is a healthy food that can help reduce weight. It is low in calories with no cholesterol, plenty of vitamins such as vitamin K, vitamin A, small amounts of vitamin C, B9, B3, and B6, including calcium, iron, potassium, phosphorus, magnesium, and selenium, that are full of fiber. That helps your body digest food and relieve constipation. Vitamin K, magnesium, and potassium nourish the blood vessels and heart. Vitamin A is essential for maintaining your eyesight. Minerals along with vitamins support bone function and muscle. Antioxidants may help reduce the risk against harmful diseases. Regular consumption may help reduce cholesterol levels.

From the past research of the group, the study of activated carbon for removal of ferric ion, which the preparation from pineapple leaf that was modified by KMnO_4 . The producing of pineapple leaf activated carbon was modified by 0% wt to 5% wt of KMnO_4 and carbonized temperature at 500°C for an hour. The results showed the pineapple leaf activated carbon with 1% wt of KMnO_4 exhibited the highest value of BET surface area of 142.8920 m^2/g and total pore volume of 0.07356 cm^3/g . While the pineapple leaf activated carbon with 3% wt of KMnO_4 exhibited the BET surface area of 115.1215 m^2/g and total pore volume of 0.6359 cm^3/g . This is because the oxygen contained on the function groups and MnO_2 blocked the pore entrances [58].

CHAPTER III

THE PREPARATION OF SUGARCANE LEAF ACTIVATED CARBON AND THEIR CHARACTERISTIC

Equipment and tools

1. Nanoparticle sizing and zeta potential analyzer (ZS, Malvern zeta sizer nano-ZS, UK)
2. Surface area and porosity analyzer (BET, Micromeritics TriStar II)
3. Scanning electron microscopy and energy dispersive X-ray spectrometer (SEM-EDS, a LEO 1455 VP Electron Microscopy, England)
4. X-ray Diffraction (XRD, PW 3040/60 X'Pert PRO Console, Philips, Netherland)
5. Fourier-transform infrared spectroscopy (FT-IR, Spectrum GX, Perkin Elmer, USA)
6. Stainless steel portable sterilizer autoclave (XFS-280B, China)
7. Analytical balance (Sartorius, Germany)
8. Muffle furnace (Fish Scientific Isotemp®, USA)
9. Hot air oven (Shel lab, USA)
10. Desiccator

Materials and Chemicals

1. Sugarcane leaves (Kamphaengphet, Thailand)
2. Potassium Permanganate (KMnO_4) (A.R. grade, Q RēC™)
3. Concentrated Hydrochloric acid (Conc. HCl) 37% wt (A.R. grade, RCI labscan)
4. Sodium hydroxide (NaOH) (A.R. grade, Sigma-Aldrich)
5. Sodium Chloride (NaCl) (A.R. grade, Loba Chemie™)

Experimental

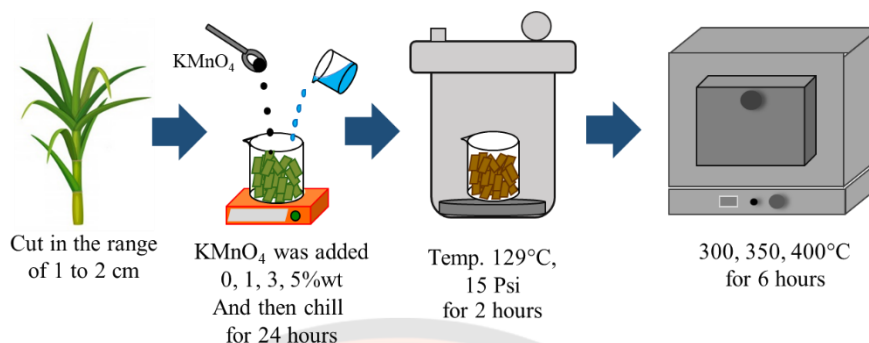


Figure 13 Schematic illustrations of the producing activated carbon process

1. The producing of sugarcane leaves activated carbon

Sugarcane leaves were used as the precursor materials for producing activated carbon. They were collected from Kamphaengphet Province. That is the one lower northern city of Thailand. After the harvest, the sugarcane leaves were dried in sunlight for a few days or until completely dried. The sugarcane leaves were cut by pruning shears. Their particle size was in the range of 1 to 2 cm (10 to 20 mm). The precursor materials were put into container with 0%, 1%, 3% and 5% wt of potassium permanganate (KMnO_4). It acted as modified carbon materials and then added distilled water. Before, the samples were put into stainless steel portable sterilizer autoclave at about 129°C and 15 Psi with reaction time of 2 hours. The samples were chilled for 24 hours. After 2 hours, the sterilized sample was cooled down at room temperature. The samples from this process were called “hydrochar”. The hydrochar samples were dried into hot air oven at 70°C until completely dry and then cooled in a desiccator. Before the samples were put into the crucible with a lid for the activation step. The exact weight of the hydrochar sample was measured. The heating temperature was designed that 300, 350 and 400°C and the maintained at the steady temperature for 6 hours. After that, the crucible was cooled in a desiccator to room temperature. The samples from this process were called “activated carbon”. The weight of activated carbon was measured and then calculated as the yield percentage (%yield), is given by:

$$\%YIELD = 100 \times \left(\frac{AC}{HS} \right) \quad \text{Equation 2}$$

AC as Mass of activated carbon (gram)

HS as Mass of hydrochar sample (gram)

2. Proximate analysis

When the activated carbon sample was heated under various conditions. Proximate analysis is the first analysis to perform on the activated carbon sample for characterizing of the individual components. It gives the gross composition of the activated carbon sample. It is relatively easy to measure and an inexpensive process. That comprises the determination of moisture content (M), ash content (ASH), volatile matter content (VM) and fixed carbon content (FC).

2.1 Moisture content (M)

This method was used to determine the percentage of water or low volatile matter in an activated carbon sample by drying it to a constant weight. The exact weight of activated carbon sample and petri plate were measured before they were dried in the hot air oven at 105 to 110°C for an hour and half to 3 hours. The petri plate was not covered during this step. After that, they were cooled in a desiccator to room temperature. The weight of dried activated carbon sample was measured and recorded. And then it was calculated as moisture content percentage (%M), is given by:

$$\%M = 100 \times \left(\frac{C-D}{C-B} \right) \quad \text{Equation 3}$$

B as Mass of petri plate (gram)

C as Mass of petri plate + activated carbon before heating (gram)

D as Mass of petri plate + activated carbon after heating (gram)

2.2 Ash content (ASH)

This method was used to determine the total ash content percentage of the activated carbon sample, including precursor materials. The activated carbon sample was dried in the hot air oven at 105 to 110°C for an hour and half to 3 hours before determination in this step. The exact weight of activated carbon sample and crucible were measured and then it was heated at high temperature about 760°C for 3 to 6 hours. The crucible was not covered during this step. After that, they were cooled in a desiccator to room temperature. The weight of ash was measured and recorded. And then it was calculated as ash content percentage (%ASH), is given by:

$$\%ASH = 100 \times \left(\frac{D-B}{C-B} \right) \quad \text{Equation 4}$$

B as Mass of empty crucible (gram)

C as Mass of empty crucible + activated carbon before heating (gram)

D as Mass of empty crucible + ash after heating (gram)

2.3 Volatile matter content (VM)

This method was used to determine the percentage of loss in mass minus the moisture that was already determined before. The exact weight of activated carbon sample and crucible with a lid were measured before they were heated at high temperature about 925 to 950°C for 7 minutes under condition without air. After that, they were cooled in a desiccator to room temperature. The weight of the activated carbon sample was measured and recorded. And then it was calculated as volatile matter content percentage (%VM), is given by:

$$\% \text{weight loss} = 100 \times \left(\frac{A-B}{A} \right) \quad \text{Equation 5}$$

A as Mass of activated carbon before heating (gram)

B as Mass of activated carbon after heating (gram)

$$\%VM = C - D - E \quad \text{Equation 6}$$

C as weight loss percentage

D as moisture content percentage

E as ash content percentage

2.4 Fixed carbon content (FC)

The fixed carbon content percentage (%FC) was calculated as follows:

$$\%FC = 100 - (\%M + \%ASH + \%VM) \quad \text{Equation 7}$$

3. The preparation for zeta potential analysis

Reagent preparation

- a) NaCl was prepared to concentration of 0.01 mol/L.
- b) NaOH was prepared to concentration of 0.01 mol/L.
- c) HCl 37%wt was diluted to 0.01 mol/L.

Procedure

- a) Activated carbon was dispersed 50 mg/L in NaCl solution by ultrasonic.
- b) The pH (3, 5, 7, 9 and 11) of the solution was adjusted with 0.01 mol/L HCl and NaOH.

4. Characterization

4.1 Fourier-transform infrared spectroscopy (FTIR)

Fourier-transform infrared spectroscopy (FTIR, Spectrum GX, Perkin Elmer, USA) was used to classify organic, inorganic and chemical bonds or functional groups of the obtained activated carbon sample.

4.2 X-ray Diffraction (XRD)

X-ray Diffraction (XRD, PW 3040/60 X'Pert PRO Console, Philips, Netherland) was used to analyze and identify the type of compound and crystal structure of the obtained activated carbon sample.

4.3 Surface area and porosity analyzer (BET)

Surface area and porosity analyzer (BET, Micromeritics TriStar II, USA) was used to analyze surface area characteristics, for example, pore size diameter, surface area, pore volume of the obtained activated carbon sample.

4.4 Scanning electron microscopy and energy dispersive X-ray spectrometer (SEM-EDS)

Scanning electron microscopy and energy dispersive X-ray spectrometer (SEM-EDS, a LEO 1455 VP Electron Microscopy, England) was used to study the surface characteristics, size, shape and analytical technique used for the elemental analysis or chemical characterization of the obtained activated carbon sample.

4.5 Zeta potential analyzer (ZS)

Zeta potential analyzer (ZS, Malvern zeta sizer nano -ZS, UK) is used to analyze particle size and potential on the surface of particles of the obtained activated carbon.

Results and Discussion

1. Proximate analysis and yield percentage of sugarcane leaf activated carbon

The yield percentage was calculated by equation 2, the results were shown in Table 1 and Figure 14a. The yield percentage of all sugarcane leaf activated carbon products decreased, which increased the activation temperature by 300, 350 and 400°C. The without hydrothermal pretreatment sample showed the yield percentage 36.5000, 23.4667 and 16.4000, respectively. As well as the hydrochar activated carbon sample with the increasing of KMnO_4 concentration by 0%, 1%, 3% and 5% by weight that showed the increasing of yield percentage. It exhibited that the increasing of the activation temperature caused the sample to decompose more thermally. When compared at the same temperature, the hydrochar activated carbon sample showed a higher yield percentage than without hydrothermal pretreatment process activated carbon samples. At 300°C of the activation temperature, the yield percentage of the hydrochar activated carbon sample with KMnO_4 concentration by 0%, 1%, 3% and 5% by weight exhibited 35.5000, 36.2333, 37.3692, 41.2670 and

42.1399, respectively. It is because the hemicellulose of the precursor material was decomposed in the hydrothermal pretreatment process. That caused the hydrochar sample to occur in the aromatization reaction. From the period work reported the decomposition of hemicellulose in the range of 180 to 240°C, while cellulose and lignin decomposed in the range of 230 to 310°C and 300 to 400°C, respectively [18]. This phenomenon made the hydrochar sample stable to thermal activation [15, 16]. Moreover, the comparison at the same temperature with increasing of KMnO_4 concentration by 0%, 1%, 3% and 5% by weight. The results showed that the yield percentage of activated carbon samples increased. The hemicellulose of the precursor material decomposed in the hydrothermal pretreatment process not only occurred during the aromatization, but also increased the surface area of the hydrochar sample. That led the hydrochar sample to enhance binding the KMnO_4 on the surface [15]. In addition, the decomposing of KMnO_4 , that occurred the oxides of Mn and K. These were resistant to decompose by thermal at temperatures in the range of 300 to 400°C. Therefore, the yield percentage of the hydrochar activated carbon sample increased as compared to activated carbon samples without KMnO_4 .

The percentage of ash content was calculated by equation 4, the results were showed in Table 1 and Figure 14c. All conditions of activated carbon sample showed increasing of the ash content percentage. This phenomenon showed the hydrothermal pretreatment process caused the sample to decompose more thermally. The increasing of activation temperature and KMnO_4 led to the decomposition of hemicellulose of precursor material. That would not only damage pore structure but also decreased specific surface area (G. Zhang et al., 2017). Therefore, the ash content percentage of the activated carbon sample increased after the increase of activation temperature and KMnO_4 , including the hydrothermal pretreatment process.

The percentage of volatile matter content was calculated by equation 5 and equation 6, the results were showed in Table 1 and Figure 14d. The percentage of volatile matter content showed lower value with increasing of activation temperature and KMnO_4 concentration, that relating to the percentage of fixed carbon content that showed higher value. Excepting, the activation temperature of 300°C with 3 and 5% of KMnO_4 showed the opposite results. The percentage of fixed carbon was

calculated by equation 7, the results were showed in Table 1 and Figure 14e. However, the percentage of moisture content showed a higher value with increasing of activation temperature and KMnO_4 concentration to 3% and it decreased at 5% of KMnO_4 in all the activation temperature. It is because the amount of KMnO_4 was too high, causing their cover on the surface area of activated carbon samples and the oxide of Mn and K resistant to decompose by thermal at temperatures of 300, 350 and 400°C. The percentage of moisture content was calculated by equation 3, the results were shown in Table 1 and Figure 14b.

Table 1 Proximate analysis and %yield of sugarcane leaf activated carbon products

Temp. (°C)	SLAC samples	Proximate analysis				% Yield
		%M	%ASH	%VM	%FC	
-	Sugarcane leaf	2.7680	7.6174	84.0102	5.6044	-
300	w/t HPT	1.8715	12.4110	73.9198	11.7977	36.5000
	0% KMnO_4	3.6202	14.7913	67.7642	13.8243	36.2333
	1% KMnO_4	3.7996	18.8124	61.3595	16.0285	37.3692
	3% KMnO_4	4.6395	19.3283	75.7749	0.2573	41.2670
	5% KMnO_4	3.8106	20.6394	75.2770	0.2730	42.1399
	350	w/t HPT	3.4509	14.5597	67.9639	14.0255
0% KMnO_4		4.2627	17.7954	56.6736	21.2683	23.3669
1% KMnO_4		4.5510	20.8530	51.1502	23.4458	26.6803
3% KMnO_4		5.1947	22.6918	48.2382	23.8753	29.9631
5% KMnO_4		3.4280	24.5007	43.3094	28.7619	30.2913
400		w/t HPT	2.8168	17.3657	55.4332	24.3843
	0% KMnO_4	4.6309	20.6003	50.2152	24.5536	20.3286
	1% KMnO_4	4.7209	22.8248	47.8662	24.5881	22.0826
	3% KMnO_4	5.3973	26.8909	38.7315	28.9803	23.7130
	5% KMnO_4	3.1097	30.4124	37.0446	29.4333	26.9947

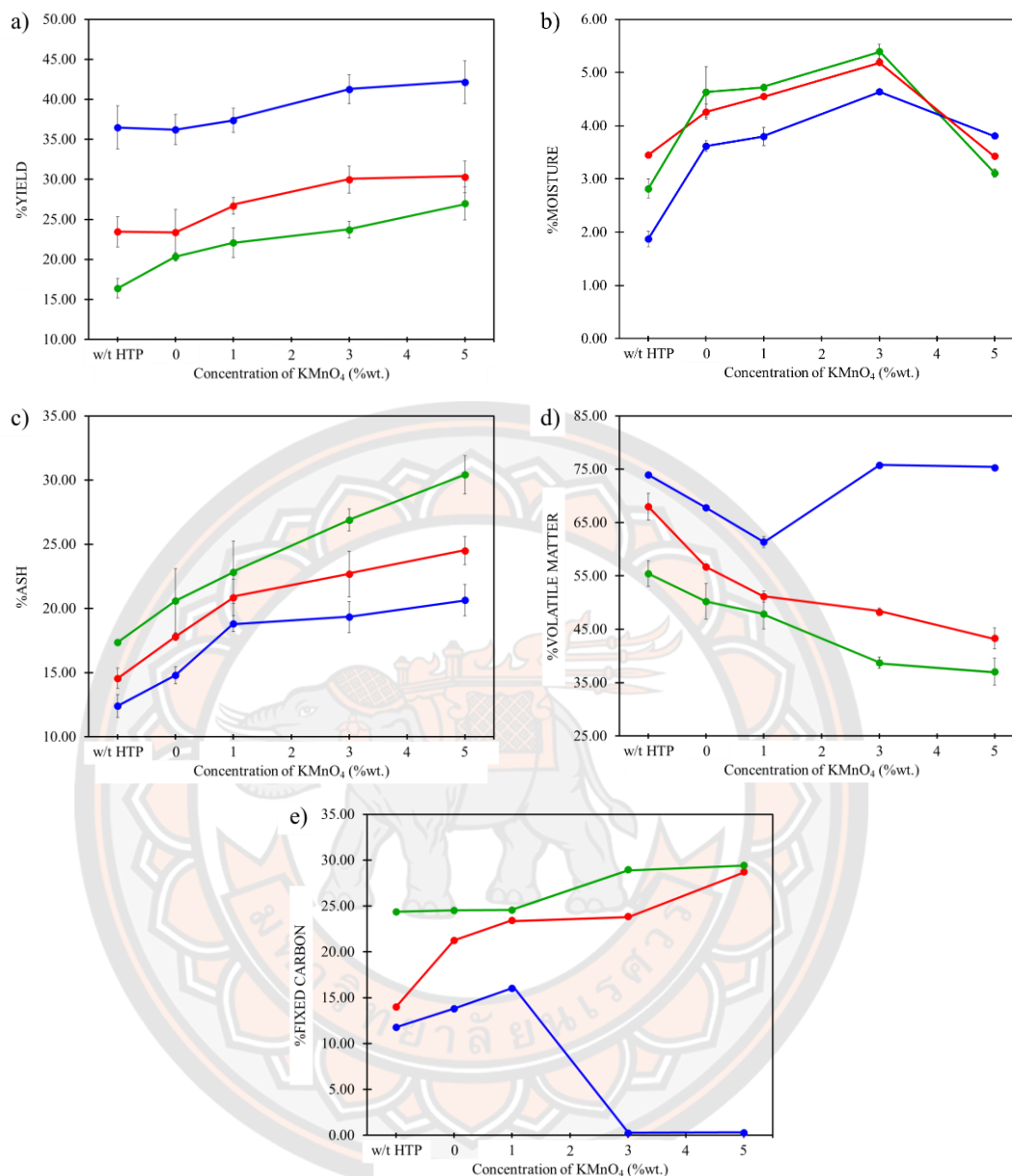


Figure 14 Proximate analysis %yield (a), %moisture content (b), %ash content (c), %volatile matter content (d) and fixed carbon content (e) of SLAC with and without hydrothermal pretreatment process and addition of 0 to 5% of KMnO₄ at 300°C (blue), 350°C (red) and 400°C (green)

2. Morphologies and elemental composition of sugarcane leaf activated carbon by SEM-EDS

All activated carbon sample was measured element composition by energy dispersive X-ray spectrometer (EDS), the analytical technique was used for the elemental analysis or chemical characterization of the obtained activated carbon sample, as shown in Table 2. The increase of the activation temperature showed the decreasing of the oxygen (O) content. This phenomenon indicates that the higher activation temperature led to the volatile matter degradation increased. In considering the effect of hydrothermal pretreatment process exhibited the carbon (C) content of the hydrochar activated carbon sample was higher than the without hydrothermal pretreatment process activated carbons sample. This is because hemicellulose contains high amounts of oxygen and hydrogen, and it was decomposed during hydrothermal pretreatment process [15]. From these results, the increase of the activation temperature showed decrease in the ratio of oxygen to carbon (O/C) of the hydrochar activated carbon sample. While the increasing of KMnO_4 concentration, the ratio of oxygen to carbon (O/C) of activated carbon sample tended to increase. This is because the oxidation of the hydrochar activated carbon sample by KMnO_4 resulting in the decreasing of carbon content and increasing of oxygen content. The other elements of activated carbon samples tended to slightly increase with the increasing of activation temperature Especially, the increasing of KMnO_4 concentration led the content of manganese (Mn) and potassium (K) to increase. Although some of these elements are dissolved and washed away by acetic acid which formed during hydrothermal pretreatment process, except Ca and Si which resisted removal to hydrothermal pretreatment process [59]. In addition, these elements are inorganic matter which was stable in high temperature. Therefore, it remained in the activated carbon products after activation step.

Table 2 Elemental composition of activated carbon products from EDS

Temp. (°C)	SLAC Sample	Elements composition (% wt.)						
		C	O	O/C ratio	Mn	Si	K	Ca
300	w/t HPT	60.87	35.85	0.59	0.38	1.32	0.57	0.81
	0%KMnO ₄	69.93	21.66	0.31	1.01	4.06	1.38	0.96
	1%KMnO ₄	62.83	27.44	0.39	1.05	4.87	2.46	1.39
	3%KMnO ₄	57.45	30.67	0.53	1.26	4.87	4.23	1.45
	5%KMnO ₄	50.55	29.86	0.59	5.64	7.04	4.70	2.18
350	w/t HPT	65.52	30.85	0.47	0.67	1.83	0.32	1.01
	0%KMnO ₄	70.69	26.10	0.37	0.45	0.58	0.59	1.27
	1%KMnO ₄	64.70	27.35	0.42	0.85	3.58	2.57	0.94
	3%KMnO ₄	61.09	28.62	0.42	1.16	5.50	2.81	1.68
	5%KMnO ₄	54.15	32.23	0.60	1.90	6.53	3.27	1.93
400	w/t HPT	68.46	28.28	0.41	0.45	1.45	0.97	1.22
	0%KMnO ₄	75.05	20.17	0.27	0.60	1.67	1.58	1.23
	1%KMnO ₄	71.68	21.29	0.30	0.66	2.43	2.54	1.40
	3%KMnO ₄	70.88	21.83	0.31	0.82	3.65	2.60	0.21
	5%KMnO ₄	59.83	26.44	0.44	1.21	7.74	3.86	0.60

All activated carbon samples were measured by scanning electron microscopy (SEM) that was used to study the surface characteristics, size and shape. The activated carbon sample of all conditions was shown in Figure 15.

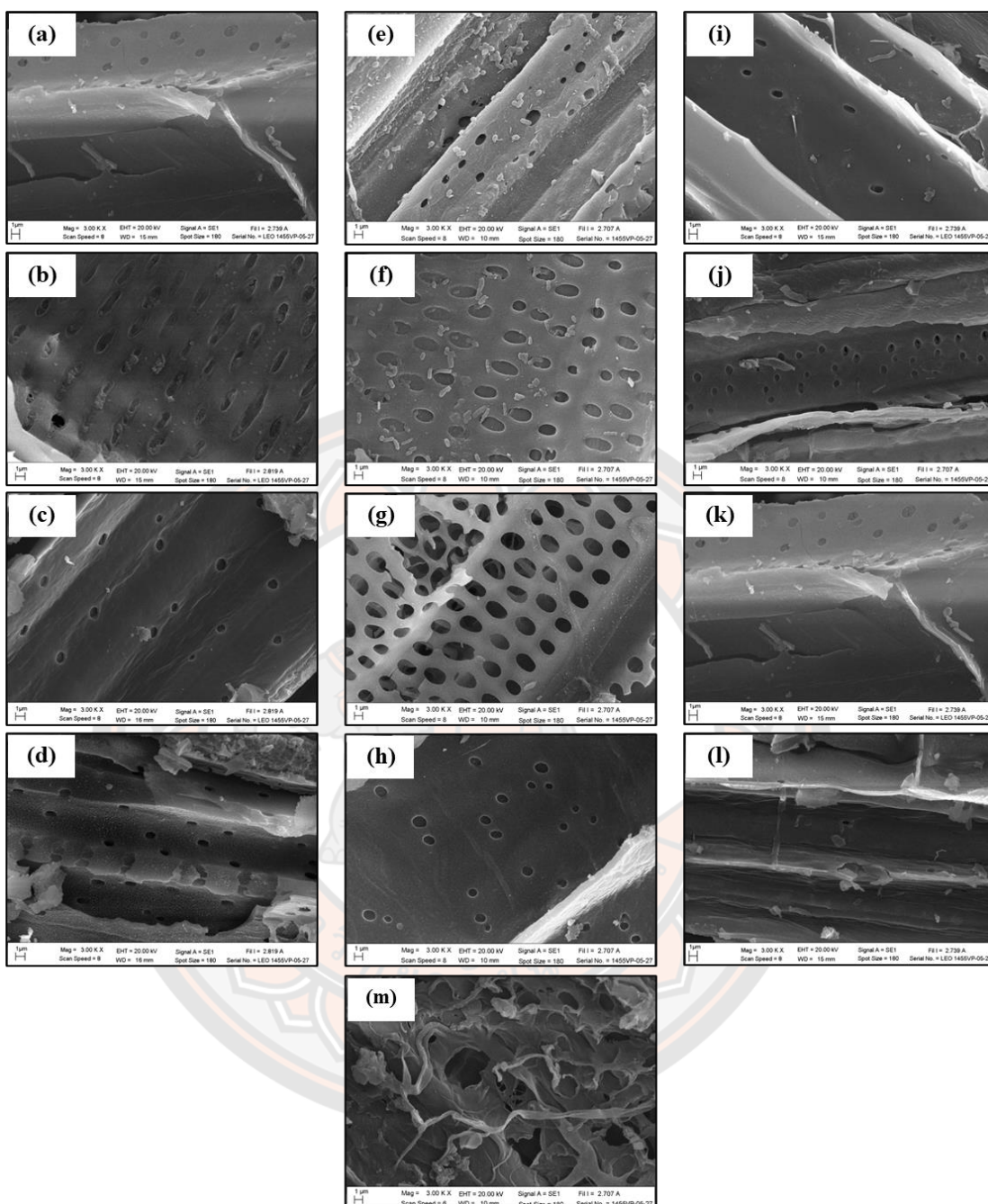


Figure 15 SEM images of the hydrochar activated carbon sample at 300°C (left) addition with 0%wt (a), 1%wt (b), 3%wt (c) and 5%wt (d) of KMnO_4 , 350°C (center) addition with 0%wt (e), 1%wt (f), 3%wt (g) and 5%wt (h) of KMnO_4 and 400°C (right) addition with 0%wt (i), 1%wt (j), 3%wt (k) and 5%wt (l) of KMnO_4 and activated carbon sample without hydrothermal pretreatment process at 350°C (m)

The without hydrothermal pretreatment process activated carbon sample at 350°C showed the cell walls and the interconnected porous lattice structures, as shown in Figure 16a. While the hydrochar activated carbon sample at the same activation temperature showed the smooth surface and the small size of particles, as shown in Figure 16b. It is because the cell walls were damaged during hydrothermal pretreatment process.

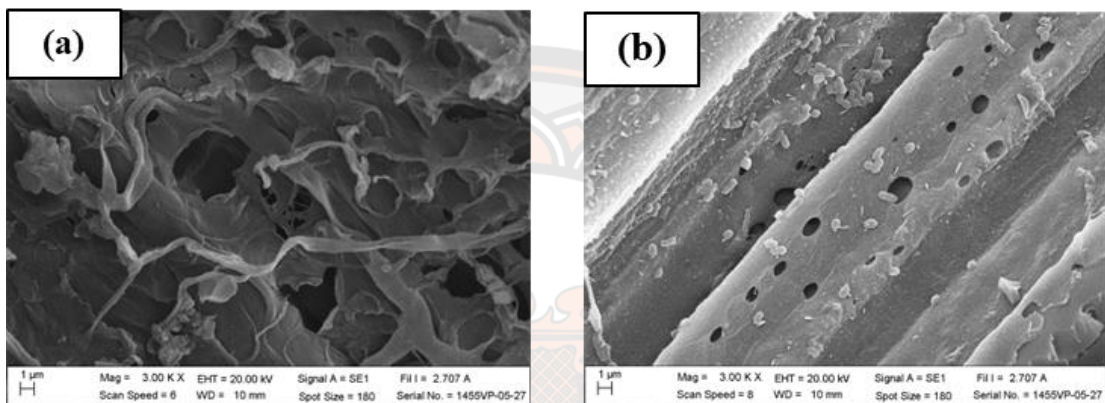


Figure 16 SEM images of the activated carbon without hydrothermal pretreatment process at 350°C (a) and hydrochar activated carbon sample at 350°C addition with 0%wt (b)

The effect of KMnO_4 concentration was considered, as shown in Figure 17. The hydrochar activated carbon sample showed the broken on the surface particles. In addition to the surface particles being more decomposed and almost all gone with the increasing of KMnO_4 . The surface of the hydrochar activated carbon sample has begun to break at 3% of KMnO_4 , as shown in Figure 17c. And the holes in the sugarcane leaf structure have begun to disappear, as shown in Figure 17d.

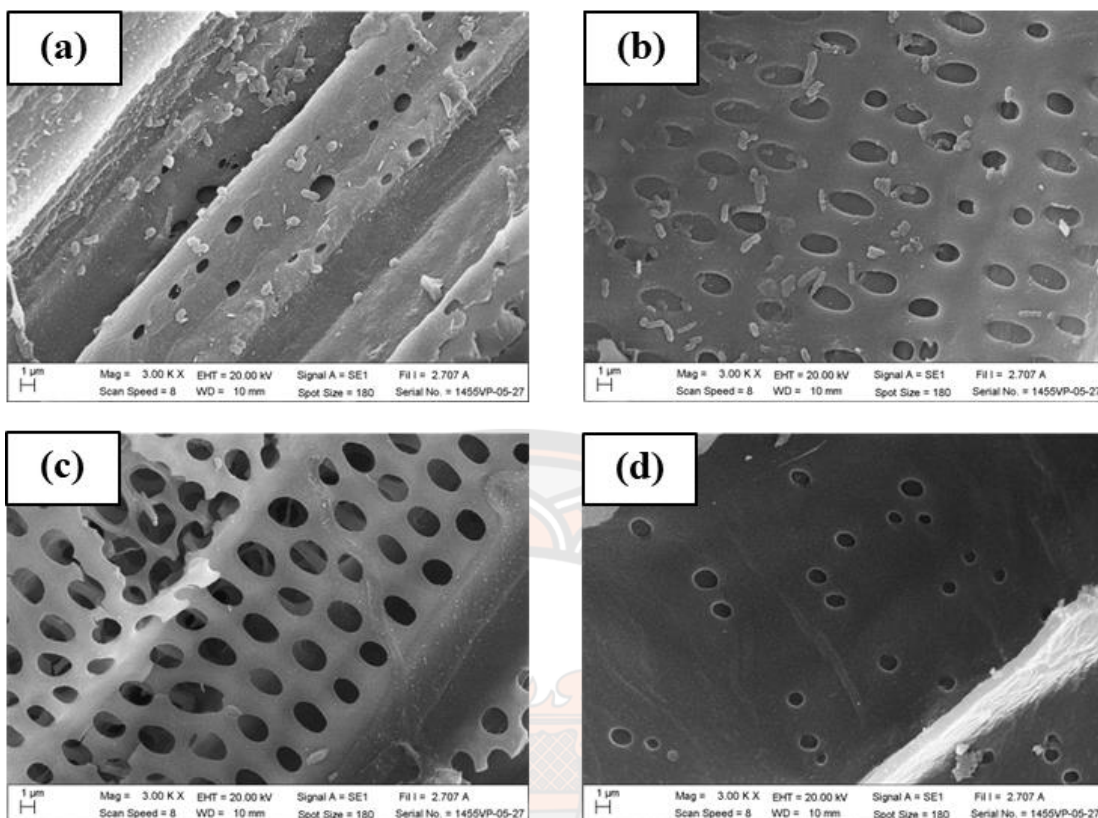


Figure 17 SEM images of the hydrochar activated carbon sample at 350°C addition with 0%wt (a), 1%wt (b), 3%wt (c) and 5%wt (d) of KMnO_4

After that, the considering the increasing of activation temperature by 300, 350 and 400°C, as shown in Figure 18. The surface of the hydrochar activated carbon sample showed the same result, which the cell walls were decomposed and formed particles, Particularly, the activation temperature of 400°C. The surface of the hydrochar activated carbon sample has been broken and showed a very cracked surface, as shown in Figure 18c and f. The effect of activation temperature was determined by comparing between 1%wt and 5%wt of KMnO_4 . The activated carbon sample surface showed the same tend when increasing the activation temperature.

These results could summarize the volatile organic compounds of sugarcane leaf were decomposed during the hydrothermal pretreatment process, the adding of KMnO_4 significant effect to decomposition of some organic matters, including the activation temperature.

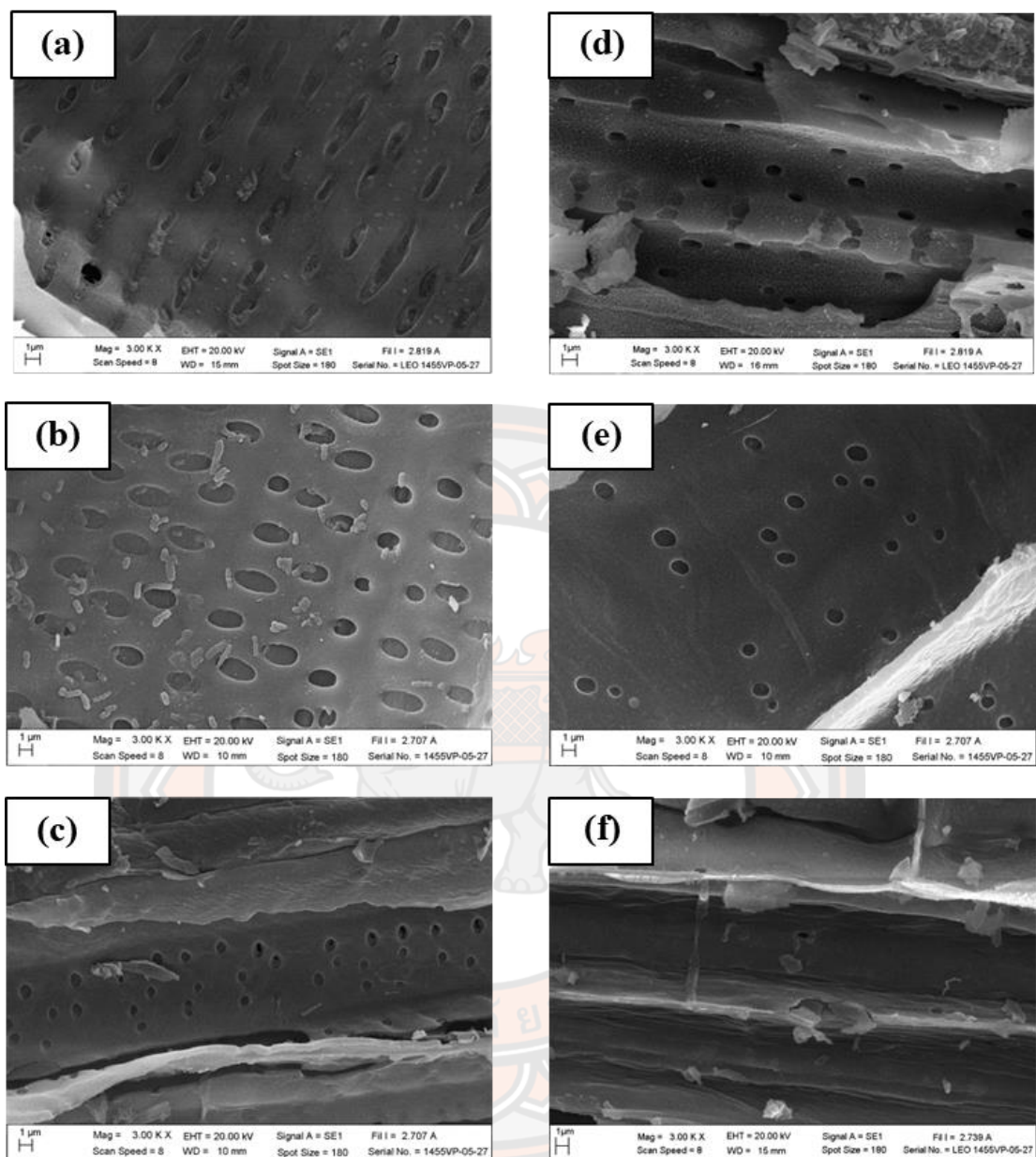


Figure 18 SEM images of the hydrochar activated carbon sample with addition 1%wt of KMnO_4 at 300°C (a), 350°C (b), 400°C (c) and 5%wt of KMnO_4 at 300°C (d), 350°C (e) and 400°C (f)

3. FTIR spectrum of activated carbon of sugarcane leaf activated carbon

The FTIR pattern was measured by Fourier-transform infrared spectroscopy, Spectrum GX, Perkin Elmer, USA. That was used to classify organic, inorganic and chemical bonds or functional groups of the obtained activated carbon sample. These results are shown in Figure 19. The activated carbon sample of all condition showed at 3200 to 3400 cm^{-1} of O-H stretching. After the increasing of the activation temperature of 300, 350 and 400°C, the FTIR pattern showed the disappearance of C-H stretching at 2900 cm^{-1} . It is because the hydrogen (H) content of activated carbon samples was decomposed with the higher activation temperature. It is because the hydrogen (H) content of activated carbon samples was decomposed with the higher activation temperature.

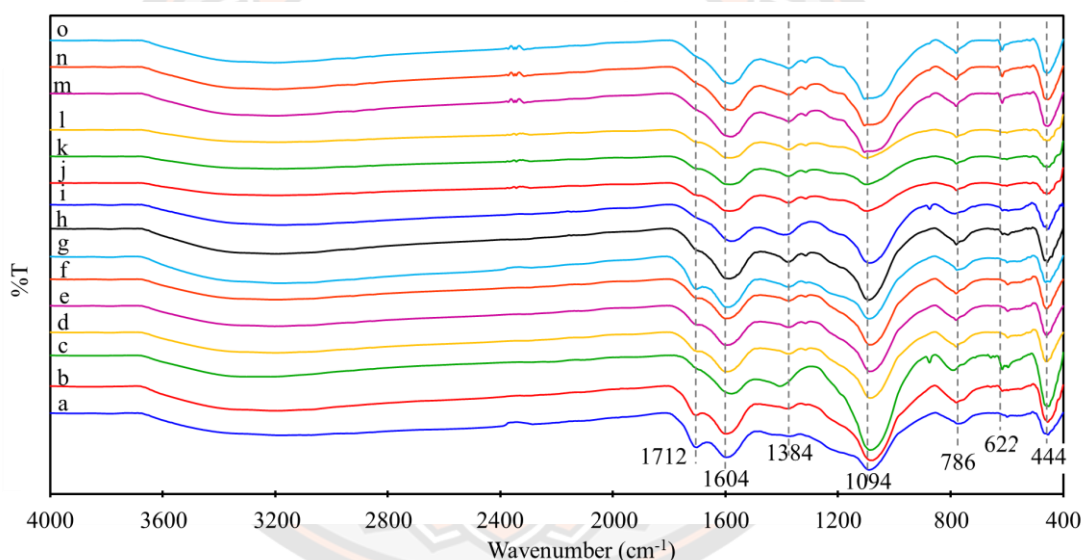


Figure 19 FTIR spectra of the without hydrothermal pretreatment process activated carbon sample 300°C (a), 350°C (b) and 400°C (c), the hydrochar activated carbon sample with 0%wt of KMnO_4 at 300°C (d), 350°C (e) and 400°C (f), 1%wt of KMnO_4 at 300°C (g), 350°C (h) and 400°C (i), 3%wt of KMnO_4 at 300°C (j), 350°C (k) and 400°C (l) and 5%wt of KMnO_4 at 300°C (m), 350°C (n) and 400°C (o)

The effect of hydrothermal pretreatment process on the functional groups of the activated carbon surface was considered, as shown in Figure 20. It was found that the C=O stretching of hemicellulose at 1712 cm^{-1} , -C-O-H at 1384 cm^{-1} [60] and C-H and/ or aryl C-O groups at 622 cm^{-1} [61]. The without hydrothermal pretreatment process activated carbon sample, as shown in Figure 20a–c, that showed the peak intensity are higher than the hydrochar activated carbon sample with 0%wt of KMnO_4 , as shown in Figure 20d–f. That showed the same results in all activation temperature. It is possible that the effect of hydrothermal pretreatment process causes the C=O group and other functional groups of hemicellulose were decomposition at 129°C and 15 Psi. In contrast, the peak intensity of aromatic C=C at 1604 cm^{-1} has opposite results. It has been suggested that the hydrothermal pretreatment process increased aromatics of the hydrochar activated carbon sample more than the without hydrothermal pretreatment process activated carbon sample with dehydration and decarboxylation reactions [61].

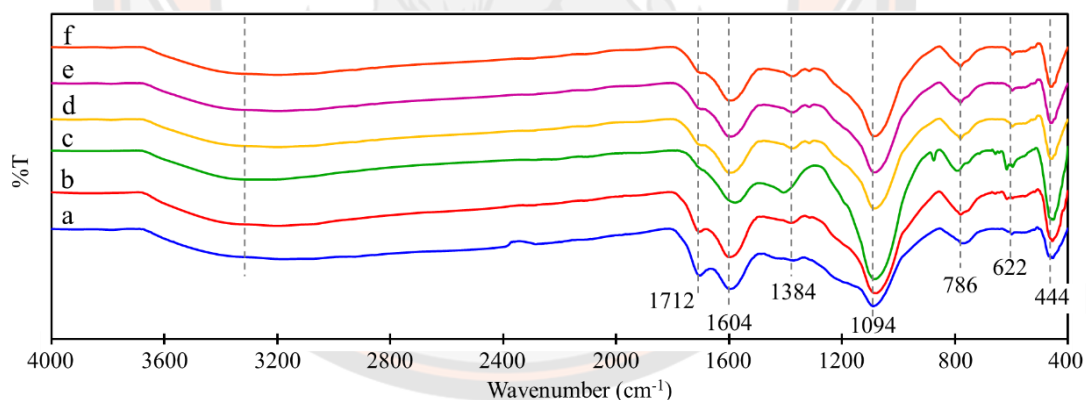


Figure 20 FTIR spectra of the without hydrothermal pretreatment process activated carbon sample at 300°C (a), 350°C (b) and 400°C (c) and the hydrochar activated carbon sample addition with 0%wt of KMnO_4 at 300°C (d), 350°C (e) and 400°C (f)

The increasing of KMnO_4 concentration decrease pattern showed the peaks intensity at 1712 cm^{-1} of C=O stretching, 1604 cm^{-1} of aromatic C=C and 622 cm^{-1} of C-H and/or aryl C-O groups tend to be decreased, as shown in Figure 21. While the

FTIR pattern showed the opposite tendency at 1094 cm^{-1} of C-O stretching, 786 cm^{-1} of Si-O bonds and 444 cm^{-1} of Mn-O bond for all the activation temperature. In this case, KMnO_4 have been more effect on surface functional decomposition of activated carbon sample which more decarboxylation and aliphatic degradation [61]. However, KMnO_4 increased partial oxidation that cause the increasing of C-O at 1094 cm^{-1} on the surface functional groups and residuals of Mn-OH at 622 cm^{-1} , O-Mn-O and Mn-O bond at 444 cm^{-1} on the surface of activated carbon sample [62].

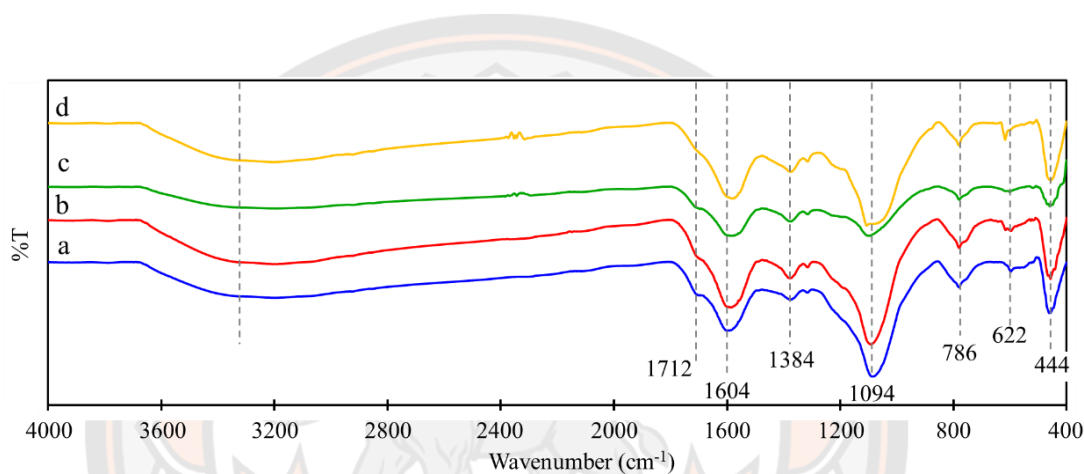


Figure 21 FTIR spectra of the hydrochar activated carbon sample at 350°C addition with 0%wt (a), 1%wt (b), 3%wt (c) and 5%wt (d) of KMnO_4

In considering the increasing of activation temperature by 300, 350 and 400°C , as shown in Figure 22. The activated carbon sample showed the increasing of peak intensity of aromatic C=C at 1604 cm^{-1} . In contrast, the spectra at 1712 cm^{-1} of C=O stretching, 1604 cm^{-1} of C=C stretching and 622 cm^{-1} of C-H and/or aryl C-O groups decreased. It was found that the aromatics increase with increasing the activation temperature with the condensation [61]. Moreover, the FTIR pattern at 1712 cm^{-1} of C=O stretching disappeared after the activation temperature at 350°C for 5% wt of KMnO_4 , as shown in Figure 22e.

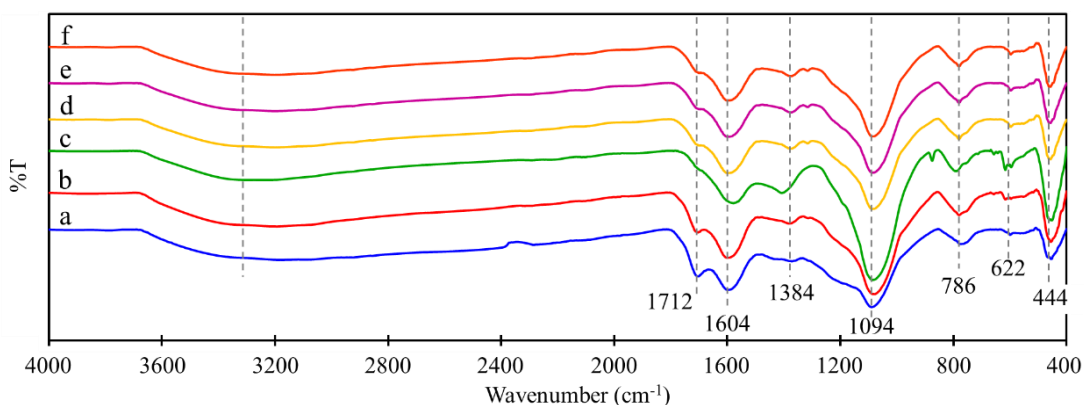


Figure 22 FTIR spectra of the hydrochar activated carbon sample with addition 1%wt of KMnO_4 at (a) 300°C, (b) 350°C and (c) 400°C, 5%wt of KMnO_4 at 300°C (d), 350°C (e) and 400°C (f)

The FTIR pattern at 1604 cm^{-1} and 1384 cm^{-1} were related to aromatic skeletal vibration in lignin [46]. In addition, the FTIR pattern at 1094 cm^{-1} was also related to the anomeric region of cellulose-like structures (C-O and C-O-C stretching) [15]. These results showed that some lignin and cellulose were loosed in the activated carbon samples. It is because the lignin and cellulose completely degradation at the activation temperatures up to 450°C [61]. And, there are the functional groups of Si-O-Si at 1094 cm^{-1} and 444 cm^{-1} , Si-O bonds at 786 cm^{-1} [63]. These functional groups were in good agreement with elementals content, as shown in Table 2. Therefore, the aromatic nature and presence of the functional groups of hydrochar activated carbon samples have shown good stability and adsorption efficiency.

4. XRD patterns of activated carbon of sugarcane leaf activated carbon

The X-ray diffraction patterns of activated carbon sample. The XRD patterns were measured by X-ray Diffraction, PW 3040/60 X'Pert PRO Console, Philips, Netherland. This method was used to analyze and identify the type of compound and crystal structure of the obtained activated carbon sample, as shown in Figure 23.

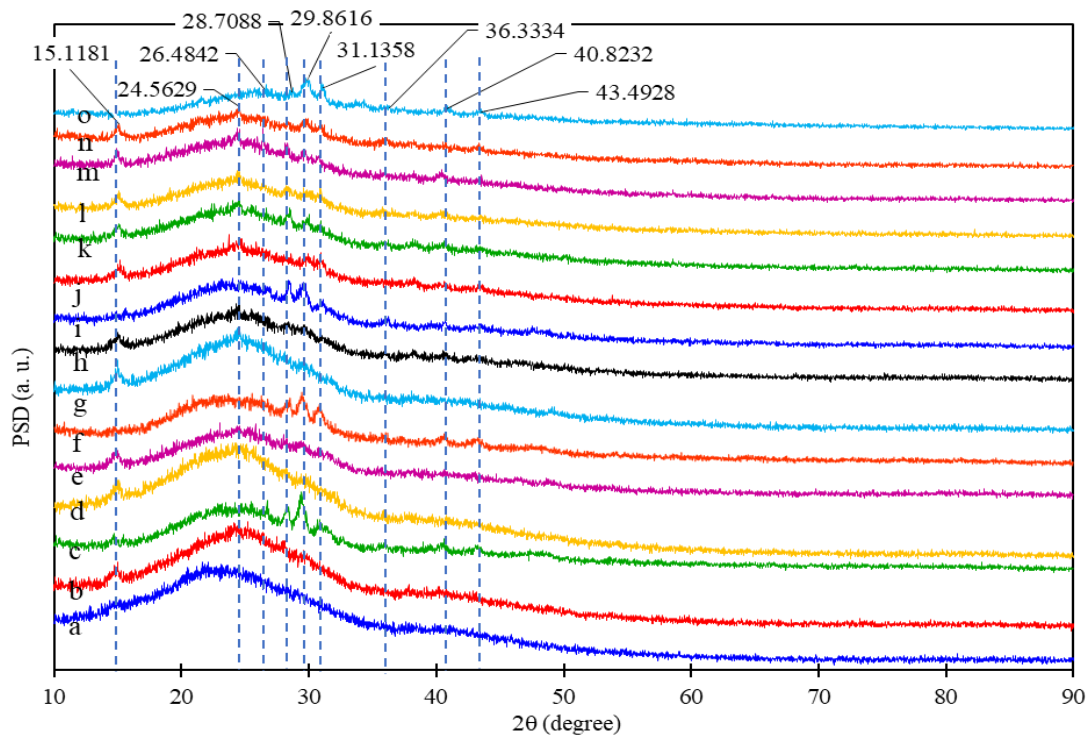


Figure 23 XRD patterns of the without hydrothermal pretreatment process activated carbon sample 300°C (a), 350°C (b) and 400°C (c), the hydrochar activated carbon sample with 0%wt of KMnO_4 at 300°C (d), 350°C (e) and 400°C (f), 1%wt of KMnO_4 at 300°C (g), 350°C (h) and 400°C (i), 3%wt of KMnO_4 at 300°C (j), 350°C (k) and 400°C (l) and 5%wt of KMnO_4 at 300°C (m), 350°C (n) and 400°C (o)

All activated carbon sample showed the bands with peak at about 26.5842° and 43.4928° of graphite flakes with the disordered layer (Yin et al., 2020). It was found that all activated carbon sample were converted to charcoal when the activation temperature was 300°C and above. Nevertheless, because the different activation temperatures cause some characteristics of these activated carbon samples to differ, as shown in Figure 24.

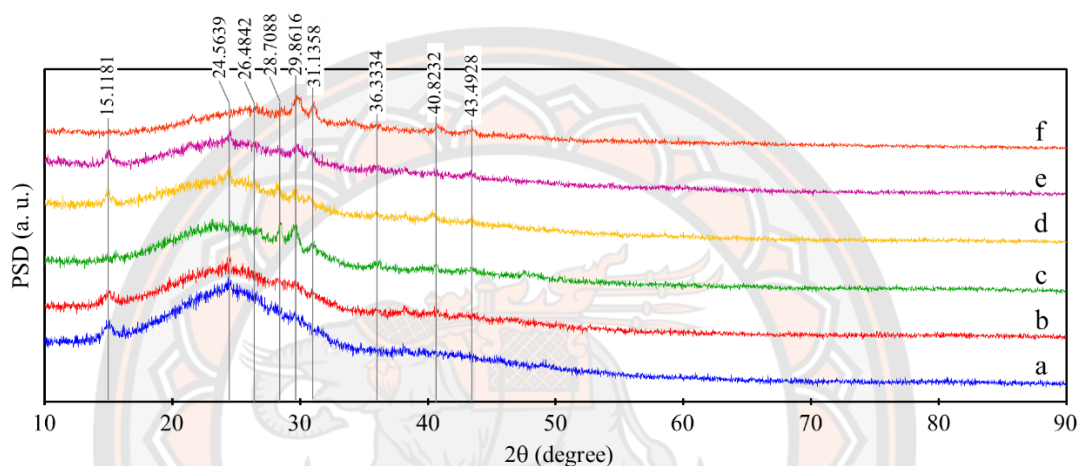


Figure 24 XRD patterns of the hydrochar activated carbon sample with addition 1%wt of KMnO_4 at (a) 300°C , (b) 350°C and (c) 400°C , 5%wt of KMnO_4 at 300°C (d), 350°C (e) and 400°C (f)

Not only did the activation temperature caused all activated carbon samples to be converted to charcoal, but also the concentration of KMnO_4 and hydrothermal pretreatment process. The without hydrothermal pretreatment process activated carbon sample showed in Figure 25, the peaks positions of these samples occurred a little peak at $\theta = 15.1181^\circ$ of cellulose for all activation temperature. It was found that the cellulose remained in the without hydrothermal pretreatment process activated carbon sample. However, the increasing activation temperature made this peak decrease. It is because cellulose was decomposed with the temperature in the range of 230 to 310°C . Hemicellulose was supposed to completely decomposition, because it was decomposed with temperature in the range of 180 to 240°C . Whereas lignin of

the without hydrothermal pretreatment process activated carbon sample remained in amorphous structure. Because lignin was decomposed over a range of activation temperature 280 to 500°C, so its disappeared in XRD pattern [64]. Moreover, the activation temperature at 400°C showed obviously peaks positions of SiO₂ at 24.5629°, 26.4842°, 28.7088°, 29.8616° and 43.4928° [65], CaO at 26.4842°, 28.7088°, 31.1358° and 36.3334°, and K₂O at 26.4842°, 28.7088° and 40.8232° [66]. It is because the volatile matter of activated carbon sample was decomposed. These elements were derived from the sugarcane leaf that was used as precursor material. In the same way, the hydrochar activated carbon sample with 0% wt of KMnO₄ showed the same position of peaks, as shown in Figure 25d-f. The XRD pattern of the hydrochar activated carbon sample with 0% wt of KMnO₄ at 400°C (Figure 25f) disappeared of cellulose at 15.1181°. It is because the cellulose structure was broken during the hydrothermal pretreatment process.

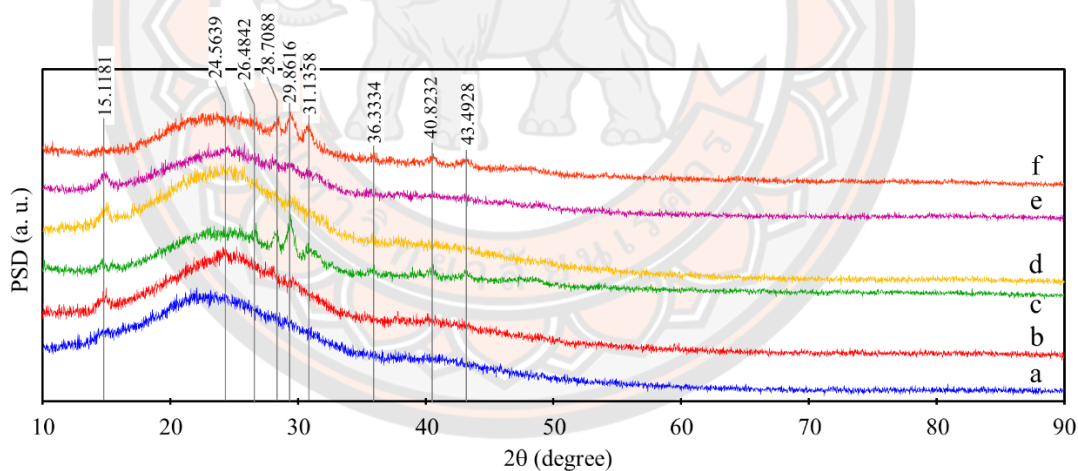


Figure 25 XRD patterns of the without hydrothermal pretreatment process activated carbon sample at 300°C (a), 350°C (b) and 400°C (c) and the hydrochar activated carbon sample addition with 0%wt of KMnO₄ at 300°C (d), 350°C (e) and 400°C (f)

When considering, the hydrochar activated carbon sample with 1 to 3% wt of KMnO_4 exhibited the same effect as the hydrochar activated carbon sample with 0% wt of KMnO_4 , as shown in Figure 26. It was suggested that the addition of KMnO_4 had no effect on cellulose decomposition in the sugarcane leaf.

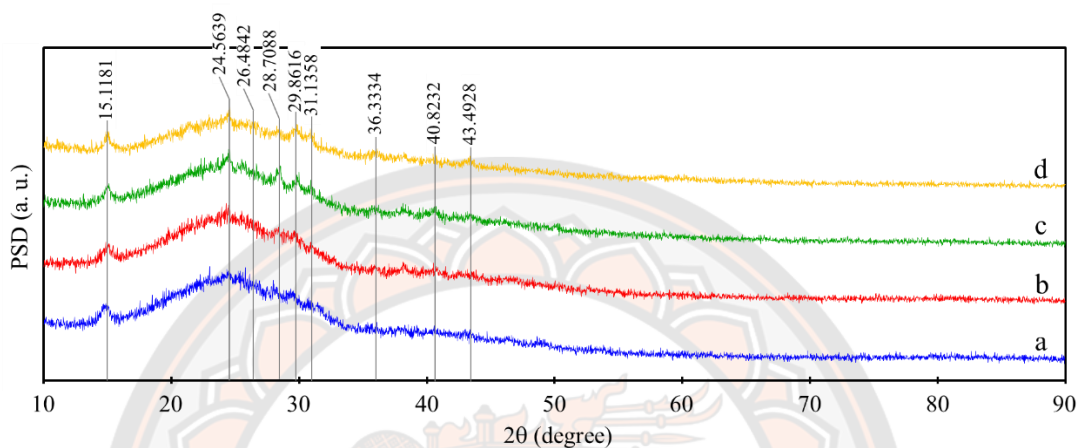


Figure 26 XRD patterns of the hydrochar activated carbon sample at 350°C addition with 0%wt (a), 1%wt (b), 3%wt (c) and 5%wt (d) of KMnO_4

5. Surface area and porous structure of sugarcane leaf activated carbon

The surface area and micropore volume were measured by Surface area and porosity analyzer, BET, Micromeritics TriStar II, USA. That was used to analyze surface area characteristics, for example, pore size diameter, surface area, pore volume of the obtained activated carbon sample. These results were shown in Table 3 and Figure 27. The surface area of activated carbon sample increased with increasing of the activation temperature. The surface areas and micropore volumes of the hydrochar activated carbon sample with 0%wt of KMnO_4 showed higher than the without hydrothermal treatment process activated carbon sample. This is because some of hemicellulose and cellulose were decomposed during the hydrothermal pretreatment process, and the porous structures were generated on the surface of activated carbon sample [15]. Moreover, the porous structure of activated carbon samples could be increased with the increase of the activation temperature. This is because increasing the activation temperature led the cellulose and lignin of precursor

material to break. The effect of KMnO_4 was considered. It was found that the hydrochar activated carbon sample with addition of KMnO_4 showed an increase of the surface area and micropore volume more than the hydrochar activated carbon samples with 0%wt of KMnO_4 in all activation temperature. Comparison of the increasing of KMnO_4 concentration in the same activation temperature. It was found that KMnO_4 could be oxidized matters in precursor material. However, the hydrochar activated carbon sample with 5%wt of KMnO_4 showed decrease of surface area and micropore volume below the hydrochar activated carbon sample with 3%wt of KMnO_4 at all activation temperature. This is because the excessive amount of KMnO_4 caused their cover on the surface area and some of MnO_2 blocked the pore entrance of activated carbon sample.

Table 3 Surface area and porosity of sugarcane leaf activated carbon by BET

Temp. (°C)	SLAC Sample	BET surface area (m ² /g)	Surface area of pores between 17Å and 3000Å (m ² /g)	Micropore volume (cm ³ /g)	Volume of pores between 17Å and 3000Å (cm ³ /g)
300	w/t HPT	0.9289	0.1997	0.000698	0.000089
	0% KMnO_4	2.9560	0.9345	0.00624	0.000921
	1% KMnO_4	5.9670	3.2251	0.00390	0.004285
	3% KMnO_4	13.5882	9.2956	0.00670	0.013424
	5% KMnO_4	7.5572	5.8829	0.00261	0.006508
350	w/t HPT	10.8815	8.8915	0.002647	0.003702
	0% KMnO_4	12.1574	11.7152	0.007006	0.011131
	1% KMnO_4	15.1145	13.6461	0.002525	0.071490
	3% KMnO_4	30.5653	26.0662	0.00423	0.2744
	5% KMnO_4	24.8480	19.5535	0.001575	0.16119
400	w/t HPT	23.7722	18.1505	0.002759	0.18773
	0% KMnO_4	24.9388	21.0224	0.005924	0.13548
	1% KMnO_4	33.3101	31.7505	0.009794	0.14507
	3% KMnO_4	45.0364	42.4550	0.002290	0.11473
	5% KMnO_4	34.7107	32.7012	0.002200	0.022678

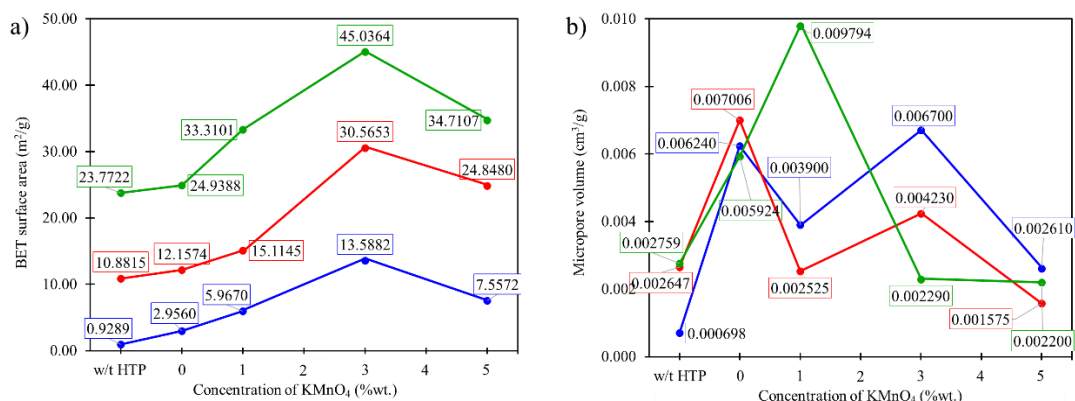


Figure 27 The surface area (a) and micropore volume (b) of activated carbon sample

6. Zeta potential of the hydrochar activated carbon sample with addition 0% wt and 1% wt of KMnO₄ at 350°C

The zeta potential of the hydrochar activated carbon sample was measured by nanoparticle sizing and zeta potential analyzer (ZS, Malvern zeta sizer nano -ZS, UK). It was used to characterize particle size and potential on the surface of particles of the obtained activated carbon sample in the solution. Zeta potential was one of the parameter that showed the association between the adsorbate and the adsorbent material, which gave a preliminary suppose of the adsorption capacity of the adsorbate on adsorbent materials [67]. Figure 28 showed the pH dependence of the zeta potential value for the hydrochar activated carbon sample with addition 0% wt and 1% wt of KMnO₄ at 350°C. It was found that the zeta potential values of both hydrochar activated carbon samples showed negative values all over the pH in the range of 3 to 11. These results exhibited that it could adsorb the positively charged adsorbate with electrostatic force [68]. It is because the electrons π - π interactions from aromatic rings on the surface of activated carbon sample [69]. Moreover, the hydrochar activated carbon sample with the addition 1% wt of KMnO₄ showed the lower zeta potential value, as shown in Figure 28 (red). It is because the aromatic ring in the surface of hydrochar activated carbon sample was being oxidized by KMnO₄. It showed the aromatic ring was damaged, including some of C-O-H surface functional groups of hemicellulose was oxidized to carbonyl group. This results in a large

amount of electric charge accumulation on the surface of the hydrochar activated carbon sample with addition of KMnO_4 and the zeta potential values decreased [70]. As considering more details, the zeta potential value of the hydrochar activated carbon sample decreased with the pH of the solution increased over the range of 3 to 7 and then maximum value at pH 9. After pH 9, the zeta potential value of hydrochar activated carbon sample decreased again to pH 11. It is because again bound by π - π interactions of second layer after the formation of the first layer on the surface of the activated carbon sample [69].

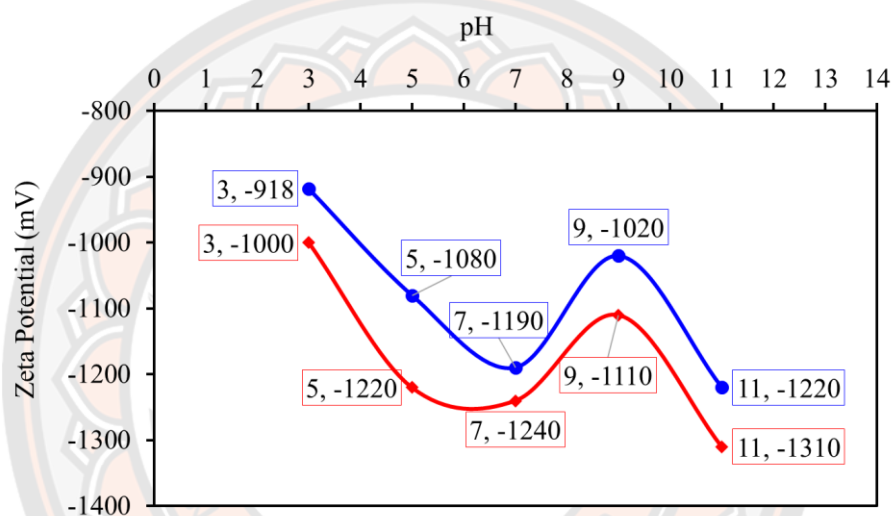


Figure 28 Zeta Potential of the hydrochar activated carbon sample at 350°C with addition 0%wt (blue) and 1%wt (red) of KMnO_4

CHAPTER IV

THE USING OF SUGARCANE LEAF ACTIVATED CARBON FOR AQUATIC TREATMENT

Equipment

1. pH meter (Mettler Toledo, USA)
2. Analytical balance (Sartorius, Germany)
3. Portable turbidimeter (Jenway 6035, UK)
4. Spectrophotometer (double beam, Jusco V650, Germany)

Apparatus

1. Glass biological oxygen demand bottle or (BOD) bottle
2. Filter paper (Whatman No.24)
3. Cuvette (10 millimeter)

Materials and Reagents

1. Sugarcane leaf activated carbon (Kamphaengphet, Thailand)
2. Conc. Hydrochloric acid (Conc. HCl), 37% wt, (A.R. grade, RCI labscan)
3. Conc. Sulfuric acid (Conc. H₂SO₄), 98% (A.R. grade, Loba Chemie™)
4. Ascorbic acid (C₆H₈O₆) (ACS reagent grade, Merck)
5. Ammonium molybdate tetrahydrate ((NH₄)₆Mo₇O₂₄·4H₂O) (ACS reagent grade, Sigma-Aldrich)
6. Potassium antimonyl tartrate (K(SbO)C₄H₄O₆·¹/₂H₂O) (A.R. grade, Loba Chemie™)
7. Ammonium chloride (NH₄Cl) (A.R. grade, Loba Chemie™)
8. Manganese (II) sulfate tetrahydrate (MnSO₄·4H₂O) (A.R. grade, Merck)
9. Potassium iodate (KIO₃) (ACS reagent grade, Sigma-Aldrich)
10. Potassium iodide (KI) (A.R. grade, Carlo Erba™)
11. Sodium thiosulphate pentahydrate (Na₂S₂O₃·5H₂O) (ACS reagent grade, Sigma-Aldrich)
12. Sodium hydroxide (NaOH) (A.R. grade, Sigma-Aldrich)

13. Sodium Iodide (NaI) (ACS reagent grade, Merck)
14. Sodium azide (NaN₃) (ACS Reagent grade, Sigma-Aldrich)
15. Sodium nitroprusside (C₅H₄FeN₆Na₂O₃) (A.R. grade, Sigma-Aldrich)
16. Sodium hypochlorite (NaClO) (A.R. grade, Carlo Erba™)
17. Sodium oxalate (Na₂C₂O₄) (A.R. grade, Carlo Erba™)
18. Trisodium citrate dihydrate (C₆H₅Na₃O₇·2H₂O) (Certified A.R. for Analysis, Fisher Chemical™)
19. Phenol (C₆H₅OH) (A.R. grade, Loba Chemie™)
20. Sulfanilamide (C₆H₈N₂O₂S) (A.R. grade, DC Finechem™)
21. N-(1-Naphthyl)-ethylenediamine dihydrochloride (C₁₀H₇NHCH₂CH₂NH₂·2HCl) (A.R. grade, Sigma-Aldrich)
22. Potato starch (Food grade, New Grade)

Experimental

1. The construction of an aquaponics system

The four fishponds were built by using interlocking bricks (10 x 10 x 20 cm) with width, length and height of 2 m, 2 m and 70 cm, respectively (Figure 29). The PVC tube and plastic sheet were used to hydroponic system and cover the bottom and side, respectively. The water storage of each pond depth 50 cm or volume 2 cubic meters. The catfish was used in aquaculture system. Which was about 40 to 45 days old and had a size in the range of 5 to 7 cm (50 fish per cubic meter). And the red oak lettuce was used in hydroponic system, that was about 15 to 20 days old (90 plant). In a system, the growth of catfish and red oak lettuce were observed for analyzing quality of water.

Pond No.1: Aquaculture system (Figure 29a)

Pond No.2: Hydroponic system (Figure 29b)

Pond No.3: Aquaponics system (Figure 29c)

Pond No.4: Aquaponics system with activated carbon powders filter (Figure 29d)

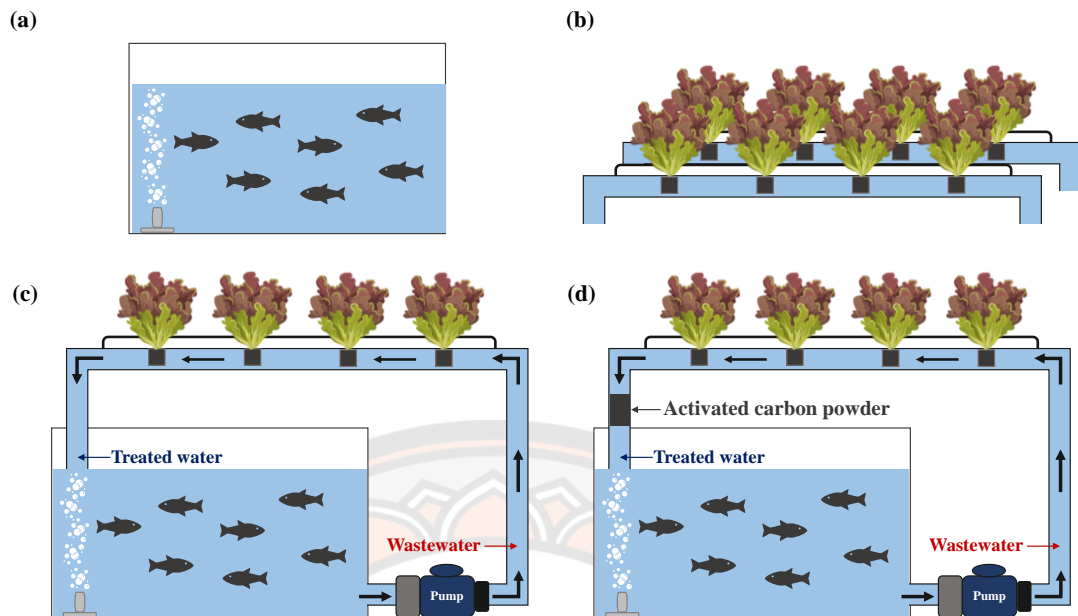


Figure 29 aquaculture system (a), hydroponic system (b), aquaponics system (c) and aquaponics system with activated carbon powders filter (d)

In pond No.4, 3 kg of hydrochar activated carbon powders with 3%wt of KMnO_4 were used as a filter in the aquaponics system. That was placed between the aquaculture system and the hydroponics system (Figure 29d). At 8 a.m. every morning (once a day), the catfish were fed that amounted to 5% total weight. Before feeding, 10% of the catfish were randomly selected for weighing. Every 7 days for 4 weeks the growth of catfish and red oak lettuce was observed by randomly selecting 10% of sample set by recording the weight for catfish (g), length of the root (cm), height of stem (cm), number of leaves to stem, weight of dried root (g/stem), weight of dried stem (g/stem), weight of dried leaf (g) and diameter of trunk (cm). Including the measurement of dissolved oxygen (DO), pH and turbidity. While the concentration of ammonia (NH_4), nitrite (NO_2^-), and orthophosphate (PO_4^{3-}) were measured at week 4.

2. Water analysis

After the use of water in an aquaculture system, hydroponic system or aquaponics system, the quality of water would be changed. It was maybe noticeable to the naked eye – it is called “physical principles”. However, it cannot be indicative of the actual water quality. Therefore, the measure of water quality was based on chemical principles to determine several parameters of water. That cannot be known by physical principles.

2.1 Dissolved oxygen (DO) by Winkler titration method

Reagent preparation

a) Manganese (II) sulfate tetrahydrate ($\text{MnSO}_4 \cdot 4\text{H}_2\text{O}$) was dissolved 480.0 g with 1000 mL distilled water in a volumetric flask. After complete dissolution, the solution was stored into a plastic bottle.

b) Sodium azide (NaN_3) was dissolved 10.0 g in distilled water 500.0 mL. After that, sodium hydroxide (NaOH) and sodium iodide (NaI) were added 500.0 and 135.0 g into the above solution. After complete mixing, the distilled water was made up to the final volume of 1000.0 mL in a volumetric flask. And the solution was storage into a glass bottle.

c) Concentrated Sulfuric acid (Conc. H_2SO_4) was diluted to 0.10 mol/L.

d) The soluble starch was used as indicator in titration method. The potato starch dissolved 2.0 g in distilled water 100.0 mL. After complete dissolution, the soluble starch was boiled for 5 minutes and constantly stirred in the hot plate and put aside to cool.

e) Sodium thiosulphate pentahydrate ($\text{Na}_2\text{S}_2\text{O}_3 \cdot 5\text{H}_2\text{O}$) was dissolved 3.5 g in boiling distilled water 500.0 mL and then set aside to cool. (The sodium thiosulphate solution must be standardized with a primary standard - potassium iodate (KIO_3) to find the exact concentration.

Titration procedures

a) The water sample from fishpond was collected below the surface of the water by using glass stoppered BOD bottle to avoid bubbles into the sample

b) The solution of $\text{MnSO}_4 \cdot 4\text{H}_2\text{O}$ was added 1.0 mL by pipette. This step must be made below the surface of water sample and slowly to avoid bubbles was entered

into the sample. And alkaline-iodide-azide solution was added 1.0 mL in the same manner and then set aside to precipitate. (The solution at this stage could be stored in a dark and cool place, but not more than 6 hours)

c) Conc. H_2SO_4 was added 2.0 mL into the solution above the step. Then stoppered and shake several times to dissolve the precipitate. (The solution at this stage could be stored for up to 8 hours in a dark and cool place)

d) The solution from above the step was placed 201.0 mL to the Erlenmeyer flask and titrated with the solution of $\text{Na}_2\text{S}_2\text{O}_3$ until the color of solution turns to light yellow. After that, the starch indicator solution was added to the flask. The color of the sample turns blue. Continue to slowly titrate by dropping the solution of $\text{Na}_2\text{S}_2\text{O}_3$ just until the solution becomes colorless. The volume of $\text{Na}_2\text{S}_2\text{O}_3$ was recorded and repeated step a) to step d) just until the volume of $\text{Na}_2\text{S}_2\text{O}_3$ was recorded 3 times that difference 0.05 mL to each other.

Calculation

$$\text{DO} \left(\frac{\text{mg}}{\text{L}} \right) = \frac{(\text{Normality of } \text{Na}_2\text{S}_2\text{O}_3)(\text{mL of } \text{Na}_2\text{S}_2\text{O}_3)}{\text{mL of water sample}} \times 8 \times 1000 \quad \text{Equation 8}$$

2.2 Ammonium ion (NH_3^+) by indophenol reaction

Reagent preparation

a) Phenol ($\text{C}_6\text{H}_6\text{OH}$) was dissolved 5.0 g in ethyl alcohol ($\text{C}_2\text{H}_5\text{OH}$) 50.0 mL. (The solution can be stored for a week)

b) Sodium nitroprusside ($\text{C}_5\text{H}_4\text{FeN}_6\text{Na}_2\text{O}_3$) was dissolved 0.5 g in deionized water 100.0 mL. (The solution can be stored for up to a month in an amber glass bottle)

c) Trisodium citrate dihydrate ($\text{C}_6\text{H}_5\text{Na}_3\text{O}_7 \cdot 2\text{H}_2\text{O}$) and sodium hydroxide (NaOH) were dissolved 50.0 and 1.0 g in deionized water 50.0 mL, respectively. After complete dissolution, the deionized water was made up to the final volume of 100.0 mL in a volumetric flask.

d) Sodium hypochlorite (NaClO) was titrated with the solution of $\text{Na}_2\text{S}_2\text{O}_3$ to check the content of ClO^- in the solution. ($\text{Na}_2\text{S}_2\text{O}_3 \cdot 5\text{H}_2\text{O}$ was dissolved 12.5 g in deionized water 500.0 mL by using a volumetric flask)

e) Oxidizing reagent was mixed between trisodium citrate solution and sodium hypochlorite in the ratio of 4:1 (trisodium citrate solution: sodium hypochlorite). This solution should be prepared every day.

Procedures

a) The water sample from fishpond was filtered and placed 25.0 mL into an Erlenmeyer flask.

b) The solution of phenol was added 1.0 mL to the above Erlenmeyer flask and then shake well.

c) The solution of sodium nitroprusside was added 1.0 mL to the above Erlenmeyer flask and then shake well.

d) The oxidizing reagent was added 2.5 mL to the above Erlenmeyer flask and then shake well. The sample in the Erlenmeyer flask was closed by parafilm and chilled in room temperature and dark place. Continue determining after 1 hour, but not more than 24 hours. (The color of the solution was stable for 24 hours)

e) The sample was measured at 640 nm with 10 mm length of cuvette.

f) The results were calculated percentage of relative removal rate by equation 9.

Calculation

$$\% \text{relative removal rate} = 100 \times \frac{(C_0 - C_t)}{C_0} \quad \text{Equation 9}$$

2.3 Nitrite ion (NO_2^-) by diazo-azo colorimetric method

Reagent preparation

a) Conc. HCl was added 25.0 mL to the distilled water 150.0 mL Sulfanilamide ($\text{C}_6\text{H}_8\text{N}_2\text{O}_2\text{S}$) was dissolved 2.5 g to this solution in a volumetric flask. After complete dissolution, the distilled water was made up to the final volume of 250.0 mL in a volumetric flask.

b) N-(1-Naphthyl)-ethylenediamine dihydrochloride was dissolved 0.25 g to the distilled water 250.0 mL in a volumetric flask. It was called "NED dihydrochloride". The solution can be stored until the color of solution turns brown in amber glass bottle.

c) Sodium oxalate ($\text{Na}_2\text{C}_2\text{O}_4$) was dissolved 3.35 g to the distilled water in a volumetric flask 1000.0 mL. The distilled water was added to make up the final volume.

d) Potassium permanganate (KMnO_4) was dissolved 8.0 g to the distilled water. This solution must be stored for a week in amber glass. Before standardized by sodium oxalate ($\text{Na}_2\text{C}_2\text{O}_4$) with sulfuric acid (H_2SO_4) [71, 72]

d) Stock Nitrite solution was prepared following the STANDARD METHODS FOR THE EXAMINATION OF WATER AND WASTEWATER [72]

Procedures

a) The sample of water that was collected. The pH of the water was adjusted to 5 to 9 with 0.01 mol/L HCl and NaOH.

b) The water sample was added 50.0 mL into the Erlenmeyer flask.

c) The sulfanilamide solution was added 1.0 mL into the Erlenmeyer flask and then shake well.

d) NED dihydrochloride solution was added 1.0 mL into the Erlenmeyer flask and then shake well. This solution can be stable after 10 minutes, but not more than 2 hours.

e) The results were calculated percentage of relative removal rate by equation 9.

2.4 Orthophosphate ion (PO_4^{3-}) by ascorbic acid method

Reagent preparation

a) Conc. H_2SO_4 was diluted to 5N. and then was added 70.0 mL into distilled water 500 mL.

b) Potassium antimonyl tartrate ($\text{K}(\text{SbO})\text{C}_4\text{H}_4\text{O}_6 \cdot \frac{1}{2}\text{H}_2\text{O}$) was dissolved 1.3715 g with distilled water 500.0 mL in a volumetric flask. The solution was stored in a glass bottle with a lid.

c) Ammonium molybdate tetrahydrate ($(\text{NH}_4)_6\text{Mo}_7\text{O}_{24} \cdot 4\text{H}_2\text{O}$) was dissolved 20.0 g with distilled water 500.0 mL in a volumetric flask. The solution was stored in a glass bottle with a lid.

d) Ascorbic acid was dissolved 1.76 g with distilled water 100.0 mL in a volumetric flask. The solution was stable for a week at 4°C in a glass bottle with a lid.

e) The solution of H₂SO₄, potassium antimonyl tartrate, ammonium molybdate tetrahydrate and ascorbic acid was mixed 50.0, 5.0, 15.0 and 30.0 mL, respectively. It was called "combined reagent". The combined reagent was mixed at room temperature. After mixed if the reagent had turbidity form. The reagent could shake and stand for a few minutes until turbidity disappears. This reagent was stable for 4 hours.

f) Anhydrous potassium dihydrogen phosphate (anhydrous KH₂PO₄) was used as stock phosphate solution. It was dissolved 0.2195 g with distilled water 1000.0 mL in a volumetric flask. The concentration of this solution was 50 mg P/L.

g) Phenolphthalein was used as an indicator. It was dissolved 5.0 g in a volumetric flask with 95% ethyl alcohol 500.0 mL and distilled water 500.0 mL.

procedures

a) The sample was added 50.0 mL in an Erlenmeyer flask by pipette.

b) The phenolphthalein indicator was added 0.05 mL or a drop. If the sample color was red. The 5N Conc. H₂SO₄ solution was dropped until the red color disappeared.

c) The combined reagent was added 8.0 mL and then mixed. After at least 10 minutes but no more than 30 minutes.

d) The solution was measured absorbance at 880 nm. The reagent blank was used as reference solution.

e) The preparation of curve was prepared by diluting the stock phosphate solution. The stock solution was diluted to 0.1, 0.2, 0.6, 0.8 and 1.0 mg/L (ppm). It was measured absorbance at 880 nm. See calibration graph at appendix CHAPTER IV.

f) The results were calculated percentage of relative removal rate by equation 9 and mg of P/L by equation 10.

Calculation

$$\text{mg P/L} = \frac{(\text{mg P}) (1000)}{\text{mL of sample}} \quad \text{Equation 10}$$

2.5 Turbidity and pH

The water samples were collected every 7 days from each pond within 20 cm of the water surface at about 09:00 AM by plastic bottles. The pH (Mettler Toledo), turbidity by turbidimeter (Jenway 6035) of water were measured.

4. The growth of catfish and red oak lettuce

The catfish were fed at a rate of 5% by weight at 8:00 AM every day. Analysis of 4 water quality systems by observation the growth of catfish (weight of the body) and the red oak lettuce (length of the root, height of stem, number of leaves, weight of dried root, weight of dried stem, weight of dried leaf and diameter of trunk) by randomly 10% of the sample every 7 days for 4 weeks.

Results and Discussion

1. The pH values of water

Pond No.1 or aquaculture system (only the catfish) showed weak acidity of water pH, as shown in Figure 30a. Pond No.2 or hydroponic system (only red oak lettuce) showed weak base of water pH, as shown in Figure 30b. Pond No.3 or aquaculture system was connected to hydroponic system, it was called “aquaponics system”, as shown in Figure 30c. The pH of water still showed a weak base in the first week and changed to weak acidity in the second week to fourth week. However, pond No.4 or aquaponics system with activated carbon powders filter showed a weak base for all 4 weeks, as shown in Figure 30d. It was found that respiration and photosynthesis process results to the changing in CO₂ and O₂. Considering pond No.1, the respiration of catfish made the CO₂ that could be dissolved in water and changed into carbonic acid (H₂CO₃), as shown in equation 11.



However, the photosynthesis process of phytoplankton or microalgae decreased a protons (H⁺) and CO₂ contents and increased the O₂ content under light conditions, resulting in pH of water slowly increased [73]. But it was not enough to remove the acidity from the water in aquaculture alone. Therefore, the pH of water increased to a

weak base in aquaponics system (pond No.3). Which contributed to the absorption of nutrients, metal ions and other salts and photosynthetic activities (H^+ uptake) by plant root [74]. Moreover, the pH of water increased when the addition of activated carbon powders filter (pond No.4). This is because activated carbon powders had negatively charged surface, that could be adsorbed positively charged protons. Therefore, all ponds showed water pH in the optimal range for the growth of phytoplankton [75].

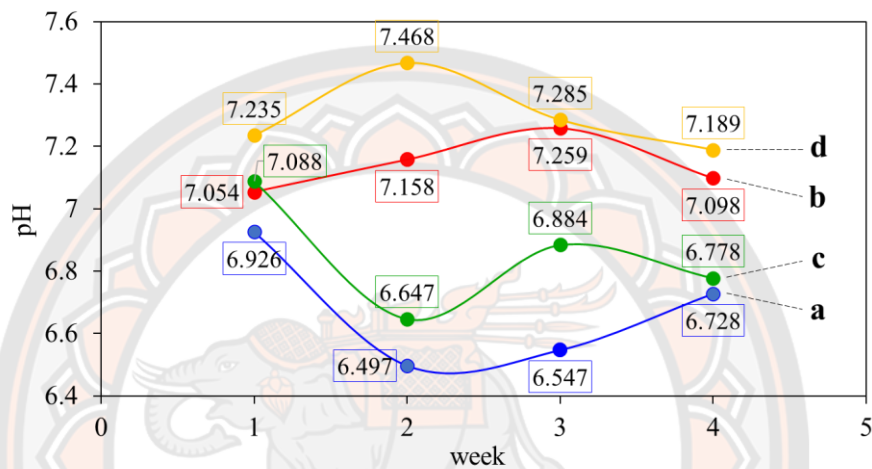


Figure 30 pH values of water of pond No.1 (a), pond No.2 (b), pond No.3 (c) and pond No.4 (d)

2. The dissolved oxygen (DO) values of water

Dissolved oxygen (DO) was an important substrate that was contained in the water. That was a measure of oxygen (O_2) content in the form of gas. It was very significant to many aquatic lives in water able to live. These aquatic lives used O_2 to breathe. The O_2 content in the form of gas was a parameter of the water quality. If the O_2 content was very low or less than 3 mg/L, that led many aquatic lives in water unable to live. While O_2 content of water from natural sources generally exhibited 5 to 7 mg/L. The quality standard of water would show the O_2 content of about 5 to 8 mg/L. The basic requirement of living for aquatic animals was dissolved oxygen (DO) [76]. The DO value was lowest in pond No.1, as shown in Figure 31a. The DO value showed a higher value in pond No.3, as shown in Figure 31c. After the use of activated carbon powders filter in pond No.4, the DO value showed as a higher value

than pond No.3, shown in Figure 31d. This is because of respiration and photosynthesis process. The catfish used O_2 for the respiration process. Plant roots, phytoplankton and microbes were adsorbed O_2 , including nitrification of ammonium ion (NH_4^+) that was used oxygen in the process [75, 77]. The photosynthesis of microalgae increased the DO value [74]. In addition, the DO value also could be increased by gas exchange from atmosphere with the water circulation system or mechanical aeration in the pond, that made the DO value increase in the aquaponics system (pond No.3). This is because the water circulation and aerenchyma of root plant zones in pond [75]. Furthermore, the addition of activated carbon powders filter could increase water pH and manganese oxide oxidation, that was more increased in pond No.4. Each pond had an increased DO value with the duration of catfish raising. This is due to the induction phase of waterborne microorganisms in the early stages, with a slight increase in cell density. or the physiological adaptation of cell metabolism to growth in the first week [78]. It also contributes to more root growth over time. which adds oxygen to the water. The different rates of oxygen exchange from the aerobic tissue to the root region contribute primarily to differences in DO levels between plant cultures. [74]. It is also related to having more plant roots over time, which adds oxygen to the water.

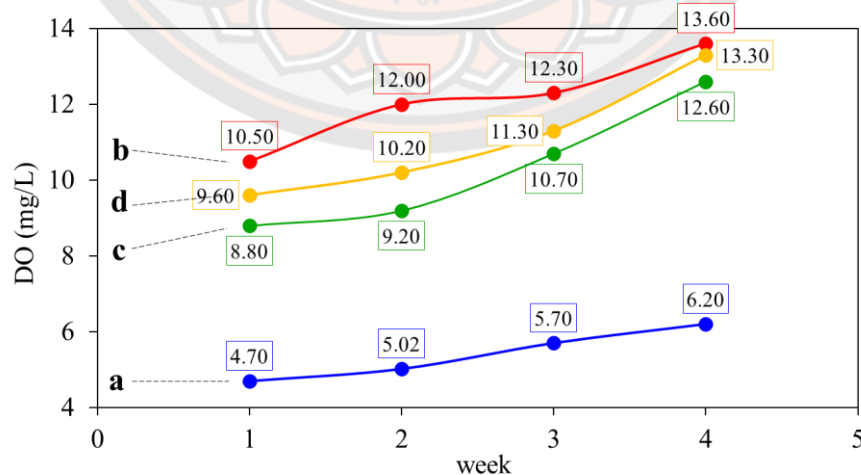


Figure 31 DO values of water of pond No.1 (a), pond No.2 (b), pond No.3 (c) and pond No.4 (d)

3. The turbidity of water

Turbidity of water was an important indicator of suspended materials and microorganisms content that could be had many negative effects on aquatic life [74]. The turbidity value could be prevented light penetration through to the water, that led to decreased photosynthetic process of phytoplankton [79]. It showed quite high in pond No.1 (Figure 32a) and low in pond No.2 (Figure 32b). Furthermore, it was lowering in the aquaponics system (pond No.3, Figure 32c) and the aquaponics system with addition activated carbon powders filter (pond No.4, Figure 32d). For pond No.1, metabolic waste from catfish after feeding is unable to filtered and adsorbed. Therefore, the turbidity value was too high and increased more over time. For pond No.3, the turbidity value was greatly decreased due to the adsorption and filtration of suspended organic matters through plant roots in circulated water, that led to the decreased more over time. This is because plant roots grow up more over time. Furthermore, the turbidity value was greatly decreased after using activated carbon powders filter, in pond No.4. This is because plant roots and activated carbon powders filtered and absorbed these suspended materials.

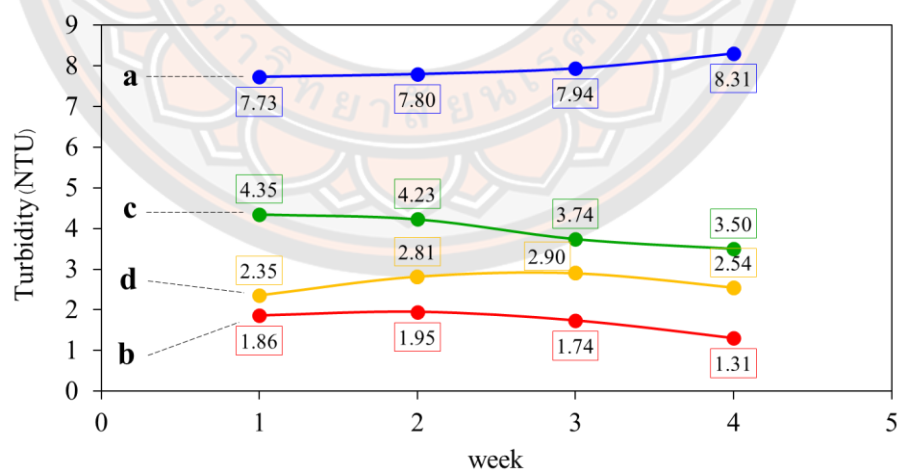


Figure 32 Turbidity values of water of pond No.1 (a), pond No.2 (b), pond No.3 (c) and pond No.4 (d)

4. The measurement of ammonia, nitrite and orthophosphate

Nitrogen compounds are essential compounds for the growth of aquatic plants. Nitrogen compounds were composed of two types: organic nitrogen compounds. That could be found in manure, feces, nucleic acids, amino acids and so on. It was a component of plants and animals. And the other type was inorganic nitrogen compounds such as ammonium ions, nitrite, and nitrate. These compounds could be found in fertilizers or salts in the urine. In addition, nitrogen compounds could change their structure from organic to inorganic through the action of microorganisms in water. Including, the change of inorganic substances forms in the ammonification, nitrification and denitrification reaction, as shown in Figure 33. This represents the relationship in the nitrogen cycle. Ammonia (NH_4) was an inorganic nitrogen compound that plays an important role in the aquaculture system. Because it was both a fertilizer for the growth of aquatic animals and toxic to aquatic lives when it accumulates in the water for a long-time. Ammonia was obtained from the excretion of aquatic animals including food residues. Therefore, in aquaculture system, it was necessary to change the water regularly to control the ammonia concentration from being too high.

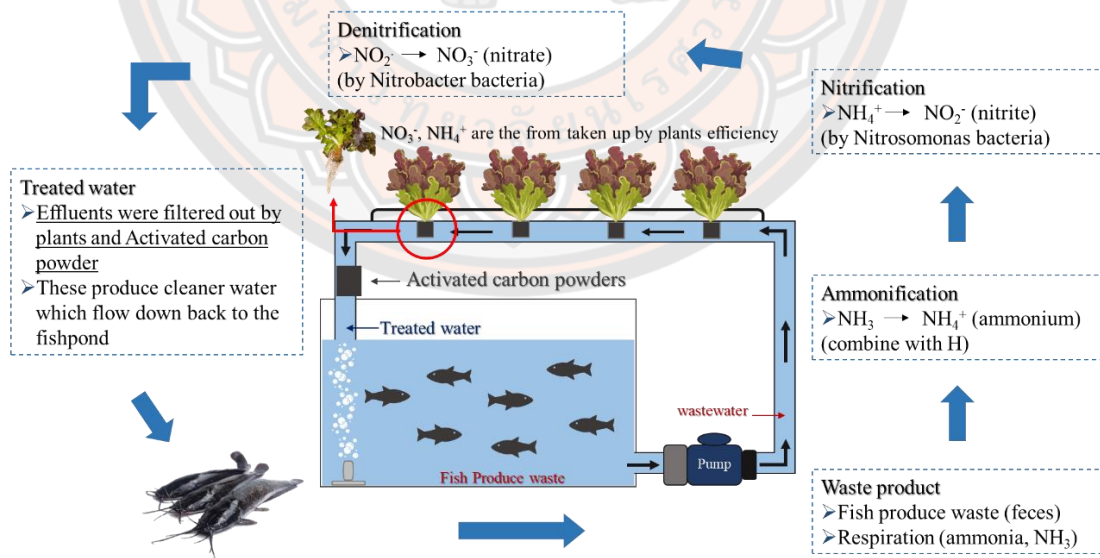


Figure 33 Nitrogen cycle in aquaponic system

The removal and relative removal rate of $\text{NH}_3\text{-N}$ (express in form of total ammonia, $\text{NH}_3 + \text{NH}_4^+$), $\text{NO}_2^- \text{-N}$ and orthophosphate of water in pond No.1 to pond No.4 at week 4 are showed in Table 4. It was showed that all matters are decreased in the aquaponics system (pond No.3) and the aquaponics system with activated carbon powders filter (pond No.4) as compared to control pond No.1. In the case of $\text{NH}_3\text{-N}$ for all pond, showed the decrease compared to the recommended production well management guidelines to no more than 2 mg/L [80]. However, it was greatly high for pond No.1, which was formed as a waste product of protein metabolism. It was oxidized and transformed to nitrate via nitrite by nitrification of ammonia - oxidizing and nitrite-oxidizing bacteria [81]. It also accumulated in the lower environment of the bottom of the pond, and it continuously released into the water [82]. Its value was lowering with 70.39% and 86.84 % of relative removal rate in pond No.3 and pond No.4, respectively. which indicated a high DO value. The high DO value promoted ammonia oxidation by nitrification and decreases the toxicity of NH_3 to fish. In addition, another nitrogen compounds were formed from nitrification and denitrification. These were absorbed by plant roots for growth. Another way to removal of ammonia, that contained in a combined form of ionized (NH_4^+) and unionized (NH_3) [76]. It was removed by ammonium ion (NH_4^+) adsorption of the hydrochar activated carbon sample, that led more ammonia to remove for pond No.4. For nitrite (NO_2^-) that was formed from nitrification step, that transformed NH_3 to NO_3^- by Nitrosomonas bacteria. This is another way to remove ammonia. However, it was still higher than the optimal amount in aquaculture system (less than 0.1 mg/L) unless pond No.2 [67]. The relative removal rate of pond No.3 and pond No.4 showed 41.46% and 73.17%, respectively. It was noticed that nitrite content of pond No.4 is close to the suitable value, which was the result of high DO values. In the case of orthophosphate (PO_4^{3-}), it decreased relative removal rate by 44.44% and 53.33% for pond No.3 and pond No.4, respectively, mainly due to root uptake for plant growth.

Table 4 The removal and percent relative removal rate of NH₃, NO₂⁻ and orthophosphate

Pond No.	Removal of					
	NH ₃		NO ₂ ⁻		PO ₄ ³⁻	
	mg/L	%Removal rate	mg/L	%Removal rate	mg/L	%Removal rate
1	1.52	-	0.41	-	0.45	-
2	0.04	-	0.02	-	0.02	-
3	0.45	70.39	0.24	41.46	0.25	44.44
4	0.20	86.84	0.11	73.17	0.21	53.33

5. The growth of catfish and red oak lettuce

The growth of catfish in weight of pond No.1, No.3 and No.4 were showed in Figure 33. In pond No.2 had no data of growth catfish due to hydroponic system only. Only in the first week, in pond No.1, No.3 and No.4, the growth of catfish tends to be higher for aquaponics system (pond No.3) and aquaponics system with activated carbon powders filter (pond No.4) as compared to aquaculture system (pond No.1). The growth of catfish at pond No.3 and pond No.4 continued to be higher than pond No.1 until the fourth week. Moreover, pond No.4 showed higher growth of catfish than pond No.3 for all 4 weeks. These results were relative to the water pH, DO value, turbidity, NH₃ and NO₂⁻ content level in pond No.3 and pond No.4. These parameters could lead the growth of catfish to better.

Considering the data of red oak lettuce growth for all crop panels at the fourth week in Table 5, among all growth parameters of plant crop tube panel No.2 (connecting with aquaponics system – pond No.3) and plant crop tube panel No.3 (connecting with aquaponics system that addition the activated carbon powders filter – pond No.4) exhibited slightly higher than crop tube panel No.1 (hydroponic system only). Higher plant growth also showed higher in NH₃, NO₂⁻ and others matters removal efficiency. Especially the growth of plant roots, it had a great effect on the adsorption of various substances and oxygen in water. The plant roots played an

important role in decreasing nitrogen compound and increasing DO value. It was the habitat of microbes which causes nitrification - denitrification and nutrient absorption in the hydroponics plant [83]. It could be expected that the level of ammonia, nitrite and turbidity would be substantially lower in an efficient aquaponics system and aquaponics system with addition the activated carbon powders filter. This is because plant root and activated carbon powders showed many efficient to uptake or adsorb and filter these substrate materials.

Table 5 The growth parameters of red oak at 4th week

crop tube panel number	Stem height (cm)	Dried stem weight (g/stem)	Root length (cm)	Dried root weight (g/stem)	Number of leaves /stems	Dried leaf weight (g)	Trunk diameter (cm)
1	15.63	1.12	9.32	0.24	9.2	0.14	16.4
2	16.87	1.26	10.22	0.26	9.3	0.15	16.4
3	16.89	1.47	11.22	0.29	9.3	0.17	17.75

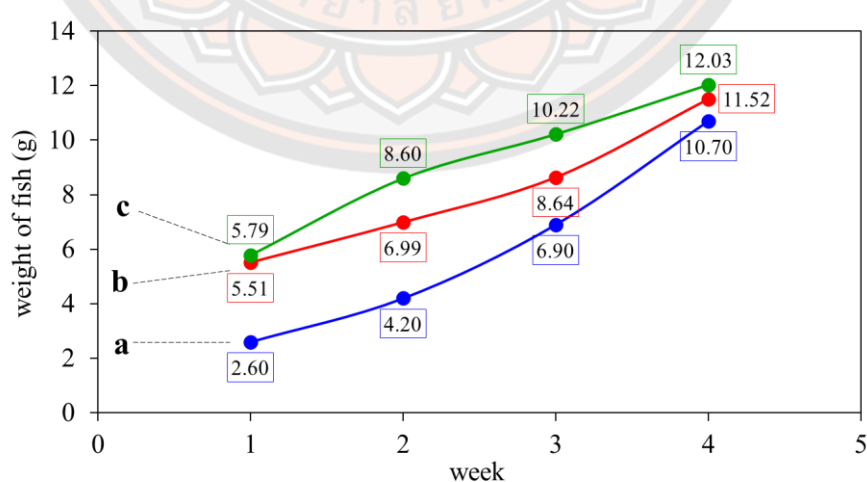


Figure 34 The catfish growth of pond No.1 (a), pond No.3 (b) and pond No.4 (c)

CHAPTER V

CONCLUSION

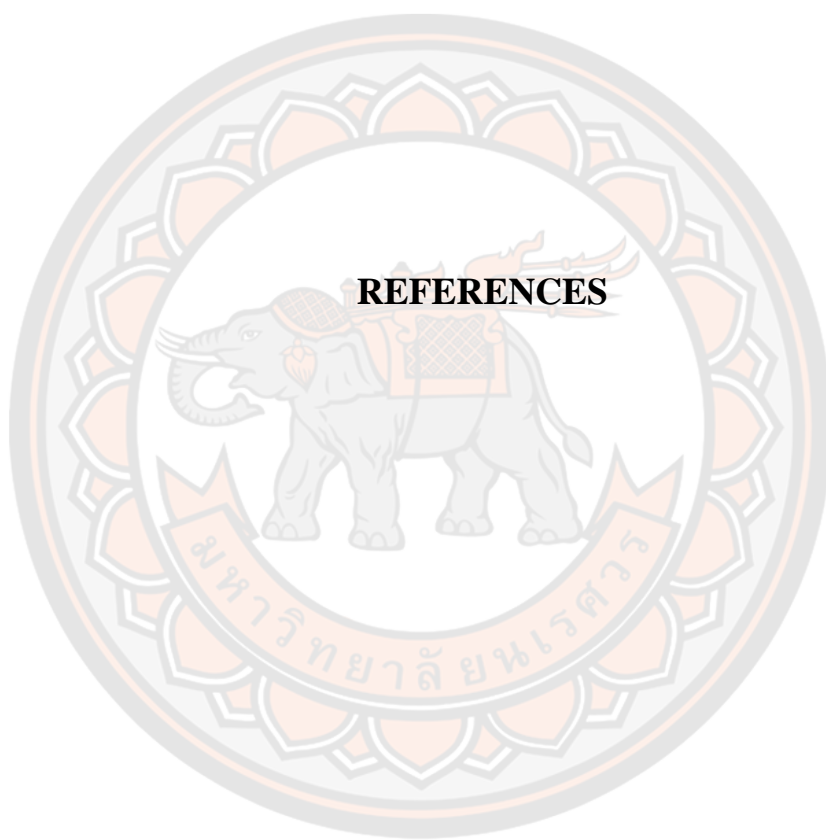
Hydrothermal pretreatment, concentration of potassium permanganate (KMnO_4) and the activation temperature had a significant effect on the characteristics of activated carbon sample that produced from sugarcane leaf. The yield percentage of all activated carbon sample decreased with increased of activation temperature from 300 to 400°C. The yield percentage of the hydrothermal pretreatment activated carbon sample was higher than without hydrothermal pretreatment activated carbon sample at the same condition. And it was higher with the concentration of potassium permanganate increased. In addition, the carbon content of activated carbon sample increased with hydrothermal pretreatment processing and increasing of the activation temperature, while the oxygen content showed the opposite results. However, the O/C ratio of activated carbon sample increased with increasing concentration of potassium permanganate. The surface functional group of activated carbon sample, it had been eliminated from the effects of hydrothermal pretreatment and increasing of activation temperature, go along with the aromatics increased. Whereas the addition of potassium permanganate increased the presence of C-O, Mn-OH, O-Mn-O and Mn-O bonds surface functional groups on the hydrochar activated carbon samples. The XRD patterns also confirmed that the hydrochar activated carbon sample with KMnO_4 adding was amorphous and contained oxides of K and Mn. Moreover, the zeta potential values of the hydrochar activated carbon sample with 0%wt of KMnO_4 showed negative charge throughout the pH range of 3 to 11 and more negative after the addition with 1%wt of KMnO_4 . Therefore, the addition of KMnO_4 and hydrothermal pretreatment process had a significant effect on the breakdown and decomposition of surface particles on activated carbon products. From these results, it has increased the surface area and porous structure of the hydrochar activated carbon sample with the addition of KMnO_4 and the hydrochar activated carbon sample with 3%wt of KMnO_4 at 400°C of activation temperature exhibited the highest value of surface area was 45.0364 m^2/g . In contrast, the surface area of the hydrochar activated

carbon sample with 5%wt of KMnO_4 all activation temperature tended to decrease. This is because KMnO_4 was too high and led to decomposition on their surface area, including particle size.

After using of the hydrochar activated carbon sample with 3%wt of KMnO_4 at 350 °C of activation temperature as the filter in an aquaponics system, it was found that the water showed the weakly alkaline pH (7.2 to 7.4), DO value suitable for fish farming (9.6 to 13.3 mg/L), and the turbidity was significantly reduced (reduced from 7.73 to 8.31 NTU to 2.35 to 2.90 NTU). It has also been found that the hydrochar activated carbon sample could be significantly decreased ammonia (NH_3) (relative removal rate = 86.84%), nitrites ion (NO_2^-) (relative removal rate = 73.17%) and orthophosphates ion (PO_4^{3-}) (relative removal rate = 53.33%), because of activated carbon powder filter could be adsorbed and filtered of these compound because its negative charge surface area, including the root of plant could be adsorbed for its growth. Based on the water properties of aquaponics system with activated carbon powders filter, the catfish showed good growth for 4 weeks.

In this research, it was concluded that the hydrothermal pretreatment process at low temperature of 129 °C at 15 bar, 1%wt to 3%wt of KMnO_4 at 350 °C of activation temperature were suitable for the activated carbon production from sugarcane leaf for using in aquaponics systems of catfish and red oak lettuce which could be reduced the surface functional groups of sugarcane leaf more easily after activation step. It has also resulted in the aromatics of the activated carbon products with high yield at only 350°C. While KMnO_4 caused partial oxidation, which increased more amorphousness and negative charge of the hydrochar activated carbon throughout the pH range of 3 to 11, which more increases the affinity between the activated carbon and the positive charge adsorbate. These results resulted in reduced energy for activated carbon production and increased adsorption properties of activated carbon.

REFERENCES



- [1] W. H. Cheung, S. S. Y. Lau, S. Y. Leung, A. W. M. Ip, and G. McKay, "Characteristics of Chemical Modified Activated Carbons from Bamboo Scaffolding," *Chinese Journal of Chemical Engineering*, vol. 20, no. 3, pp. 515-523, 2012/06/01/ 2012, doi: [https://doi.org/10.1016/S1004-9541\(11\)60213-9](https://doi.org/10.1016/S1004-9541(11)60213-9).
- [2] J. Choma and M. Jaroniec, "Chapter 3 Characterization of nanoporous carbons by using gas adsorption isotherms," in *Interface Science and Technology*, vol. 7, T. J. Bandosz Ed.: Elsevier, 2006, pp. 107-158.
- [3] R. DiPanfilo and N. O. Egiebor, "Activated carbon production from synthetic crude coke," *Fuel Processing Technology*, vol. 46, no. 3, pp. 157-169, 1996/03/01/ 1996, doi: [https://doi.org/10.1016/0378-3820\(95\)00054-2](https://doi.org/10.1016/0378-3820(95)00054-2).
- [4] O. F. Olorundare, R. W. M. Krause, J. O. Okonkwo, and B. B. Mamba, "Potential application of activated carbon from maize tassel for the removal of heavy metals in water," *Physics and Chemistry of the Earth, Parts A/B/C*, vol. 50-52, pp. 104-110, 2012/01/01/ 2012, doi: <https://doi.org/10.1016/j.pce.2012.06.001>.
- [5] L. Muniandy, F. Adam, A. R. Mohamed, and E.-P. Ng, "The synthesis and characterization of high purity mixed microporous/mesoporous activated carbon from rice husk using chemical activation with NaOH and KOH," *Microporous and Mesoporous Materials*, vol. 197, pp. 316-323, 2014/10/01/ 2014, doi: <https://doi.org/10.1016/j.micromeso.2014.06.020>.
- [6] S. Yorgun, N. Vural, and H. Demiral, "Preparation of high-surface area activated carbons from Paulownia wood by ZnCl₂ activation," *Microporous and Mesoporous Materials*, vol. 122, no. 1, pp. 189-194, 2009/06/01/ 2009, doi: <https://doi.org/10.1016/j.micromeso.2009.02.032>.
- [7] S. Başakçılardan Kabakçı and S. S. Baran, "Hydrothermal carbonization of various lignocellulosics: Fuel characteristics of hydrochars and surface characteristics of activated hydrochars," *Waste Management*, vol. 100, pp. 259-268, 2019/12/01/ 2019, doi: <https://doi.org/10.1016/j.wasman.2019.09.021>.

- [8] J. K. Buttner, R. W. Soderberg, and D. E. Terlizzi, "An Introduction to Water Chemistry in Freshwater Aquaculture," in "Northeastern Regional Aquaculture Center," 1993.
- [9] R. D. Zweig, J. D. Morton, and M. M. Stewart, *Source water quality for aquaculture: a guide for assessment*. (in English), 1999, p. 72 pp.
- [10] P. Q. dziwiatr, D. Zawadzki, and K. Michalska, "Aquaculture waste management," *Acta Innovations*, pp. 20-29, 2017.
- [11] A. B. Dauda, A. Ajadi, A. S. Tola-Fabunmi, and A. O. Akinwole, "Waste production in aquaculture: Sources, components and managements in different culture systems," *Aquaculture and Fisheries*, vol. 4, no. 3, pp. 81-88, 2019/05/01/ 2019, doi: <https://doi.org/10.1016/j.aaf.2018.10.002>.
- [12] J. Pastor-Villegas and C. J. Durán-Valle, "Pore structure of activated carbons prepared by carbon dioxide and steam activation at different temperatures from extracted rockrose," *Carbon*, vol. 40, no. 3, pp. 397-402, 2002/03/01/ 2002, doi: [https://doi.org/10.1016/S0008-6223\(01\)00118-X](https://doi.org/10.1016/S0008-6223(01)00118-X).
- [13] H. Demiral and I. Uzun, "Preparation and characterization of activated carbons from poplar wood (*Populus L.*)," *Surface and Interface Analysis*, vol. 42, no. 6-7, pp. 1338-1341, 2010/06/01 2010, doi: 10.1002/sia.3276.
- [14] Q.-S. Liu, T. Zheng, P. Wang, and L. Guo, "Preparation and characterization of activated carbon from bamboo by microwave-induced phosphoric acid activation," *Industrial Crops and Products*, vol. 31, no. 2, pp. 233-238, 2010/03/01/ 2010, doi: <https://doi.org/10.1016/j.indcrop.2009.10.011>.
- [15] G. Sun, L. Qiu, M. Zhu, K. Kang, and X. Guo, "Activated carbons prepared by hydrothermal pretreatment and chemical activation of *Eucommia ulmoides* wood for supercapacitors application," *Industrial Crops and Products*, vol. 125, pp. 41-49, 2018/12/01/ 2018, doi: <https://doi.org/10.1016/j.indcrop.2018.08.082>.
- [16] F. Mbarki *et al.*, "Hydrothermal pre-treatment, an efficient tool to improve activated carbon performances," *Industrial Crops and Products*, vol. 140, p. 111717, 2019/11/15/ 2019, doi: <https://doi.org/10.1016/j.indcrop.2019.111717>.

- [17] E. Yagmur, M. S. Tunc, A. Banford, and Z. Aktas, "Preparation of activated carbon from autohydrolysed mixed southern hardwood," *Journal of Analytical and Applied Pyrolysis*, vol. 104, pp. 470-478, 2013/11/01/ 2013, doi: <https://doi.org/10.1016/j.jaap.2013.05.025>.
- [18] A. Zeriouh and L. Belkbir, "Thermal decomposition of a Moroccan wood under a nitrogen atmosphere," *Thermochimica Acta*, vol. 258, pp. 243-248, 1995/07/01/ 1995, doi: [https://doi.org/10.1016/0040-6031\(94\)02246-K](https://doi.org/10.1016/0040-6031(94)02246-K).
- [19] T. H. Tran *et al.*, "Comparative study on methylene blue adsorption behavior of coffee husk-derived activated carbon materials prepared using hydrothermal and soaking methods," *Journal of Environmental Chemical Engineering*, vol. 9, no. 4, p. 105362, 2021/08/01/ 2021, doi: <https://doi.org/10.1016/j.jece.2021.105362>.
- [20] S. M. Ibrahim, A. F. Al-Hossainy, B. Saha, and M. A. El-Aal, "Removal of bromothymol blue dye by the oxidation method using KMnO₄: Accelerating the oxidation reaction by Ru (III) catalyst," *Journal of Molecular Structure*, vol. 1268, p. 133679, 2022/11/15/ 2022, doi: <https://doi.org/10.1016/j.molstruc.2022.133679>.
- [21] W. A. Welch, "Potassium Permanganate in Water Treatment," *Journal AWWA*, <https://doi.org/10.1002/j.1551-8833.1963.tb01082.x> vol. 55, no. 6, pp. 735-741, 1963/06/01 1963, doi: <https://doi.org/10.1002/j.1551-8833.1963.tb01082.x>.
- [22] T. Lin, L. Li, W. Chen, and S. Pan, "Effect and mechanism of preoxidation using potassium permanganate in an ultrafiltration membrane system," *Desalination*, vol. 286, pp. 379-388, 2012/02/01/ 2012, doi: <https://doi.org/10.1016/j.desal.2011.11.052>.
- [23] L. W. K. M. M. Sailus, *Home water treatment*. 1995.
- [24] G. Zhang, Y. Sun, P. Zhao, Y. Xu, A. Su, and J. Qu, "Characteristics of activated carbon modified with alkaline KMnO₄ and its performance in catalytic reforming of greenhouse gases CO₂/CH₄," *Journal of CO₂ Utilization*, vol. 20, pp. 129-140, 2017/07/01/ 2017, doi: <https://doi.org/10.1016/j.jcou.2017.05.013>.

- [25] F. Tavakoli Foroushani, H. Tavanai, and F. A. Hosseini, "An investigation on the effect of KMnO₄ on the pore characteristics of pistachio nut shell based activated carbon," *Microporous and Mesoporous Materials*, vol. 230, pp. 39-48, 2016/08/01/ 2016, doi: <https://doi.org/10.1016/j.micromeso.2016.04.030>.
- [26] Y. Zhang, Y. Wang, and L. Zhou, "Influence of excess KMnO₄ on the adsorption of powdered activated carbon," *Chemical Engineering Journal*, vol. 226, pp. 279-285, 2013/06/15/ 2013, doi: <https://doi.org/10.1016/j.cej.2013.03.063>.
- [27] T. Adinaveen, L. J. Kennedy, J. J. Vijaya, and G. Sekaran, "Studies on structural, morphological, electrical and electrochemical properties of activated carbon prepared from sugarcane bagasse," *Journal of Industrial and Engineering Chemistry*, vol. 19, no. 5, pp. 1470-1476, 2013/09/25/ 2013, doi: <https://doi.org/10.1016/j.jiec.2013.01.010>.
- [28] J. Sreńscek-Nazzal, W. Kamińska, B. Michalkiewicz, and Z. C. Koren, "Production, characterization and methane storage potential of KOH-activated carbon from sugarcane molasses," *Industrial Crops and Products*, vol. 47, pp. 153-159, 2013/05/01/ 2013, doi: <https://doi.org/10.1016/j.indcrop.2013.03.004>.
- [29] A. Yadav, R. Abbassi, A. Gupta, and M. Dadashzadeh, "Removal of fluoride from aqueous solution and groundwater by wheat straw, Sawdust and activated bagasse carbon of sugarcane," *Ecological Engineering*, vol. 62, pp. 211-218, 03/01 2013, doi: 10.1016/j.ecoleng.2012.12.069.
- [30] H. C. Lin, L. T. Liu, and N. Fujimoto, "Source water purification of bamboo activated carbon prepared from bamboo charcoal by using the multi-layer filtration method," *Journal of the Faculty of Agriculture, Kyushu University*, vol. 62, pp. 459-467, 09/01 2017.
- [31] O. Boujibar, A. Souikny, F. Ghamouss, O. Achak, M. Dahbi, and T. Chafik, "CO₂ capture using N-containing nanoporous activated carbon obtained from argan fruit shells," *Journal of Environmental Chemical Engineering*, vol. 6, no. 2, pp. 1995-2002, 2018/04/01/ 2018, doi: <https://doi.org/10.1016/j.jece.2018.03.005>.

- [32] R. A. Fiuza-Jr, R. C. Andrade, and H. M. C. Andrade, "CO₂ capture on KOH-activated carbons derived from yellow mombin fruit stones," *Journal of Environmental Chemical Engineering*, vol. 4, no. 4, Part A, pp. 4229-4236, 2016/12/01/ 2016, doi: <https://doi.org/10.1016/j.jece.2016.09.025>.
- [33] C. Dalai, R. Jha, and V. R. Desai, "Rice Husk and Sugarcane Baggase Based Activated Carbon for Iron and Manganese Removal," *Aquatic Procedia*, vol. 4, pp. 1126-1133, 2015/01/01/ 2015, doi: <https://doi.org/10.1016/j.aqpro.2015.02.143>.
- [34] S. Babel and T. A. Kurniawan, "Cr(VI) removal from synthetic wastewater using coconut shell charcoal and commercial activated carbon modified with oxidizing agents and/or chitosan," *Chemosphere*, vol. 54, no. 7, pp. 951-967, 2004/02/01/ 2004, doi: <https://doi.org/10.1016/j.chemosphere.2003.10.001>.
- [35] L. Niazi, A. Lashanizadegan, and H. Sharififard, "Chestnut oak shells activated carbon: Preparation, characterization and application for Cr (VI) removal from dilute aqueous solutions," *Journal of Cleaner Production*, vol. 185, pp. 554-561, 2018/06/01/ 2018, doi: <https://doi.org/10.1016/j.jclepro.2018.03.026>.
- [36] H.-C. Tao, H.-R. Zhang, J.-B. Li, and W.-Y. Ding, "Biomass based activated carbon obtained from sludge and sugarcane bagasse for removing lead ion from wastewater," *Bioresource Technology*, vol. 192, pp. 611-617, 2015/09/01/ 2015, doi: <https://doi.org/10.1016/j.biortech.2015.06.006>.
- [37] A. Jain and S. K. Tripathi, "Nano-porous activated carbon from sugarcane waste for supercapacitor application," *Journal of Energy Storage*, vol. 4, pp. 121-127, 2015/12/01/ 2015, doi: <https://doi.org/10.1016/j.est.2015.09.010>.
- [38] Y. M. Awad *et al.*, "Biochar, a potential hydroponic growth substrate, enhances the nutritional status and growth of leafy vegetables," *Journal of Cleaner Production*, vol. 156, pp. 581-588, 2017/07/10/ 2017, doi: <https://doi.org/10.1016/j.jclepro.2017.04.070>.
- [39] A. Mosa, M. F. El-Banna, and B. Gao, "Biochar filters reduced the toxic effects of nickel on tomato (*Lycopersicon esculentum* L.) grown in nutrient film technique hydroponic system," *Chemosphere*, vol. 149, pp. 254-262, 2016/04/01/ 2016, doi: <https://doi.org/10.1016/j.chemosphere.2016.01.104>.

- [40] G. Jin, Y. Eom, and T. G. Lee, "Removal of Hg(II) from aquatic environments using activated carbon impregnated with humic acid," *Journal of Industrial and Engineering Chemistry*, vol. 42, pp. 46-52, 2016/10/25/ 2016, doi: <https://doi.org/10.1016/j.jiec.2016.07.029>.
- [41] Y. Zou, Z. Hu, J. Zhang, H. Xie, C. Guimbaud, and Y. Fang, "Effects of pH on nitrogen transformations in media-based aquaponics," *Bioresource Technology*, vol. 210, pp. 81-87, 2016/06/01/ 2016, doi: <https://doi.org/10.1016/j.biortech.2015.12.079>.
- [42] K. M. Buzby, N. L. Waterland, K. J. Semmens, and L.-S. Lin, "Evaluating aquaponic crops in a freshwater flow-through fish culture system," *Aquaculture*, vol. 460, pp. 15-24, 2016/07/01/ 2016, doi: <https://doi.org/10.1016/j.aquaculture.2016.03.046>.
- [43] E.-S. G. Khater, A. H. Bahnasawy, A. E.-H. S. Shams, M. S. Hassaan, and Y. A. Hassan, "Utilization of effluent fish farms in tomato cultivation," *Ecological Engineering*, vol. 83, pp. 199-207, 2015/10/01/ 2015, doi: <https://doi.org/10.1016/j.ecoleng.2015.06.010>.
- [44] F. Martínez, S. Castillo, C. Borrero, S. Pérez, P. Palencia, and M. Avilés, "Effect of different soilless growing systems on the biological properties of growth media in strawberry," *Scientia Horticulturae*, vol. 150, pp. 59-64, 2013/02/04/ 2013, doi: <https://doi.org/10.1016/j.scienta.2012.10.016>.
- [45] L. Chekli *et al.*, "Fertilizer drawn forward osmosis process for sustainable water reuse to grow hydroponic lettuce using commercial nutrient solution," *Separation and Purification Technology*, vol. 181, pp. 18-28, 2017/06/30/ 2017, doi: <https://doi.org/10.1016/j.seppur.2017.03.008>.
- [46] J. Pan *et al.*, "Hydroponic plate/fabric/grass system for treatment of aquacultural wastewater," *Aquacultural Engineering*, vol. 37, no. 3, pp. 266-273, 2007/11/01/ 2007, doi: <https://doi.org/10.1016/j.aquaeng.2007.09.001>.
- [47] J. Zhang, X. Wang, and Q. Zhou, "Co-cultivation of *Chlorella* spp and tomato in a hydroponic system," *Biomass and Bioenergy*, vol. 97, pp. 132-138, 2017/02/01/ 2017, doi: <https://doi.org/10.1016/j.biombioe.2016.12.024>.
- [48] D. C. Sikawa and A. Yakupitiyage, "The hydroponic production of lettuce (*Lactuca sativa* L) by using hybrid catfish (*Clarias macrocephalus*×*C.*

- gariepinus) pond water: Potentials and constraints," *Agricultural Water Management*, vol. 97, no. 9, pp. 1317-1325, 2010/09/01/ 2010, doi: <https://doi.org/10.1016/j.agwat.2010.03.013>.
- [49] I. Domeño, I. Irigoyen, and J. Muro, "Comparison of traditional and improved methods for estimating the stability of organic growing media," *Scientia Horticulturae*, vol. 130, no. 1, pp. 335-340, 2011/08/26/ 2011, doi: <https://doi.org/10.1016/j.scienta.2011.07.012>.
- [50] C. I. A. Ferreira, V. Calisto, M. Otero, H. Nadais, and V. I. Esteves, "Comparative adsorption evaluation of biochars from paper mill sludge with commercial activated carbon for the removal of fish anaesthetics from water in Recirculating Aquaculture Systems," *Aquacultural Engineering*, vol. 74, pp. 76-83, 2016/09/01/ 2016, doi: <https://doi.org/10.1016/j.aquaeng.2016.06.003>.
- [51] Z. Khiari, K. Alka, S. Kelloway, B. Mason, and N. Savidov, "Integration of Biochar Filtration into Aquaponics: Effects on Particle Size Distribution and Turbidity Removal," *Agricultural Water Management*, vol. 229, p. 105874, 2020/02/28/ 2020, doi: <https://doi.org/10.1016/j.agwat.2019.105874>.
- [52] R. Uchida, "Essential nutrients for plant growth: nutrient functions and deficiency symptoms," *Plant nutrient management in Hawaii's soils*, vol. 4, pp. 31-55, 2000.
- [53] V. Römheld and H. Marschner, "Function of Micronutrients in Plants," *Micronutrients in Agriculture*, <https://doi.org/10.2136/sssabookser4.2ed.c9> pp. 297-328, 1991/01/01 1991, doi: <https://doi.org/10.2136/sssabookser4.2ed.c9>.
- [54] M. A. Grusak, "Plant Macro-and Micronutrient Minerals," *e LS*, 2001.
- [55] U. Na-Nakorn and R. E. Brummett, "Use and exchange of aquatic genetic resources for food and aquaculture: Clarias catfish," *Reviews in Aquaculture*, vol. 1, pp. 214-223, 2009.
- [56] U. Na-Nakorn, W. Kamonrat, and T. Ngamsiri, "Genetic diversity of walking catfish, *Clarias macrocephalus*, in Thailand and evidence of genetic introgression from introduced farmed *C. gariepinus*," *Aquaculture*, vol. 240, pp. 145-163, 10/01 2004, doi: 10.1016/j.aquaculture.2004.08.001.
- [57] Y. K. Avsar, Y. Karagul-Yuceer, M. A. Drake, T. K. Singh, Y. Yoon, and K. R. Cadwallader, "Characterization of Nutty Flavor in Cheddar Cheese,"

- Journal of Dairy Science*, vol. 87, no. 7, pp. 1999-2010, 2004/07/01/ 2004, doi: [https://doi.org/10.3168/jds.S0022-0302\(04\)70017-X](https://doi.org/10.3168/jds.S0022-0302(04)70017-X).
- [58] S. Mopoung, "KMnO₄ Modified Carbon Prepared from Waste of Pineapple Leaf Fiber Production Processing for Removal of Ferric Ion from Aqueous Solution," *American Journal of Applied Sciences*, vol. 13, pp. 814-826, 07/25 2016, doi: 10.3844/ajassp.2016.814.826.
- [59] Y. Su *et al.*, "Syngas production at low temperature via the combination of hydrothermal pretreatment and activated carbon catalyst along with value-added utilization of tar and bio-char," *Energy Conversion and Management*, vol. 205, p. 112382, 2020/02/01/ 2020, doi: <https://doi.org/10.1016/j.enconman.2019.112382>.
- [60] Y. Iradukunda *et al.*, "High performance of activated carbons prepared from mangosteen (*Garcinia mangostana*) peels using the hydrothermal process," *Journal of Energy Storage*, vol. 39, p. 102577, 2021/07/01/ 2021, doi: <https://doi.org/10.1016/j.est.2021.102577>.
- [61] F. Benstoem *et al.*, "Elimination of micropollutants by activated carbon produced from fibers taken from wastewater screenings using hydrothermal carbonization," *Journal of Environmental Management*, vol. 211, pp. 278-286, 2018/04/01/ 2018, doi: <https://doi.org/10.1016/j.jenvman.2018.01.065>.
- [62] Y. Dessie, S. Tadesse, and R. Eswaramoorthy, "Physicochemical parameter influences and their optimization on the biosynthesis of MnO₂ nanoparticles using *Vernonia amygdalina* leaf extract," *Arabian Journal of Chemistry*, vol. 13, no. 8, pp. 6472-6492, 2020/08/01/ 2020, doi: <https://doi.org/10.1016/j.arabjc.2020.06.006>.
- [63] M. Ghebleh Goydaragh, R. Taghizadeh-Mehrjardi, A. Golchin, A. Asghar Jafarzadeh, and M. Lado, "Predicting weathering indices in soils using FTIR spectra and random forest models," *CATENA*, vol. 204, p. 105437, 2021/09/01/ 2021, doi: <https://doi.org/10.1016/j.catena.2021.105437>.
- [64] N. A. Mahat and S. A. Shamsudin, "Transformation of oil palm biomass to optical carbon quantum dots by carbonisation-activation and low temperature hydrothermal processes," *Diamond and Related Materials*, vol. 102, p.

- 107660, 2020/02/01/ 2020, doi: <https://doi.org/10.1016/j.diamond.2019.107660>.
- [65] C. Li, Y. Sun, Z. Yi, L. Zhang, S. Zhang, and X. Hu, "Co-pyrolysis of coke bottle wastes with cellulose, lignin and sawdust: Impacts of the mixed feedstock on char properties," *Renewable Energy*, vol. 181, pp. 1126-1139, 2022/01/01/ 2022, doi: <https://doi.org/10.1016/j.renene.2021.09.103>.
- [66] I. Istadi, S. A. Prasetyo, and T. S. Nugroho, "Characterization of K₂O/CaO-ZnO Catalyst for Transesterification of Soybean Oil to Biodiesel," *Procedia Environmental Sciences*, vol. 23, pp. 394-399, 2015/01/01/ 2015, doi: <https://doi.org/10.1016/j.proenv.2015.01.056>.
- [67] L. Li *et al.*, "Study of the interaction mechanism between GO/rGO and trypsin," *Journal of Hazardous Materials Advances*, vol. 3, p. 100011, 2021/11/01/ 2021, doi: <https://doi.org/10.1016/j.hazadv.2021.100011>.
- [68] D. Ying *et al.*, "Removal of uranium using MnO₂/orange peel biochar composite prepared by activation and in-situ deposit in a single step," *Biomass and Bioenergy*, vol. 142, p. 105772, 2020/11/01/ 2020, doi: <https://doi.org/10.1016/j.biombioe.2020.105772>.
- [69] R. Maršálek and M. Švidrnoch, "The adsorption of amitriptyline and nortriptyline on activated carbon, diosmectite and titanium dioxide," *Environmental Challenges*, vol. 1, p. 100005, 2020/12/01/ 2020, doi: <https://doi.org/10.1016/j.envc.2020.100005>.
- [70] Y. Zhuang, J. Liu, J. Chen, and P. Fei, "Modified pineapple bran cellulose by potassium permanganate as a copper ion adsorbent and its adsorption kinetic and adsorption thermodynamic," *Food and Bioproducts Processing*, vol. 122, pp. 82-88, 2020/07/01/ 2020, doi: <https://doi.org/10.1016/j.fbp.2020.04.008>.
- [71] V. D. Adams, *Water and wastewater examination manual*. Routledge, 2017.
- [72] E. W. Rice, R. B. Baird, A. D. Eaton, and L. S. Clesceri, *Standard methods for the examination of water and wastewater*. American public health association Washington, DC, 2012.
- [73] S. Zerveas, M. S. Mente, D. Tsakiri, and K. Kotzabasis, "Microalgal photosynthesis induces alkalization of aquatic environment as a result of H⁺ uptake independently from CO₂ concentration – New perspectives for

- environmental applications," *Journal of Environmental Management*, vol. 289, p. 112546, 2021/07/01/ 2021, doi: <https://doi.org/10.1016/j.jenvman.2021.112546>.
- [74] K. Nahar and S. Hoque, "Phytoremediation to improve eutrophic ecosystem by the floating aquatic macrophyte, water lettuce (*Pistia stratiotes* L.) at lab scale," *The Egyptian Journal of Aquatic Research*, vol. 47, no. 2, pp. 231-237, 2021/06/01/ 2021, doi: <https://doi.org/10.1016/j.ejar.2021.05.003>.
- [75] F. Li *et al.*, "Effects of Rice-Fish Co-culture on Oxygen Consumption in Intensive Aquaculture Pond," *Rice Science*, vol. 26, no. 1, pp. 50-59, 2019/01/01/ 2019, doi: <https://doi.org/10.1016/j.rsci.2018.12.004>.
- [76] M. A. Hossain, M. A. Hossain, M. A. Haque, M. M. R. Mondol, M. Harun-Ur-Rashid, and S. K. Das, "Determination of suitable stocking density for good aquaculture practice-based carp fattening in ponds under drought-prone areas of Bangladesh," *Aquaculture*, vol. 547, p. 737485, 2022/01/30/ 2022, doi: <https://doi.org/10.1016/j.aquaculture.2021.737485>.
- [77] L. M. Schuijt, T. J. H. M. van Bergen, L. P. M. Lamers, A. J. P. Smolders, and P. F. M. Verdonchot, "Aquatic worms (Tubificidae) facilitate productivity of macrophyte *Azolla filiculoides* in a wastewater biocascade system," *Science of The Total Environment*, vol. 787, p. 147538, 2021/09/15/ 2021, doi: <https://doi.org/10.1016/j.scitotenv.2021.147538>.
- [78] F. Sekli Belaïdi *et al.*, "Accurate physiological monitoring using lab-on-a-chip platform for aquatic micro-organisms growth and optimized culture," *Sensors and Actuators B: Chemical*, vol. 321, p. 128492, 2020/10/15/ 2020, doi: <https://doi.org/10.1016/j.snb.2020.128492>.
- [79] M. E. Cunha *et al.*, "Understanding the individual role of fish, oyster, phytoplankton and macroalgae in the ecology of integrated production in earthen ponds," *Aquaculture*, vol. 512, p. 734297, 2019/10/15/ 2019, doi: <https://doi.org/10.1016/j.aquaculture.2019.734297>.
- [80] S. D. Rawles, B. W. Green, M. E. McEntire, T. G. Gaylord, and F. T. Barrows, "Reducing dietary protein in pond production of hybrid striped bass (*Morone chrysops* × *M. saxatilis*): Effects on fish performance and water

- quality dynamics," *Aquaculture*, vol. 490, pp. 217-227, 2018/03/01/ 2018, doi: <https://doi.org/10.1016/j.aquaculture.2018.01.045>.
- [81] H. Liu *et al.*, "Biofloc formation improves water quality and fish yield in a freshwater pond aquaculture system," *Aquaculture*, vol. 506, pp. 256-269, 2019/05/15/ 2019, doi: <https://doi.org/10.1016/j.aquaculture.2019.03.031>.
- [82] R. Hoess and J. Geist, "Nutrient and fine sediment loading from fish pond drainage to pearl mussel streams - Management implications for highly valuable stream ecosystems," *J Environ Manage*, vol. 302, no. Pt A, p. 113987, Jan 15 2022, doi: 10.1016/j.jenvman.2021.113987.
- [83] S. R. Paudel, "Nitrogen transformation in engineered aquaponics with water celery (*Oenanthe javanica*) and koi carp (*Cyprinus carpio*): Effects of plant to fish biomass ratio," *Aquaculture*, vol. 520, p. 734971, 2020/04/15/ 2020, doi: <https://doi.org/10.1016/j.aquaculture.2020.734971>.
- [84] K. Tawatbundit and S. Mopoung, "Activated Carbon Preparation from Sugarcane Leaf via a Low Temperature Hydrothermal Process for Aquaponic Treatment," *Materials*, vol. 15, p. 2133, 03/14 2022, doi: 10.3390/ma15062133.



APPENDIX

มหาวิทยาลัยนครพนม

APPENDIX A CHAPTER III

Table 6 The %moisture calculation of sugarcane leaf

No.	Beaker	SL (before)	Beaker + Dry SL	Dry SL	%M
1	104.8807	2.0181	106.8512	1.9705	2.3587
2	98.3622	2.0217	100.3374	1.9752	2.3000
3	95.6567	2.0172	97.6184	1.9617	2.7513
4	98.5819	2.0584	100.5834	2.0015	2.7643
5	104.5404	2.0062	106.4879	1.9475	2.9259
6	98.9762	2.0119	100.9320	1.9558	2.7884
				Average	2.7680
				S.D.	0.0188

Table 7 The %ash calculation of sugarcane leaf

No.	Crucible	AC (before)	Crucible + AC (after)	AC (after)	%ASH
1	209.9868	5.3567	210.2756	0.2888	5.3914
2	210.1205	5.1802	210.5282	0.4077	7.8704
3	212.9370	5.4002	213.2958	0.3588	6.6442
4	209.2268	4.9065	209.6054	0.3786	7.7163
5	208.0038	5.1984	208.4018	0.3980	7.6562
6	212.6299	5.5224	213.0290	0.3991	7.2269
				Average	7.6174
				S.D.	0.2755

Table 8 The %volatile matter calculation of sugarcane leaf

No.	C+L	AC (before)	C+L+AC (after)	AC (after)	%WL	%VM
1	311.6283	1.9306	311.7444	0.1161	93.9863	83.6009
2	305.6256	1.9307	305.6348	0.0092	99.5235	89.1381
3	296.0173	1.9321	296.0877	0.0704	96.3563	85.9709
4	310.8766	1.9339	310.9631	0.0865	95.5272	85.1418
5	290.0954	1.9268	290.2173	0.1219	93.6734	83.2880
					Average	84.0102
					S.D.	0.9923

Table 9 The %moisture calculation of SLAC without hydrothermal pretreatment at 300°C activation temperature

No.	Beaker	AC (before)	Beaker + Dry AC	AC (after)	%M
1	97.2968	1.0086	98.2930	0.9962	1.2294
2	119.0124	1.0026	120.0028	0.9904	1.2168
3	106.1607	1.0026	107.1590	0.9983	0.4289
4	98.2780	2.0128	100.2532	1.9752	1.8680
5	123.1433	2.1850	125.2842	2.1409	2.0183
6	100.6967	2.0020	102.6641	1.9674	1.7283
				Average	1.8715
				S.D.	0.1450

Table 10 The %ash calculation of SLAC without hydrothermal pretreatment at 300°C activation temperature

No.	Crucible	AC (before)	Crucible + AC (after)	AC (after)	%ASH
1	41.2229	1.0122	41.3540	0.1311	12.9520
2	38.4014	1.0399	38.4989	0.0975	9.3759
3	38.3986	1.0185	38.5145	0.1159	11.3795
4	39.7836	1.0165	39.9310	0.1474	14.5007
5	43.7126	1.0049	43.8822	0.1696	16.8773
6	41.0959	1.3200	41.2662	0.1703	12.9015
Average					12.4110
S.D.					0.8937

Table 11 The %volatile mater calculation of SLAC without hydrothermal pretreatment at 300°C activation temperature

No.	C+L	AC (before)	C+L+AC (After)	AC (after)	%WL	%VM
1	59.9225	1.0012	60.0422	0.1197	88.0443	73.7618
2	68.1136	1.0021	68.2562	0.1426	85.7699	71.4874
3	67.6003	1.0039	67.7514	0.1511	84.9487	70.6662
4	67.2493	1.0014	67.3786	0.1293	87.0881	72.8056
5	67.6282	1.0006	67.7434	0.1152	88.4869	74.2044
6	72.6565	1.0013	72.7759	0.1194	88.0755	73.7930
Average						73.9198
S.D.						0.2470

Table 12 The %yield calculation of SLAC without hydrothermal pretreatment at 300°C activation temperature

No.	Crucible	AC (before)	Crucible + AC (after)	AC (after)	%Yield
1	209.9700	10.0100	213.3800	3.4100	34.1000
2	210.3900	10.0200	213.9900	3.6000	36.0000
3	212.9600	10.0100	217.6600	4.7000	47.0000
4	209.6000	10.0400	214.5200	4.9200	49.2000
5	208.1900	10.0100	210.9300	2.7400	27.4000
6	212.7800	10.0100	216.7200	3.9400	39.4000
				Average	36.5000
				S.D.	2.6851

Table 13 The %moisture calculation of SLAC 0%KMnO₄ with hydrothermal pretreatment at 300°C activation temperature

No.	Beaker	AC (before)	Beaker + AC (after)	AC (after)	%M
1	117.5617	1.0034	118.5276	0.9659	3.7373
2	95.6474	1.1524	96.7559	1.1085	3.8094
3	98.5760	1.2803	99.8103	1.2343	3.5929
4	98.9657	1.0909	100.0113	1.0456	4.1525
5	107.9994	1.1307	109.0870	1.0876	3.8118
6	103.9007	1.3341	105.1877	1.2870	3.5305
				Average	3.6202
				S.D.	0.1061

Table 14 The %ash calculation of SLAC 0%KMnO₄ with hydrothermal pretreatment at 300°C activation temperature

No.	Crucible	AC (before)	Crucible + AC (after)	AC (after)	%ASH
1	41.2267	1.0015	41.3134	0.0867	8.6570
2	38.3860	1.0185	38.4942	0.1082	10.6235
3	38.4262	1.0078	38.5404	0.1142	11.3316
4	41.0221	1.0054	41.1729	0.1508	14.9990
5	38.6896	1.0428	38.8361	0.1465	14.0487
6	41.2770	1.1601	41.4548	0.1778	15.3263
Average					14.7913
S.D.					0.6636

Table 15 The %volatile matter calculation of SLAC 0%KMnO₄ with hydrothermal pretreatment at 300°C activation temperature

No.	C+L	AC (before)	C+L+AC (After)	AC (after)	%WL	%VM
1	69.1817	1.0095	69.3265	0.1448	85.6563	67.2448
2	58.6475	1.0025	58.6927	0.0452	95.4913	77.0798
3	67.5524	1.0076	67.6898	0.1374	86.3636	67.9521
4	67.2464	1.0035	67.3818	0.1354	86.5072	68.0957
5	67.6280	1.0180	67.7554	0.1274	87.4853	69.0738
6	70.1823	1.0018	70.3040	0.1217	87.8519	69.4404
Average						67.7642
S.D.						0.4555

Table 16 The %yield calculation of SLAC 0%KMnO₄ with hydrothermal pretreatment at 300°C activation temperature

No.	Crucible	SL (before)	Crucible + AC (after)	AC (after)	%Yield
1	209.8200	10.0100	213.8500	4.0300	40.3000
2	210.2500	10.0100	214.0900	3.8400	38.4000
3	212.9000	10.0300	218.7500	5.8500	58.5000
4	209.3900	10.0200	213.9700	4.5800	45.8000
5	207.9900	10.0100	211.4700	3.4800	34.8000
6	212.6300	10.0100	216.1800	3.5500	35.5000
				Average	36.2333
				S.D.	1.9088

Table 17 The %moisture calculation of SLAC 1%KMnO₄ with hydrothermal pretreatment at 300°C activation temperature

No.	Pedri plate	AC (before)	Pedri plate + AC (after)	AC (after)	%M
1	43.1736	1.0410	44.1764	1.0028	3.6695
2	40.8024	1.0189	41.7806	0.9782	3.9945
3	45.9371	1.0389	46.9372	1.0001	3.7347
4	40.6086	1.0642	41.6352	1.0266	3.5332
5	47.3512	1.0145	48.3314	0.9802	3.3810
6	42.2356	1.0284	43.2275	0.9919	3.5492
				Average	3.7996
				S.D.	0.1719

Table 18 The %ash calculation of SLAC 1%KMnO₄ with hydrothermal pretreatment at 300°C activation temperature

No.	Pedri plate	AC (before)	Pedri plate + AC (after)	AC (after)	%ASH
1	38.4012	1.0009	38.5221	0.1209	12.0791
2	41.0576	1.5544	41.3539	0.2963	19.0620
3	31.9077	1.5944	32.1721	0.2644	16.5830
4	38.6137	1.6385	38.8628	0.2491	15.2029
5	38.8098	1.5120	39.0835	0.2737	18.1019
6	40.0640	1.9265	40.4353	0.3713	19.2733
				Average	18.8124
				S.D.	0.6243

Table 19 The %volatile matter calculation of SLAC 1%KMnO₄ with hydrothermal pretreatment at 300°C activation temperature

No.	C + L	AC (before)	C + L + AC (after)	AC (after)	%WL	%VM
1	69.1888	1.0055	69.3575	0.1687	83.2223	60.6103
2	58.4805	1.0027	58.6795	0.1990	80.1536	57.5416
3	67.5421	1.0064	67.7077	0.1656	83.5453	60.9333
4	67.2572	1.0086	67.3637	0.1065	89.4408	66.8288
5	67.6356	1.0074	67.7672	0.1316	86.9367	64.3247
6	70.1849	0.8436	70.3102	0.1253	85.1470	62.5350
				Average		61.3595
				S.D.		1.0307

Table 20 The %yield calculation of SLAC 1%KMnO₄ with hydrothermal pretreatment at 300°C activation temperature

No.	Crucible	SL (Before)	Crucible + AC (after)	AC (after)	%Yield
1	209.8500	9.1600	213.6900	3.8400	41.9214
2	210.3100	9.4200	213.9200	3.6100	38.3227
3	212.9200	9.0100	216.1300	3.2100	35.6271
4	209.4200	9.0500	214.4000	4.9800	55.0276
5	207.9900	9.3000	212.4600	4.4700	48.0645
6	212.6200	9.1200	216.1000	3.4800	38.1579
				Average	37.3692
				S.D.	1.5110

Table 21 The %moisture calculation of SLAC 3%KMnO₄ with hydrothermal pretreatment at 300°C activation temperature

No.	Pedri plates	AC (before)	Pedri plates + AC (after)	AC (after)	%M
1	40.8034	1.0021	41.7572	0.9538	4.8199
2	42.2397	1.0028	43.1958	0.9561	4.6570
3	43.1736	1.0977	44.2240	1.0504	4.3090
4	40.7994	1.0793	41.8287	1.0293	4.6326
5	45.9368	1.0490	46.9339	0.9971	4.9476
6	40.6087	1.0823	41.6409	1.0322	4.6290
				Average	4.6395
				S.D.	0.0152

Table 22 The %ash calculation of SLAC 3%KMnO₄ with hydrothermal pretreatment at 300°C activation temperature

No.	Pedri plates	AC (before)	Pedri plates + AC (after)	AC (after)	%ASH
1	31.7066	1.0034	31.8390	0.1324	13.1951
2	38.4068	1.0015	38.5868	0.1800	17.9730
3	38.4008	1.0075	38.5603	0.1595	15.8313
4	38.5265	1.0001	38.7234	0.1969	19.6880
5	39.8723	1.0249	40.0806	0.2083	20.3239
6	41.2611	1.2538	41.5577	0.2966	23.6561
				Average	19.3283
				S.D.	1.2160

Table 23 The %volatile matter calculation of SLAC 3%KMnO₄ with hydrothermal pretreatment at 300°C activation temperature

No.	C + L	AC (before)	C + L + AC (after)	AC (after)	%WL	%Volatile
1	69.1928	1.0005	69.3647	0.1719	99.7516	75.7838
2	58.5493	1.0050	58.7638	0.2145	99.6336	75.6658
3	67.5558	1.0020	67.7036	0.1478	99.7812	75.8134
4	67.2695	1.0072	67.4388	0.1693	99.7483	75.7805
5	67.6430	1.0152	67.8269	0.1839	99.7281	75.7603
6	70.1848	0.7519	70.3236	0.1388	99.8022	75.8344
				Average		75.7749
				S.D.		0.0127

Table 24 The %yield calculation of SLAC 3%KMnO₄ with hydrothermal pretreatment at 300°C activation temperature

No.	Crucible	SLs (before)	Crucible + AC (after)	AC (after)	% Yield
1	205.0900	9.1300	208.9800	3.8900	42.6068
2	212.6400	9.0500	217.4300	4.7900	52.9282
3	196.6800	9.1200	200.7200	4.0400	44.2982
4	198.1200	9.1200	203.5400	5.4200	59.4298
5	208.6100	9.1900	212.4700	3.8600	42.0022
6	208.2100	9.1600	211.8000	3.5900	39.1921
				Average	41.2670
				S.D.	1.8222

Table 25 The %moisture calculation of SLAC 5%KMnO₄ with hydrothermal pretreatment at 300°C activation temperature

No.	Beaker	AC (before)	Beaker + AC (after)	AC (after)	%M
1	106.1573	1.0324	107.1508	0.9935	3.7679
2	95.1172	1.0052	96.0836	0.9664	3.8599
3	107.5320	1.1909	108.6776	1.1456	3.8038
4	119.0062	1.1045	120.0767	1.0705	3.0783
5	117.5744	1.0154	118.5561	0.9817	3.3189
6	123.1156	1.0595	124.1439	1.0283	2.9448
				Average	3.8106
				S.D.	0.0464

Table 26 The %ash calculation of SLAC 5%KMnO₄ with hydrothermal pretreatment at 300°C activation temperature

No.	Crucible	AC (before)	Crucible + AC (after)	AC (after)	%ASH
1	31.7140	1.0012	31.9303	0.2163	21.6041
2	41.2380	1.0002	41.4485	0.2105	21.0458
3	38.4089	1.0012	38.6500	0.2411	24.0811
4	32.0744	1.2089	32.2295	0.1551	12.8298
5	38.8575	1.3374	39.0675	0.2100	15.7021
6	40.0972	0.9046	40.2715	0.1743	19.2682
Average					20.6394
S.D.					1.2198

Table 27 The %volatile matter calculation of SLAC 5%KMnO₄ with hydrothermal pretreatment at 300°C activation temperature

No.	C + L	AC (before)	C + L + AC (after)	AC (after)	%WL	%VM
1	69.2036	1.0094	69.4035	0.1999	99.7111	75.2611
2	58.5547	1.7068	59.0314	0.4767	99.1859	74.7359
3	67.5696	1.0150	67.7581	0.1885	99.7210	75.2710
4	67.2912	1.1660	67.6369	0.3457	99.4863	75.0363
5	67.6546	1.0855	67.8246	0.1700	99.7487	75.2987
6	70.1930	1.0023	70.3313	0.1383	99.8030	75.3530
Average						75.2770
S.D.						0.0195

Table 28 The %yield calculation of SLAC 5%KMnO₄ with hydrothermal pretreatment at 300°C activation temperature

No.	Crucible	SL (before)	Crucible + AC (after)	AC (after)	% Yield
1	209.7800	12.7000	213.8900	4.1100	32.3622
2	210.1900	9.6300	214.2300	4.0400	41.9522
3	212.8800	6.5400	217.6400	4.7600	72.7829
4	209.4100	9.6200	215.4000	5.9900	62.2661
5	207.9300	9.6300	211.7400	3.8100	39.5639
6	212.5700	7.2600	215.8300	3.2600	44.9036
				Average	42.1399
				S.D.	2.6748

Table 29 The %moisture calculation of SLAC without hydrothermal pretreatment at 350°C activation temperature

No.	Beaker	AC (before)	Beaker + AC (after)	AC (after)	%M
1	100.7107	1.0085	101.6881	0.9774	3.0838
2	107.5343	1.0060	108.5116	0.9773	2.8529
3	117.5773	1.0072	118.5501	0.9728	3.4154
4	98.2962	1.0080	99.2568	0.9606	4.7024
5	103.9148	1.0017	104.8815	0.9667	3.4941
6	95.1171	1.0020	96.0846	0.9675	3.4431
				Average	3.4509
				S.D.	0.0399

Table 30 The %ash calculation of SLAC without hydrothermal pretreatment at 350°C activation temperature

No.	Crucible	AC (before)	Crucible + AC (after)	AC (after)	%ASH
1	41.0098	1.0259	41.1577	0.1479	14.4166
2	42.0773	1.0193	42.2184	0.1411	13.8428
3	42.1378	1.2455	42.3299	0.1921	15.4195
4	43.1450	1.2780	43.2900	0.1450	11.3459
5	37.5569	1.2491	37.7179	0.1610	12.8893
6	42.1456	1.1215	42.2831	0.1375	12.2604
				Average	14.5597
				S.D.	0.7980

Table 31 The %volatile matter calculation of SLAC without hydrothermal pretreatment at 350°C activation temperature

No.	C + L	AC (before)	C + L + AC (after)	AC (after)	%WL	%VM
1	66.9365	1.0007	67.0526	0.1161	88.3981	70.3875
2	68.0189	1.0022	68.1577	0.1388	86.1505	68.1399
3	71.2877	1.0014	71.5690	0.2813	71.9093	53.8988
4	64.6895	1.0006	64.9607	0.2712	72.8963	54.8857
5	69.4382	1.0057	69.6054	0.1672	83.3748	65.3642
6	66.9329	1.0014	67.1395	0.2066	79.3689	61.3583
				Average		67.9639
				S.D.		2.5163

Table 32 The %yield calculation of SLAC without hydrothermal pretreatment at 350°C activation temperature

No.	Crucible	SL (before)	Crucible + AC (after)	AC (after)	% Yield
1	205.6500	10.0100	208.0800	2.4300	24.3000
2	212.7000	10.0100	214.3000	1.6000	16.0000
3	197.0700	10.0200	199.5500	2.4800	24.8000
4	198.4000	10.0400	202.3800	3.9800	39.8000
5	208.7100	10.0200	210.8400	2.1300	21.3000
6	208.3600	10.0400	212.0400	3.6800	36.8000
				Average	23.4667
				S.D.	1.8930

Table 33 The %moisture calculation of SLAC 0%KMnO₄ with hydrothermal pretreatment at 350°C activation temperature

No.	Pedri plate	AC (before)	Pedri plates + AC (after)	AC (after)	%M
1	43.3345	1.0096	44.3200	0.9855	2.3871
2	43.0654	1.0018	44.0230	0.9576	4.4121
3	44.2706	1.0047	45.2225	0.9519	5.2553
4	41.9815	1.0045	42.9446	0.9631	4.1215
5	42.1963	1.0006	43.1574	0.9611	3.9476
6	46.1245	1.0036	47.0854	0.9609	4.2547
				Average	4.2627
				S.D.	0.1455

Table 34 The %ash calculation of SLAC 0%KMnO₄ with hydrothermal pretreatment at 350°C activation temperature

No.	Crucible	AC (Before)	Crucible + AC (after)	AC (after)	%Moisture
1	41.0265	1.0046	41.1635	0.1370	13.6373
2	44.5905	1.0088	44.7734	0.1829	18.1305
3	42.1598	1.0156	42.3390	0.1792	17.6447
4	41.3443	1.0238	41.5246	0.1803	17.6109
5	42.6206	1.0463	42.7682	0.1476	14.1069
6	37.3306	1.0214	37.4899	0.1593	15.5962
				Average	17.7954
				S.D.	0.2907

Table 35 The %volatile matter calculation of SLAC 0%KMnO₄ with hydrothermal pretreatment at 350°C activation temperature

No.	C + L	AC (before)	C + L + AC (after)	AC (after)	%WL	%VM
1	66.9387	1.0006	67.1472	0.2085	79.1625	57.1044
2	68.0052	1.0048	68.2589	0.2537	74.7512	52.6931
3	71.3373	1.0024	71.5515	0.2142	78.6313	56.5732
4	64.6893	1.0108	64.9013	0.2120	79.0265	56.9684
5	69.3991	1.0058	69.6546	0.2555	74.5973	52.5392
6	66.9273	1.0064	67.1433	0.2160	78.5374	56.4792
				Average		56.6736
				S.D.		0.2596

Table 36 The %yield calculation of SLAC 0%KMnO₄ with hydrothermal pretreatment at 350°C activation temperature

No.	Crucible	SL (before)	Crucible + AC (after)	AC (after)	% Yield
1	205.4100	9.4300	207.8700	2.4600	26.0870
2	212.6200	9.3500	214.5500	1.9300	20.6417
3	196.8500	9.4200	198.8400	1.9900	21.1253
4	198.4100	9.4000	202.2500	3.8400	40.8511
5	208.6200	9.3500	211.4500	2.8300	30.2674
6	208.3300	9.3700	210.7300	2.4000	25.6137
				Average	23.3669
				S.D.	2.8809

Table 37 The %moisture calculation of SLAC 1%KMnO₄ with hydrothermal pretreatment at 350°C activation temperature

No.	Pedri plate	AC (before)	Pedri plate + AC (after)	AC (after)	%M
1	43.3299	1.0538	44.3348	1.0049	4.6403
2	43.0598	1.0055	44.0156	0.9558	4.9428
3	44.2651	1.0057	44.2253	0.9602	4.5242
4	41.9767	1.0607	42.9887	1.0120	4.5913
5	42.1921	1.0725	43.2119	1.0198	4.9138
6	46.1188	1.0380	47.1097	0.9909	4.5376
				Average	4.5510
				S.D.	0.0355

Table 38 The %ash calculation of SLAC 1%KMnO₄ with hydrothermal pretreatment at 350°C activation temperature

No.	Crucible	AC (before)	Crucible + AC (after)	AC (after)	%ASH
1	41.9066	1.0037	42.1088	0.2022	20.1455
2	41.0419	1.0069	41.2427	0.2008	19.9424
3	42.1151	1.0066	42.3019	0.1868	18.5575
4	41.4830	1.6389	41.7739	0.2909	17.7497
5	42.7330	1.5749	43.0869	0.3539	22.4713
6	37.3995	1.2437	37.7360	0.3365	27.0564
				Average	20.8530
				S.D.	1.4051

Table 39 The %volatile matter calculation of SLAC 1%KMnO₄ with hydrothermal pretreatment at 350°C activation temperature

No.	C + L	AC (before)	C + L + AC (after)	AC (after)	%WL	%VM
1	66.9542	1.0060	67.1954	0.2412	76.0239	50.6198
2	68.0149	1.0072	68.2390	0.2241	77.7502	52.3462
3	71.3479	1.0021	71.5449	0.1970	80.3413	54.9372
4	64.6959	1.0140	65.0001	0.3042	70.0000	44.5960
5	69.4057	1.0016	69.6472	0.2415	75.8886	50.4845
6	66.9301	0.7777	67.1366	0.2065	73.4473	48.0433
				Average		51.1502
				S.D.		1.0380

Table 40 The %yield calculation of SLAC 1%KMnO₄ with hydrothermal pretreatment at 350°C activation temperature

No.	Crucible	SL (before)	Crucible + AC (after)	AC (after)	%Yield
1	205.3300	9.7100	207.4300	2.1000	21.6272
2	212.6400	11.3200	215.5300	2.8900	25.5300
3	198.8100	7.2600	198.8200	0.0100	0.1377
4	198.9100	9.3200	201.4800	2.5700	27.5751
5	208.6400	9.1700	211.1100	2.4700	26.9357
6	208.3200	9.1800	209.3800	1.0600	11.5468
				Average	26.6803
				S.D.	1.0462

Table 41 The %moisture calculation of SLAC 3%KMnO₄ with hydrothermal pretreatment at 350°C activation temperature

No.	Pedri plates	AC (before)	Pedri plates + AC (after)	AC (after)	%M
1	43.3332	1.0070	44.2936	0.9604	4.6276
2	43.0645	1.0009	44.0134	0.9489	5.1953
3	44.2697	1.0088	45.2279	0.9582	5.0159
4	41.9808	1.0018	42.9306	0.9498	5.1907
5	42.1958	1.0023	43.1460	0.9502	5.1980
6	46.1242	1.0011	47.0784	0.9542	4.6848
				Average	5.1947
				S.D.	0.0037

Table 42 The %ash calculation of SLAC 3%KMnO₄ with hydrothermal pretreatment at 350°C activation temperature

No.	Crucible	AC (before)	Crucible + AC (after)	AC (after)	%ASH
1	41.8935	1.0048	42.0419	0.1484	14.7691
2	41.9752	1.0046	42.1681	0.1929	19.2017
3	39.6928	1.0040	39.9007	0.2079	20.7072
4	41.9745	1.0016	42.2070	0.2325	23.2129
5	41.1243	1.0358	41.3745	0.2502	24.1552
6	42.3999	1.0147	42.6544	0.2545	25.0813
				Average	22.6918
				S.D.	1.7821

Table 43 The %volatile matter calculation of SLAC 3%KMnO₄ with hydrothermal pretreatment at 350°C activation temperature

No.	C + L	AC (Before)	C + L + AC (after)	AC (after)	%WL	%VM
1	66.9812	1.6490	67.5146	0.5334	67.6531	39.7244
2	68.0438	1.0019	68.2730	0.2292	77.1235	49.1948
3	71.3743	1.0028	71.5894	0.2151	78.5501	50.6214
4	64.8536	1.1008	65.1944	0.3408	69.0407	41.1120
5	69.4444	1.0034	69.7175	0.2731	72.7825	44.8538
6	66.9367	1.0164	67.2224	0.2857	71.8910	43.9623
				Average		48.2233
				S.D.		3.0040

Table 44 The %yield calculation of SLAC 3%KMnO₄ with hydrothermal pretreatment at 350°C activation temperature

No.	Crucible	SL (before)	Crucible + AC (after)	AC (after)	% Yield
1	209.8100	9.1300	212.3700	2.5600	28.0394
2	210.2700	9.2000	212.7600	2.4900	27.0652
3	212.8800	9.1700	216.4100	3.5300	38.4951
4	209.4100	9.2600	213.9100	4.5000	48.5961
5	207.9900	9.1400	210.8400	2.8500	31.1816
6	212.6000	9.1300	215.4000	2.8000	30.6681
				Average	29.9631
				S.D.	1.6856

Table 45 The %moisture calculation of SLAC 5%KMnO₄ with hydrothermal pretreatment at 350°C activation temperature

No.	Beaker	AC (before)	Beaker + AC (after)	AC (after)	%M
1	107.8005	1.0199	108.7723	0.9718	4.7161
2	118.3787	1.0268	119.3802	1.0015	2.4640
3	114.8371	1.1512	115.9609	1.1238	2.3801
4	118.4125	1.0459	119.4229	1.0104	3.3942
5	114.8255	1.0248	115.8151	0.9896	3.4348
6	123.1443	1.0130	124.1223	0.9780	3.4551
				Average	3.4280
				S.D.	0.0310

Table 46 The %ash calculation of SLAC 5%KMnO₄ with hydrothermal pretreatment at 350°C activation temperature

No.	Crucible	AC (before)	Crucible + AC (after)	AC (after)	%ASH	
1	41.0585	1.0034	41.2505	0.1920	19.1349	
2	44.6156	1.0008	44.8100	0.1944	19.4245	
3	39.6900	1.0069	39.9272	0.2372	23.5575	
4	42.0346	1.0258	42.2497	0.2151	20.9690	
5	42.1269	1.2010	42.4178	0.2909	24.2215	
6	39.7062	1.5488	40.1046	0.3984	25.7231	
					Average	24.5007
					S.D.	1.1095

Table 47 The %volatile matter calculation of SLAC 5%KMnO₄ with hydrothermal pretreatment at 350°C activation temperature

No.	C + L	AC (before)	C + L + AC (After)	AC (after)	%WL	%VM
1	66.9812	1.6490	67.5146	0.5334	67.6531	39.7244
2	68.0438	1.0019	68.2730	0.2292	77.1235	49.1948
3	71.3743	1.0028	71.5894	0.2151	78.5501	50.6214
4	64.8536	1.1008	65.1944	0.3408	69.0407	41.1120
5	69.4444	1.0034	69.7175	0.2731	72.7825	44.8538
6	66.9367	1.0164	67.2224	0.2857	71.8910	43.9623
					Average	43.3094
					S.D.	1.9545

Table 48 The %yield calculation of SLAC 5%KMnO₄ with hydrothermal pretreatment at 350°C activation temperature

No.	Crucible	SL (before)	Crucible + AC (after)	AC (after)	%Yield
1	205.1500	9.4300	207.6700	2.5200	26.7232
2	212.6600	9.5400	216.3700	3.7100	38.8889
3	196.7000	10.9500	199.7700	3.0700	28.0365
4	198.1800	8.0000	202.4000	4.2200	52.7500
5	208.6300	9.5500	211.6000	2.9700	31.0995
6	208.2000	9.6100	211.2500	3.0500	31.7378
				Average	30.2913
				S.D.	1.9786

Table 49 The %moisture calculation of SLAC without hydrothermal pretreatment at 400°C activation temperature

No.	Beaker	AC (before)	Beaker + AC (after)	AC (after)	%M
1	114.8414	1.0027	115.8143	0.9729	2.9720
2	118.2983	1.0053	119.2748	0.9765	2.8648
3	123.1312	1.0086	124.1077	0.9765	3.1826
4	123.2218	1.0041	124.1389	0.9171	8.6645
5	98.5174	1.0024	99.4936	0.9762	2.6137
6	108.0159	1.0061	108.9972	0.9813	2.4650
				Average	2.8168
				S.D.	0.1839

Table 50 The %ash calculation of SLAC without hydrothermal pretreatment at 400°C activation temperature

No.	Crucible	AC (before)	Crucible + AC (after)	AC (after)	%ASH	
1	38.5324	0.9984	38.6807	0.1483	14.8538	
2	40.8922	1.0097	41.0400	0.1478	14.6380	
3	40.6204	1.0267	40.7263	0.1059	10.3146	
4	29.8460	1.0091	30.0228	0.1768	17.5206	
5	42.4964	1.0369	42.6741	0.1777	17.1376	
6	39.4983	1.0144	39.6752	0.1769	17.4389	
					Average	17.3657
					S.D.	0.2017

Table 51 The %volatile matter calculation of SLAC without hydrothermal pretreatment at 400°C activation temperature

No.	C + L	AC (before)	C + L + AC (after)	AC (after)	%WL	%VM
1	56.2760	1.0022	56.7028	0.4268	57.4137	37.2312
2	67.7162	1.0002	67.9684	0.2522	74.7850	54.6025
3	60.5991	1.0018	60.8620	0.2629	73.7572	53.5747
4	53.8362	1.0028	54.0529	0.2167	78.3905	58.2080
5	46.0617	1.0004	46.3677	0.3060	69.4122	49.2297
					Average	55.4617
					S.D.	2.4332

Table 52 The %yield calculation of SLAC without hydrothermal pretreatment at 400°C activation temperature

No.	Crucible	SL (before)	Crucible + AC (after)	AC (after)	% Yield
1	200.0300	10.0100	201.5300	1.5000	15.0000
2	213.7500	10.0600	216.2700	2.5200	25.2000
3	215.1300	10.0100	215.8800	0.7500	7.5000
4	210.4600	10.0100	212.1800	1.7200	17.2000
5	209.8100	10.0100	211.5100	1.7000	17.0000
6	210.5400	10.0400	214.0200	3.4800	34.8000
				Average	16.4000
				S.D.	1.2166

Table 53 The %moisture calculation of SLAC 0%KMnO₄ with hydrothermal pretreatment at 400°C activation temperature

No.	Pedri plate	AC (before)	Pedri plates + AC (after)	AC (after)	%M
1	47.0836	1.0017	48.0365	0.9529	4.8717
2	44.1133	1.0015	45.0653	0.9520	4.9426
3	44.3599	1.0004	45.3195	0.9596	4.0784
4	42.9261	1.0003	43.8867	0.9606	3.9688
				Average	4.6309
				S.D.	0.4798

Table 54 The %ash calculation of SLAC 0%KMnO₄ with hydrothermal pretreatment at 400°C activation temperature

No.	Crucible	AC (before)	Crucible + AC (after)	AC (after)	%ASH
1	38.5421	1.0099	38.7401	0.1980	19.6059
2	40.9034	1.0006	41.0912	0.1878	18.7687
3	40.5735	1.0023	40.8083	0.2348	23.4261
4	29.8548	1.0021	30.1235	0.2687	26.8137
5	42.4694	1.0041	42.7688	0.2994	29.8177
6	39.5164	0.8319	39.7763	0.2599	31.2417
				Average	20.6003
				S.D.	2.4828

Table 55 The %volatile matter calculation of SLAC 0%KMnO₄ with hydrothermal pretreatment at 400°C activation temperature

No.	C + L	AC (before)	C + L + AC (after)	AC (after)	%WL	%VM
1	69.4418	1.0023	69.7996	0.3578	64.3021	39.0709
2	60.6004	1.0030	60.8814	0.2810	71.9840	46.7529
3	53.8327	1.0021	54.1034	0.2707	72.9867	47.7555
4	46.0650	1.0072	46.3392	0.2742	72.7760	47.5448
				Average		47.3511
				S.D.		0.5287

Table 56 The %yield calculation of SLAC 0%KMnO₄ with hydrothermal pretreatment at 400°C activation temperature

No.	Crucible	SL (before)	Crucible + AC (after)	AC (after)	% Yield
1	199.7400	9.3400	201.6100	1.8700	20.0214
2	213.5600	9.4800	216.2300	2.6700	28.1646
3	214.7900	9.3700	216.4100	1.6200	17.2892
4	210.1200	9.4200	211.9400	1.8200	19.3206
5	209.7900	9.3700	211.6700	1.8800	20.0640
6	210.4500	9.3300	212.4000	1.9500	20.9003
Average					20.3286
S.D.					0.4956

Table 57 The %moisture calculation of SLAC 1%KMnO₄ with hydrothermal pretreatment at 400°C activation temperature

No.	Beaker	AC (before)	Beaker + AC (after)	AC (after)	%M
1	118.3789	1.0033	119.3560	0.9771	2.6114
2	98.2863	1.0538	99.3401	0.9926	4.6403
3	107.5295	1.0086	108.5054	0.9759	3.2421
4	95.1136	1.0038	96.0828	0.9692	3.4469
5	119.0056	1.0055	119.9633	0.9577	4.7539
6	117.5747	1.0066	118.5333	0.9586	4.7685
Average					4.7209
S.D.					0.0642

Table 58 The %ash calculation of SLAC 1%KMnO₄ with hydrothermal pretreatment at 400°C activation temperature

No.	Crucible	AC (before)	Crucible + AC (after)	AC (after)	%ASH
1	41.9066	1.0037	42.1088	0.2022	20.1455
2	41.0419	1.0069	41.2427	0.2008	19.9424
3	42.1151	1.0066	42.3019	0.1868	18.5575
4	44.6030	1.0166	44.7785	0.1755	17.2634
5	41.4830	1.6389	41.7739	0.2909	17.7497
6	42.7330	1.5749	43.0869	0.3539	22.4713
Average					20.8530
S.D.					1.4051

Table 59 The %volatile matter calculation of SLAC 1%KMnO₄ with hydrothermal pretreatment at 400°C activation temperature

No.	C + L	AC (before)	C + L + AC (after)	AC (after)	%WL	%VM
1	56.2772	1.0006	56.5034	0.2262	77.3936	49.8479
2	70.4540	1.0001	70.7307	0.2767	72.3328	44.7871
3	69.4595	1.0063	69.6670	0.2075	79.3799	51.8342
4	60.6262	1.0091	60.6670	0.0408	95.9568	68.4111
5	53.8364	1.0080	54.1095	0.2731	72.9067	45.3610
6	46.1427	0.7335	46.3875	0.2448	66.6258	39.0801
Average						46.6653
S.D.						2.7711

Table 60 The %yield calculation of SLAC 1%KMnO₄ with hydrothermal pretreatment at 400°C activation temperature

No.	Crucible	SL (before)	Crucible + AC (after)	AC (after)	% Yield
1	199.6400	9.3000	200.7000	1.0600	11.3978
2	213.5600	9.3000	215.7500	2.1900	23.5484
3	214.7600	9.2700	216.6100	1.8500	19.9569
4	210.0600	8.9700	212.1000	2.0400	22.7425
5	209.8000	9.3100	212.5900	2.7900	29.9678
6	210.3600	9.9200	213.5600	3.2000	32.2581
				Average	22.0826
				S.D.	1.8845

Table 61 The %moisture calculation of SLAC 3%KMnO₄ with hydrothermal pretreatment at 400°C activation temperature

No.	Pedri plate	AC (before)	Pedri plate + AC (after)	AC (after)	%M
1	42.4298	1.0027	43.3768	0.9470	5.5550
2	48.0806	1.0024	49.0296	0.9490	5.3272
3	47.0828	1.0004	48.0252	0.9424	5.7977
4	44.1129	1.0044	45.0585	0.9456	5.8542
5	44.3594	1.0095	45.3153	0.9559	5.3096
6	42.9257	1.0054	43.8900	0.9643	4.0879
				Average	5.3973
				S.D.	0.1369

Table 62 The %ash calculation of SLAC 3%KMnO₄ with hydrothermal pretreatment at 400°C activation temperature

No.	Crucible	AC (before)	Crucible+ AC (after)	AC (after)	%ASH
1	38.5590	1.0020	38.8289	0.2699	26.9361
2	40.5832	1.0055	40.8347	0.2515	25.0124
3	43.8688	1.0383	44.1206	0.2518	24.2512
4	41.3312	1.0189	41.5593	0.2281	22.3869
5	30.2718	1.0575	30.5469	0.2751	26.0142
6	42.5361	1.0551	42.8286	0.2925	27.7225
Average					26.8909
S.D.					0.8550

Table 63 The %volatile matter calculation of SLAC 3%KMnO₄ with hydrothermal pretreatment at 400°C activation temperature

No.	C + L	AC (before)	C + L + AC (after)	AC (after)	%WL	%VM
1	56.2826	1.0027	56.5628	0.2802	72.0555	39.7673
2	70.4964	1.0012	70.9039	0.4075	59.2988	27.0106
3	69.4832	1.0012	69.7730	0.2898	71.0547	38.7665
4	60.6466	1.0184	60.9716	0.3250	68.0872	35.7990
5	53.8451	1.0166	54.1506	0.3055	69.9488	37.6607
Average						38.7315
S.D.						1.0537

Table 64 The %yield calculation of SLAC 3%KMnO₄ with hydrothermal pretreatment at 400°C activation temperature

No.	Crucible	SL (before)	Crucible + AC (after)	AC (after)	% Yield
1	199.6000	9.4600	201.5900	1.9900	21.0359
2	213.4200	8.8600	215.6000	2.1800	24.6050
3	214.7200	9.4400	216.8500	2.1300	22.5636
4	210.0300	9.3900	211.0100	0.9800	10.4366
5	209.8000	9.4700	212.0700	2.2700	23.9704
6	210.3600	9.4500	213.6600	3.3000	34.9206
				Average	23.7130
				S.D.	1.0448

Table 65 The %moisture calculation of SLAC 5%KMnO₄ with hydrothermal pretreatment at 400°C activation temperature

No.	Beaker	AC (before)	Beaker + AC (after)	AC (after)	%M
1	103.9017	1.0277	104.8967	0.9950	3.1819
2	108.0006	1.0555	109.0166	1.0160	3.7423
3	98.5039	1.0025	99.4735	0.9696	3.2818
4	98.9650	1.0951	100.0269	1.0619	3.0317
5	118.9968	1.0785	120.0417	1.0449	3.1154
6	117.5618	1.1819	118.7090	1.1472	2.9360
				Average	3.1097
				S.D.	0.0753

Table 66 The %ash calculation of SLAC 5%KMnO₄ with hydrothermal pretreatment at 400°C activation temperature

No.	Crucible	AC (before)	Crucible + AC (after)	AC (after)	%ASH
1	40.5975	1.0076	41.0599	0.4624	45.8912
2	29.8856	1.0060	30.1904	0.3048	30.2982
3	42.4468	1.0004	42.9631	0.5163	51.6094
4	39.5280	1.0070	40.0107	0.4827	47.9345
5	43.1640	1.2018	43.5123	0.3483	28.9815
6	42.6977	1.6475	43.2242	0.5265	31.9575
				Average	30.4124
				S.D.	1.4913

Table 67 The %volatile matter calculation of SLAC 5%KMnO₄ with hydrothermal pretreatment at 400°C activation temperature

No.	C + L	AC (before)	C + L + AC (After)	AC (after)	%WL	%VM
1	70.5979	1.0012	70.9007	0.3028	69.7563	36.2342
2	69.7411	1.0020	70.1777	0.4366	56.4271	22.9050
3	60.9386	1.0004	61.1676	0.2290	77.1092	43.5871
4	53.8597	1.0020	54.1751	0.3154	68.5230	35.0009
5	46.1868	1.2032	46.5066	0.3198	73.4209	39.8988
				Average		37.0446
				S.D.		2.5475

Table 68 The %yield calculation of SLAC 5%KMnO₄ with hydrothermal pretreatment at 400°C activation temperature

No.	Crucible	SL (before)	Crucible + AC (after)	AC (after)	% Yield
1	199.5700	9.3600	201.2600	1.6900	18.0556
2	213.3600	9.3300	216.0900	2.7300	29.2605
3	214.7200	9.3500	217.0800	2.3600	25.2406
4	210.0300	9.4200	211.4600	1.4300	15.1805
5	209.8400	9.4400	212.3400	2.5000	26.4831
6	210.4000	9.4900	213.8500	3.4500	36.3541
				Average	26.9947
				S.D.	2.0582

APPENDIX B CHAPTER IV

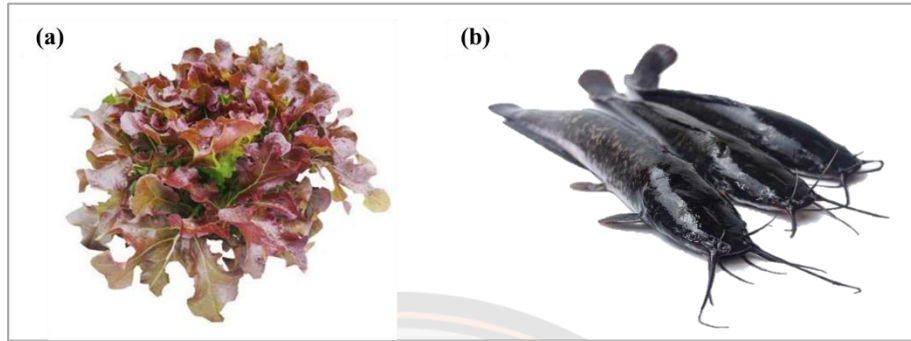


Figure 35 Red oak lettuce (a) and catfish (b)



Figure 36 3 kg of sugarcane leaf activated carbon powders



Figure 37 The fishponds were built by using interlocking bricks with 2 m of width, 2 m of length and 70 cm of height



Figure 38 The PVC tube was used to hydroponic system



Figure 39 The hydroponic system without connecting to aquaculture systems with sugarcane leaf activated carbon powders filter

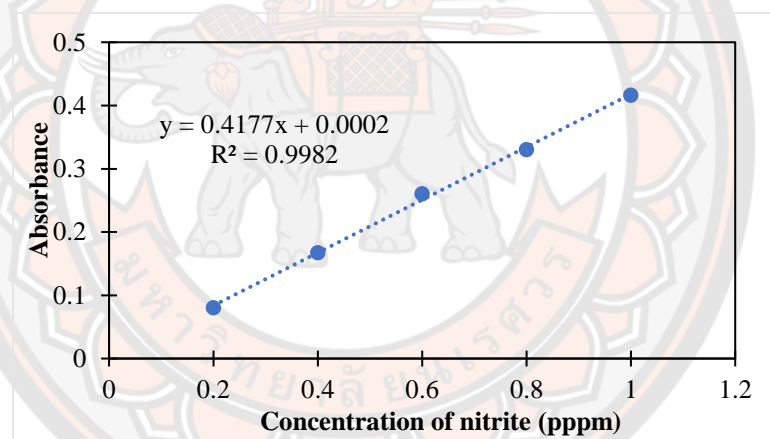


Figure 40 The calibration curve for determination the nitrites concentration in aquaponics system by spectrophotometer at the wavelength 540 nm

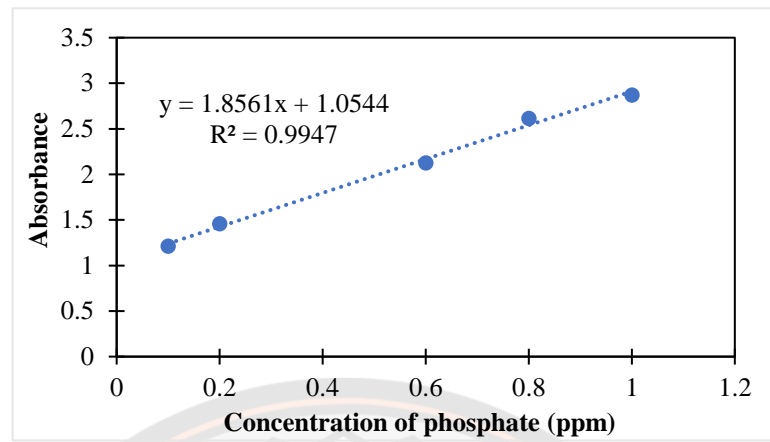


Figure 41 The calibration curve for determination the orthophosphate concentration in aquaponics system by spectrophotometer at the wavelength 880 nm

Article

Activated Carbon Preparation from Sugarcane Leaf via a Low Temperature Hydrothermal Process for Aquaponic Treatment

Kanyanat Tawatbundit and Sumrit Mopoung * 

Chemistry Department, Faculty of Science, Naresuan University, Phitsanulok 65000, Thailand;
kanyanat58@nu.ac.th

* Correspondence: sumritm@nu.ac.th; Tel.: +66-5596-3100

Abstract: The effects of hydrothermal treatment, 0–5% KMnO_4 content, and 300–400 °C pyrolysis temperature, were studied for activated carbon preparation from sugar cane leaves in comparison with non-hydrothermal treatment. The percent yield of activated carbon prepared by the hydrothermal method (20.33–36.23%) was higher than that prepared by the non-hydrothermal method (16.40–36.50%) and was higher with conditions employing the same content of KMnO_4 (22.08–42.14%). The hydrothermal and pyrolysis temperatures have the effect of increasing the carbon content and aromatic nature of the synthesized activated carbons. In addition, KMnO_4 utilization increased the O/C ratio and the content of C-O, Mn-OH, O-Mn-O, and Mn-O surface functional groups. KMnO_4 also decreases zeta potential values throughout the pH range of 3 to 11 and the surface area and porosity of the pre-hydrothermal activated carbons. The use of the pre-hydrothermal activated carbon prepared with 3% KMnO_4 and pyrolyzed at 350 °C as a filter in an aquaponic system could improve the quality of water with pH of 7.2–7.4, DO of 9.6–13.3 mg/L, and the turbidity of 2.35–2.90 NTU. It could also reduce the content of ammonia, nitrite, and phosphate with relative removal rates of 86.84%, 73.17%, and 53.33%, respectively. These results promoted a good growth of catfish and red oak lettuce.

Keywords: hydrothermal; activated carbon; aquaponic treatment; sugarcane leaf



Citation: Tawatbundit, K.; Mopoung, S. Activated Carbon Preparation from Sugarcane Leaf via a Low Temperature Hydrothermal Process for Aquaponic Treatment. *Materials* **2022**, *15*, 2133. <https://doi.org/10.3390/ma15062133>

Academic Editor: Rui Miguel Novais

Received: 30 December 2021

Accepted: 8 March 2022

Published: 14 March 2022

Publisher's Note: MDPI stays neutral with regard to jurisdictional claims in published maps and institutional affiliations.



Copyright: © 2022 by the authors. Licensee MDPI, Basel, Switzerland. This article is an open access article distributed under the terms and conditions of the Creative Commons Attribution (CC BY) license (<https://creativecommons.org/licenses/by/4.0/>).

1. Introduction

Hydrothermal carbonization is a chemical process, which can convert an organic precursor to biochar in aqueous solution under an oxygen-free atmosphere with temperatures between 150 °C and 270 °C and high pressures between 10 bar and 55 bar [1,2]. It is a low energy demand and environmentally friendly procedure, which can improve the chemical and physical characteristics of the charcoal and result in a high amount of porous structures and surface functional groups [1,3]. Importantly, the process uses water for the treatment, which is economical, non-toxic, and environmentally friendly [4]. The factors that greatly affect the efficiency of the hydrothermal process are the reaction temperature, reaction time, biomass to water ratio, and pressure [5]. Various reactions such as hydrolysis, decarboxylation, dehydration, condensation, aromatization, and polymerization occur during the hydrothermal process [2]. The process starts with hydrolysis and fragmentation of the organic compounds followed by polymerization and condensation reactions to form colloidal coal particles and dewaterability of the char product [1]. During the hydrothermal process, subcritical water is produced, which exhibits high ionic strength in a homogeneous reaction system. This subcritical water can improve the oxygen-containing surface functional groups of hydrocarbons, which enhances the activity of the activating agent and thus yields improved porosity in the carbon during activation [6]. The process also allows stabilizing the macrocellular structure of biomass before pyrolysis, resulting in higher mesoporosity [2]. However, the carbon atoms inside the hydrochar are still hindered by its functional groups or its attachment to other compounds [7]. Thus, after hydrothermal pretreatment of the wet

materials, the hydrochar product must be carbonized and activated to obtain true carbon materials and activated carbons with increased carbon content and improved the textural properties [8]. Tests of the application of the hydrothermal pretreated activated carbon have shown that it could exhibit enhanced adsorption of methylene blue by electrostatic interactions and hydrogen bonding interactions of surface oxygen-containing functional groups on the carbon surface [6]. The activated carbons were also used for water treatment and soil amendment, as a solid fuel, and for biomedical purposes [4,5]. In general, wet materials such as sewage sludge [1], organic matter [9], and wet biomass [4] with high water content are suitable for hydrothermal treatment. Especially, the lignocellulosic materials, such as plants and their derived residues and wastes, have been pretreated by the hydrothermal process for hydrochar, bio-oil, and synthesis gas production. This is because organic materials respond well in subcritical water conditions, which are maintained during the hydrothermal process [4]. In addition, the hydrothermal treatment is also performed for the purposes of ash and nitrogen removal, hemi-cellulose decomposition, reduction of H/C and O/C ratios of biomass, and biological sterilization [5,8,9]. Corn stigmata treated with CO₂ [2], acacia [5], cassava and tapioca flour treated with KOH [7], agave americana fibers and mimosa tannin [8], and rice husk treated with NaOH [9], have been used for activated carbon preparation by hydrothermal pretreatment. Sugarcane leaves are one of the waste products of sugarcane farming, produced with the rate of 6–8 tonnes of dry weight per hectare. It is lignocellulosic biomass waste, which consists of solid and polymeric organic compounds as well as silica. Sugarcane leaves consist of cellulose (31–45%), hemicelluloses (20–30%), and lignin (12–31%) [10]. It has been used for the fabrication of mesoporous materials and silica gel preparation [11]. It was also used for the reinforcement of polymer composites [12]. In addition, sugar cane leaves have been used to produce bioproducts and biomaterials such as ethanol, xylitol, biogas, enzymes, and oligosaccharides after pretreatment by physical, physicochemical, chemical, and biological processes [10]. In this research, the activated carbon from sugarcane leaves was used for water treatment in an aquaponics system. Aquaponics is an integrated system of aquaculture and hydroponics with closed-loop recycling of fresh water within the system between fish and plants [13]. The water in the aquaculture system is circulated to the hydroponics system. During water circulation in the hydroponics system, the nutrients in the water, which are the waste materials from the fish, are absorbed by the plants. The treated water is then recycled back to the aquaculture system [14]. This system could thus reduce the use of land [15]. It is also less energy-intensive, is environmentally friendly, and requires less water consumption with a minimum requirement of chemicals or fertilizers [16]. In addition, it also qualifies as an organic farming method for vegetables and fish production, utilizing sustainable food production technology [17]. However, this system is still more popular as a hobby rather than for commercial-scale production [18]. The problems with this system are turbidity, a high content of toxic nitrogen compounds (ammonia, and nitrite), and low dissolved oxygen in water. To solve these problems, factors such as stocking density, cultivation media, ratios of plants to fish, and water recirculation rates [19] were investigated. Filter suction devices are also used for water treatment in aquaponics [20]. Biological treatments (nitrifying biofilters) and solid capture via mechanical means were used for wastewater treatment [21]. According to previous reports, oyster shell [22], biochar [14], sand, rock-wool, glass wool, anthracite, pumice, calcined clay, crushed brick, polyethylene beads [19], rice biofilter [23], and vetiver [24] have been used for solid capture in the water treatment of aquaponics.

In this research, the effects of hydrothermal pretreatment and KMnO₄ addition used for activated carbon preparation from sugarcane leaves with a high content of functional surface groups were studied to achieve a decrease in the activation temperature. The final activated carbon product with a high content of surface functional groups, percent yield and good stability, which were prepared by the lowest of activation temperatures, was used for the water treatment of aquaponics.

2. Materials and Methods

The hydrothermal modification and KMnO_4 addition were used for the pretreatment of sugarcane leaves at 120 °C, 15 bar, and 0–5% KMnO_4 concentrations carried out for 6 h with the hope that the constituents in sugarcane leaves will be more easily disintegrated. The products of the hydrothermal pretreatment were activated at 300–400 °C without the addition of activating reagents, to find the lowest temperature for activated carbon production, resulting in products with a high performance in terms of chemical and physical properties and a higher mass yield. The activated carbon was applied for water treatment in an aquaponics system. The water parameters monitored in this study were pH, NH_3 , NO_2^- , DO, orthophosphate and turbidity removal efficiency, and growth of catfish and red oak lettuce.

2.1. The Production of Sugarcane Leaf-Activated Carbon

Sugarcane leaves were collected from Kamphaengphet, a province in northern Thailand. The precursor materials (10 g) were washed with distilled water, sun-dried, and cut by pruning shears to a particle size in the range of 10–20 mm. The precursor materials were weighted and placed in a container and then potassium permanganate solution with concentration of 0%, 1%, 3%, or 5%wt in distilled water was added (10 mL). The samples were immersed in the container for 24 h. After 24 h, the sample container was placed into a stainless-steel autoclave and treated at 120 °C and 15 bar with a reaction time of 6 h. The autoclave was then cooled down to room temperature (the samples produced from this process will be called hydrochar in further discussion). For samples made without hydrothermal pretreatment, the precursor materials were dried at 100 °C after being immersed in 0%, 1%, 3%, or 5%wt KMnO_4 in distilled water. The hydrochar samples and non-hydrothermal pretreatment samples were then placed into a crucible with a lid for the heating step. The pyrolysis was conducted at 300 °C, 350 °C, or 400 °C and the pyrolysis temperature was maintained constant for 6 h. The pyrolysis temperature for the preparation of activated carbon from biomass should not exceed 400 °C, a temperature at which hemicellulose, cellulose, and lignin all decompose [25].

2.2. Characteristics of Sugarcane Leaf and Sugarcane Leaf Activated Carbon

The sugarcane leaf and sugarcane leaf activated carbon were characterized by Fourier transform infrared spectrometer (FT-IR, Spectrum GX, Perkin Elmer Frontier, Richmond, Llantrisant, UK; to classify the organic, inorganic, and chemical bonds or functional groups), scanning electron microscopy and energy dispersive X-ray spectrometer (SEM, a LEO 1455 VP Electron Microscopy, Oxford instruments, Oxon, Cambridge, UK; and EDS, Edax LED1455P, AMETEK, San Luis Obispo, CA, USA; To study the surface characteristics, size, shape, and as an analytical technique used for the elemental analysis or chemical characterization), X-ray diffraction (XRD, PW 3040/60 X'Pert PRO Console, Philips, Bruker D2 PHASER, Billerica, MA, USA; To analyze and identify the type of compounds and crystal structure of the obtained activated carbon), surface area and porosity analyzer (BET, Micromeritics TriStar II3020, Bavaria, Germany; to analyze surface area characteristics, for example, pore size diameter, surface area, pore volume), and Zeta potential analyzer (Malvern zeta sizer nano -ZS Almelo, Netherlands; to investigate the potential on the surface of particles).

2.3. Using the Sugarcane Leaf Activated Carbon for Aquaponic Treatment

Four systems containing fishponds and PVC tube hydroponic systems (2 m × 2 m × 0.7 m) were built. Growth of catfish (50 fish per cubic meter) and red oak lettuce (90 plant per system) was observed and the quality of water was analyzed. A comparison between 4 sets of experiments (Figure 1) was carried out.

1. Aquaculture system (pond 1) without a hydroponics system for control experiment (Figure 1a)
2. Hydroponic system without aquaculture system (Figure 1b)

3. Aquaponics system (pond 2 and hydroponic system) without activated carbon filter (Figure 1c)
4. Aquaponics system (pond 3 and hydroponic system) with 3 kg activated carbon filter (Figure 1d)

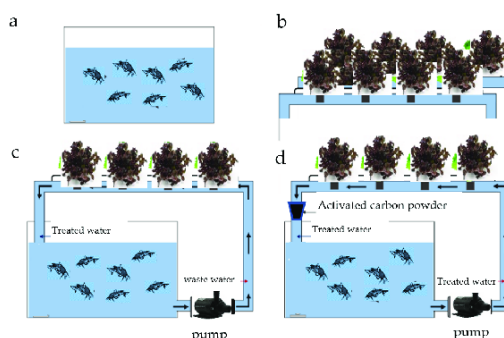


Figure 1. (a) aquaculture system; (b) hydroponic system; (c) aquaponics system; and (d) aquaponics system with activated carbon filter.

For the aquaponics system, 3 kg of activated carbon was filled in a 50 L plastic tank, which was placed between the hydroponic system and the aquaculture system (Figure 1d). The fish were fed at a rate of 5% by weight at 8:00 a.m. Analysis of the 4 water systems was made through an observation of the growth of catfish (weight of the body) every 7 days for 4 weeks and red oak lettuce by randomly selecting 10% of the sample set at week 4. Dissolved oxygen (DO), pH, and turbidity of water were measured every 7 days for 4 weeks. The content of ammonia, nitrite, and orthophosphate were measured at week 4.

2.4. Water Analysis

Water samples were collected weekly from each pond within 20 cm of the water surface at about 09:00 AM by plastic bottles. Turbidity, by turbidimeter (Jenway 6035, Jenway, Mortdale, Australia), and pH (Mettler Toledo) of water were measured. For NH_3 , NO_2^- , PO_4^{3-} , and DO analysis, the water samples were filtered through Whatman No.42 paper. NH_3 was determined by indophenol reaction, nitrite by the diazo-azo colorimetric method, and orthophosphate by an ascorbic acid method with the resulting solutions being measured by spectrophotometer (double beam, Jasco V650) at 422 nm, 540 nm, and 880 nm, respectively. Dissolved oxygen (DO) was also measured by titration with sodium thiosulphate [26]. The percent relative removal rate was used for evaluating the removal efficiency of NH_3 , NO_2^- , and orthophosphate from water.

$$\text{Relative removal rate (\%)} = [(C_0 - C_t)/C_0] \times 100\%$$

where C_0 refers to the concentration of the control (pond 1), and C_t refers to the concentration of each treatment (pond 3 or 4).

3. Results and Discussion

The aim of this study was to obtain activated carbon with sufficient chemical and physical stability for wastewater treatment applications. The beneficial properties of the final activated carbon material are its high micropore volume, surface functional groups, and its percent yield.

3.1. Percent Yield

Figure 2 shows that the percent yield of all activated carbons prepared from sugar cane leaf decreased as the activation temperature increased from 300 °C to 400 °C. This shows that the samples have undergone more extensive thermal degradation at higher activation temperatures. Furthermore, percent yields of samples prepared with hydrothermal pretreatment are higher than for samples prepared without hydrothermal pretreatment and activated at the same temperature. This is because the pre-hydrothermal process can decompose the hemicellulose in the sugar cane leaves, which causes the aromatisation reaction of pre-hydrothermal samples to begin to take place. This phenomenon makes the pre-hydrothermal samples stable to thermal activation [2,3]. Moreover, the percent yields of pyrolyzed hydrothermal samples also increase with the increasing amount of KMnO_4 from 1% to 5%. In this case, the surface areas of pre-hydrothermal samples formed after hemicellulose degradation increase with the increasing amount of KMnO_4 . The higher surface area of pre-hydrothermal samples can enhance binding of KMnO_4 to the samples [3]. In addition, the oxides of Mn and K, which are formed by the decomposition of potassium permanganate, are resistant to thermal degradation at temperatures in the 300 °C–400 °C range, thereby increasing the percent yield of pre-hydrothermal samples as compared to samples made in the absence of potassium permanganate.

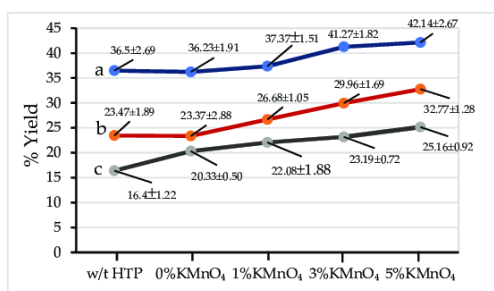


Figure 2. Percent yield of activated carbon materials made with or without hydrothermal pretreatment and with addition of KMnO_4 of 0–5% by weight at (a) 300 °C (b) 350 °C and (c) 400 °C.

3.2. Elemental Composition from EDS

For samples made at the same conditions, the carbon content of all pyrolyzed products increases with the increasing activation temperature, while the amount of oxygen shows the opposite trend (Table 1). This phenomenon indicates that the volatile matters were degraded to a greater extent at higher activation temperatures. Considering the effect of the hydrothermal pretreatment, it was found that the carbon content of the pyrolyzed pre-hydrothermal products was higher than that for the without-hydrothermal ones. This is because hemicellulose, which has a high O and H content of pre-hydrothermal samples, decomposes during the hydrothermal exposure [3] at 120 °C and 15 bar for 6 h. These results indicate that the O/C ratios of the pyrolyzed products tend to decrease with the increasing activation temperature as a result of the non-hydrothermal treatment and 0% KMnO_4 hydrothermal pre-treatment. However, the O/C ratio of pyrolyzed products tends to increase in response to the addition of potassium permanganate and is increased even further when the amount of potassium permanganate used is increased. This is due to the oxidation of the samples with potassium permanganate, resulting in a reduction in carbon content and an increase in oxygen content. Content of other elements in the pyrolyzed products tended to slightly increase with the increase in the activation temperature. In addition, the content of Mn and K increased with the increasing amount of added potassium permanganate. While some of these elements are dissolved and washed away by acetic

acid, which forms during the hydrothermal process, Ca and Si resist removal during the hydrothermal treatment [9]. In addition, these elements constitute inorganic matter, which is stable at high temperatures; therefore, it remains in the pyrolyzed products after activation.

Table 1. Elemental composition of pyrolyzed products from EDS.

Temp. (°C)	SLACs * Sample with	Elements Composition (%wt.)						
		C	O	O/C Ratio	Mn	Si	K	Ca
300	w/t HTP	60.87	35.85	0.59	0.38	1.32	0.57	0.81
	0%KMnO ₄ ⁻ HTP	69.93	21.66	0.31	1.01	4.06	1.38	0.96
	1%KMnO ₄ ⁻ HTP	62.83	27.44	0.39	1.05	4.87	2.46	1.39
	3%KMnO ₄ ⁻ HTP	57.45	30.67	0.53	1.26	4.87	4.23	1.45
	5%KMnO ₄ ⁻ HTP	50.55	29.86	0.59	5.64	7.04	4.70	2.18
350	w/t HTP	65.52	30.85	0.47	0.67	1.83	0.32	1.01
	0%KMnO ₄ ⁻ HTP	70.69	26.10	0.37	0.45	0.58	0.59	1.27
	1%KMnO ₄ ⁻ HTP	64.70	27.35	0.42	0.85	3.58	2.57	0.94
	3%KMnO ₄ ⁻ HTP	61.09	28.62	0.42	1.16	5.50	2.81	1.68
	5%KMnO ₄ ⁻ HTP	54.15	32.23	0.60	1.90	6.53	3.27	1.93
400	w/t HTP	68.46	28.28	0.41	0.45	1.45	0.97	1.22
	0%KMnO ₄ ⁻ HTP	75.05	20.17	0.27	0.60	1.67	1.58	1.23
	1%KMnO ₄ ⁻ HTP	71.68	21.29	0.30	0.66	2.43	2.54	1.40
	3%KMnO ₄ ⁻ HTP	70.88	21.83	0.31	0.82	3.65	2.60	0.21
	5%KMnO ₄ ⁻ HTP	59.83	26.44	0.44	1.21	7.74	3.86	0.60

* SLACs is sugar cane leaves; w/t HTP signifies samples without hydrothermal pre-treatment and KMnO₄ treatment.

3.3. FTIR Spectrum of Pyrolyzed Products

The peaks in the FTIR spectra of the pre-hydrothermal samples and the samples without hydrothermal treatment at 3200–3400 cm⁻¹ (O-H stretching) and about 2900 cm⁻¹ (C-H stretching) disappeared after activation at 300 °C or higher temperatures (Figure 3a–o), which is due to the pyrolytic degradation of hydrogen. Furthermore, when considering the effect of hydrothermal treatment on the surface functional groups of activated carbon, the results show that the peaks in the FTIR spectrum at 1712 cm⁻¹ (C=O stretching of hemicellulose), 1384 cm⁻¹ (-C-O-H) [27], and 622 cm⁻¹ (C-H and/or aryl C-O groups, 1) of samples without hydrothermal treatment (Figure 3a–c) are more intense than those for the pre-hydrothermal samples (Figure 3d–f) for 0% KMnO₄ at the equivalent activation temperature. It is possible that the hydrothermal effect causes the degradation of the C=O group and other functional groups of hemicellulose at 120 °C and 15 bar. Conversely, the peak at 1604 cm⁻¹ (aromatic C=C) shows the opposite result. It has been suggested that the hydrothermal effect increases the content of aromatics in the pre-hydrothermal samples to a larger extent than in samples without hydrothermal treatment due to dehydration and decarboxylation reactions [1]. Moreover, the 1604 cm⁻¹ peak intensity of both samples increases as the activation temperature increases from 300 °C to 400 °C (Figure 3a–o). It has been shown that the content of aromatics in pyrolyzed products increases with the increasing activation temperature, which promotes the condensation [1]. In regards to the effects of pre-hydrothermal treatment and activation temperature, the FTIR peaks in pre-hydrothermal samples at 1712 cm⁻¹, 1604 cm⁻¹, and 622 cm⁻¹ decrease with the increasing activation temperature from 300 °C to 400 °C for samples with 0% KMnO₄ content (Figure 3d–f). In addition, increasing the content of KMnO₄ in pre-hydrothermal samples results in FTIR spectra where the intensity of peaks at 1712 cm⁻¹, 1604 cm⁻¹ (C=C stretching), and 622 cm⁻¹ have the tendency to decrease with the increasing content of KMnO₄, while the peaks at 1094 cm⁻¹ (C-O stretching), 786 cm⁻¹, and 444 cm⁻¹ have the opposite trend for all activation temperatures between 300 °C and 400 °C (Figure 3d–o). Furthermore, the peaks in the FTIR spectrum of the pre-hydrothermal samples at 1712 cm⁻¹ disappeared

after activation at 350 °C for samples pretreated with 1–5% KMnO_4 (Figure 3h,i,k,l,n,o). In this case, potassium permanganate was expected to have a greater effect on the degradation of surface functional groups in activation products through more extensive decarboxylation and aliphatic degradation [1]. These reactions were complete for samples activated at 350 °C after pretreatment with 3–5% KMnO_4 , which indicates the stability of the final products. However, potassium permanganate also increased partial oxidation, resulting in an increased content of C-O (peak at 1094 cm^{-1}) surface functional groups and residual content of Mn-OH (622 cm^{-1}), O-Mn-O, and Mn-O bonds (444 cm^{-1}) [28] on the surface of activation products. The peaks at 1604 cm^{-1} and 1384 cm^{-1} are related to aromatic skeletal vibrations of lignin [29]. In addition, the peak at 1094 cm^{-1} is also related to the C-O and C-O-C stretching vibrations, which is characteristic of the anomeric region of cellulose-like structures [3]. These features show that there was still lignin and cellulose left in the pyrolyzed samples. This is because cellulose and lignin completely degrade at pyrolysis temperatures of 450 °C or more [1]. Furthermore, the products also exhibit FTIR vibrations consistent with the presence of functional groups containing Si-O-Si (1094 cm^{-1} and 444 cm^{-1}) and Si-O bonds (786 cm^{-1}) [30]. The presence of these functional groups in the pyrolyzed products is in good agreement with the elemental composition of the pyrolyzed products, as shown in Table 1. Therefore, the aromatic nature and presence of these functional groups in the pyrolyzed pre-hydrothermal products shows their good stability and potential for adsorption efficiency.

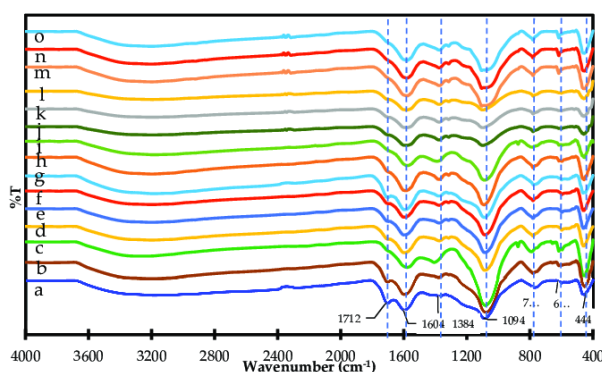


Figure 3. FTIR transmission of (a) activated carbon w/t HTP prepared at 300 °C; (b) activated carbon w/t HTP prepared at 350 °C; (c) activated carbon w/t HTP prepared at 400 °C; (d) activated carbon made with 0% KMnO_4 HTP and prepared at 300 °C; (e) activated carbon made with 0% KMnO_4 HTP and prepared at 350 °C; (f) activated carbon made with 0% KMnO_4 HTP and prepared at 400 °C; (g) activated carbon made with 1% KMnO_4 HTP and prepared at 300 °C; (h) activated carbon made with 1% KMnO_4 HTP and prepared at 350 °C; (i) activated carbon made with 1% KMnO_4 HTP and prepared at 400 °C; (j) activated carbon made with 3% KMnO_4 HTP and prepared at 300 °C; (k) activated carbon made with 3% KMnO_4 HTP and prepared at 350 °C; (l) activated carbon made with 3% KMnO_4 HTP and prepared at 400 °C; (m) activated carbon made with 5% KMnO_4 HTP and prepared at 300 °C; (n) activated carbon made with 5% KMnO_4 HTP and prepared at 350 °C; (o) and activated carbon made with 5% KMnO_4 HTP and prepared at 400 °C.

3.4. XRD Diffractogram of Pyrolyzed Products

X-ray diffraction patterns of pyrolyzed samples are shown in Figure 4. The bands with peaks at about 26.5° and 43.5° in the XRD patterns of all pyrolyzed samples are assigned to graphite flakes in a disordered layer [31]. It should be pointed out that all samples were converted to charcoal by pyrolysis in the temperature range of 300 °C to

400 °C. However, the products also have differing characteristics as a result of pyrolysis temperature, hydrothermal treatment, and the addition of various amounts of KMnO_4 . For the effect of pyrolysis temperature on the samples without hydrothermal pretreatment (Figure 4a–c), the diffractogram peaks of all pyrolyzed samples without hydrothermal pretreatment show a little peak of cellulose at $\theta = 15.1^\circ$ for pyrolysis in the temperature range of 300 °C to 400 °C. This shows that there still was cellulose left in the pyrolyzed products made without hydrothermal treatment. However, this peak decreased with the increasing pyrolysis temperature. This is because cellulose does partially decompose in the temperature range of 240 °C to 350 °C [25]. For hemicellulose, it is expected that it completely degrades in the pyrolysis temperature range of 200 °C to 260 °C [25]. In addition, these pyrolyzed products made without hydrothermal pretreatment were assumed to still contain lignin as lignin decomposes over a range of pyrolysis temperatures from 280 °C to 500 °C [25]. Lignin is amorphous [25] and therefore its XRD peak is not observed. In addition, the diffractogram peaks for products made at pyrolysis temperature of 400 °C also show more pronounced peaks of SiO_2 (24.6° , 26.5° , 28.4° , 29.9° , and 43.5°) [32], CaO (26.5° , 28.4° , 31.1° , and 36.3°), and K_2O (26.5° , 28.4° , and 40.8°) [33], due to the decomposition of various volatile substances. The compositions of these substances are derived from the elements, which are present in the original sugar cane leaves. In the same way, pyrolyzed products made with pre-hydrothermal treatment have shown the same trend of diffractogram peaks (Figure 4d–f) to that of the pyrolyzed products made without hydrothermal treatment. One exception is the XRD peak at 15.1° corresponding to cellulose, which has completely disappeared at the pyrolysis temperature of 400 °C (Figure 4f). This suggests that hydrothermal treatment affects the breakdown of cellulose in sugarcane leaves. Likewise, when 1–3% KMnO_4 was added to the pre-hydrothermal samples (Figure 4g–o), it was found that the XRD diffractograms of these pyrolyzed products exhibit the same effect as the products made with pre-hydrothermal treatment without KMnO_4 addition in the pyrolysis temperature range of 300 °C to 400 °C. This suggests that the addition of KMnO_4 had no effect on cellulose degradation in sugarcane leaves.

3.5. Zeta Potential of Pyrolyzed 0–1% KMnO_4 Pre-Hydrothermal Products

Zeta potential is used to characterize the surface electric charge of an adsorbent in solution [31]. It is one parameter that affects the affinity between the adsorbent material and the adsorbate [34], which could give a preliminary estimate of the adsorption capacity of the adsorbate for adsorbent materials [35]. Figure 5 shows only the pH dependence of the zeta potential for 0% and 1% KMnO_4 pre-hydrothermal activated carbon prepared at 350 °C. This experiment was carried out only to determine the effect of potassium permanganate on activated carbon that will be used for further water treatment. The results show that the zeta potential values of both activated carbons are negative throughout the pH range from 3 to 11, and are thus able to capture positively charged adsorbates with electrostatic force [31]. This is due to the electrons from aromatic rings on the surface of the activated carbon being involved in π - π interactions [34]. Furthermore, adding 1% KMnO_4 to pre-hydrothermal sample results in a lowering of the zeta potential value of activated carbon (Figure 3b). This is caused by the aromatic ring on the surface of the activated carbon being oxidized with potassium permanganate, which results in the destruction of the aromatic rings. In addition, C-O-H surface functional groups of hemicellulose were partially oxidized to carbonyl groups. This results in a large amount of electric charge accumulation on the surface of the KMnO_4 -treated pre-hydrothermal activated carbon and the decrease of the zeta potential values [36]. Furthermore, the zeta potential of activated carbons decreases with the increase of the solution pH over a range of pH 3.0–7.0 and then increases to a maximum value at pH 9. After pH 9, the zeta potentials of the activated carbons decrease again until pH 11, which is once again due to π - π interactions within the second layer, formed after the formation of the first layer on the surface of the activated carbon [34].

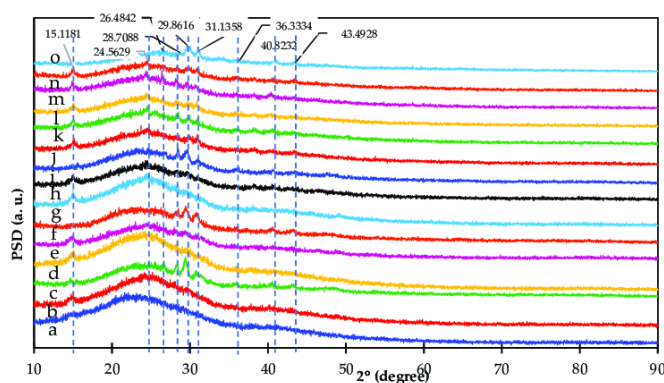


Figure 4. XRD patterns of (a) activated carbon w/t HTP prepared at 300 °C; (b) activated carbon w/t HTP prepared at 350 °C; (c) activated carbon w/t HTP prepared at 400 °C; (d) activated carbon made with 0% KMnO_4 HTP and prepared at 300 °C; (e) activated carbon made with 0% KMnO_4 HTP and prepared at 350 °C; (f) activated carbon made with 0% KMnO_4 HTP and prepared at 400 °C; (g) activated carbon made with 1% KMnO_4 HTP and prepared at 300 °C; (h) activated carbon made with 1% KMnO_4 HTP and prepared at 350 °C; (i) activated carbon made with 1% KMnO_4 HTP and prepared at 400 °C; (j) activated carbon made with 3% KMnO_4 HTP and prepared at 300 °C; (k) activated carbon made with 3% KMnO_4 HTP and prepared at 350 °C; (l) activated carbon made with 3% KMnO_4 HTP and prepared at 400 °C; (m) activated carbon made with 5% KMnO_4 HTP and prepared at 300 °C; (n) activated carbon made with 5% KMnO_4 HTP and prepared at 350 °C; (o) and activated carbon made with 5% KMnO_4 HTP and prepared at 400 °C.

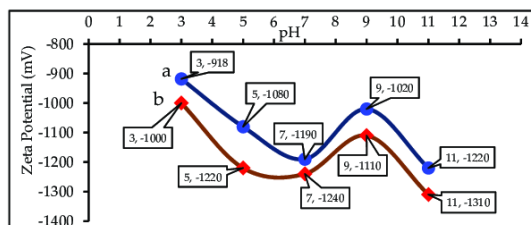


Figure 5. Zeta Potential of (a) activated carbon treated with 0% KMnO_4 HTP and prepared at 350 °C and (b) activated carbon treated with 1% KMnO_4 HTP and prepared at 350 °C.

3.6. Morphologies of Pyrolyzed Products

The hydrothermal treatment effect is evident in that it can cause a more extensive decay of the sugar cane leaves. It is evident that the pyrolyzed product made without hydrothermal treatment from sugar cane leaves and prepared at 350 °C has a cellular structure with interconnected porous lattice structures and undamaged cell walls (Figure 6a). The pyrolysis products of the pre-hydrothermal sugar cane leaves show damaged cell walls even at the pyrolysis temperature of 300 °C (Figure 6b). The cell walls of hydrothermal sugarcane leaves are further decomposed and form particles on the surface of the pyrolyzed product with an increasing pyrolysis temperature from 350 °C to 400 °C (Figure 6c,d). Especially at the pyrolysis temperature of 400 °C, the surface of the pyrolyzed product has been disintegrated to a large extent (Figure 6d). When adding potassium permanganate, small particles present on the pyrolyzed products of the pre-hydrothermal sugar leaf are

destroyed to an even greater extent and few remain as compared with the pyrolyzed products made without hydrothermal treatment (Figure 6c) and with pre-hydrothermal treatment (Figure 6e) prepared at the same pyrolysis temperature (only products made at pyrolysis temperature of 350 °C are shown). Likewise, the addition of potassium permanganate has a significant effect on the breakdown of surface particles on pyrolyzed products of pre-hydrothermal samples with more surface particles being decomposed and almost completely gone after adding potassium permanganate in the concentration range from 1% to 5% (Figure 6e–g). The surface structure of the pyrolyzed pre-hydrothermal product begins to break at 3% KMnO_4 , and the holes in the sugar cane leaf structure become apparent. Moreover, the surface structures of pyrolyzed pre-hydrothermal samples were very fractured after preparation at a pyrolysis temperature of 400 °C in comparison with pyrolyzed and 5% KMnO_4 -treated pre-hydrothermal products prepared at 350 °C (Figure 6g) and pyrolyzed and 5% KMnO_4 -treated pre-hydrothermal products prepared at 400 °C (Figure 6h). This is because the decomposition of volatile organic compounds of sugar cane leaves, which is due to hydrothermal treatment, KMnO_4 , and pyrolysis temperature.

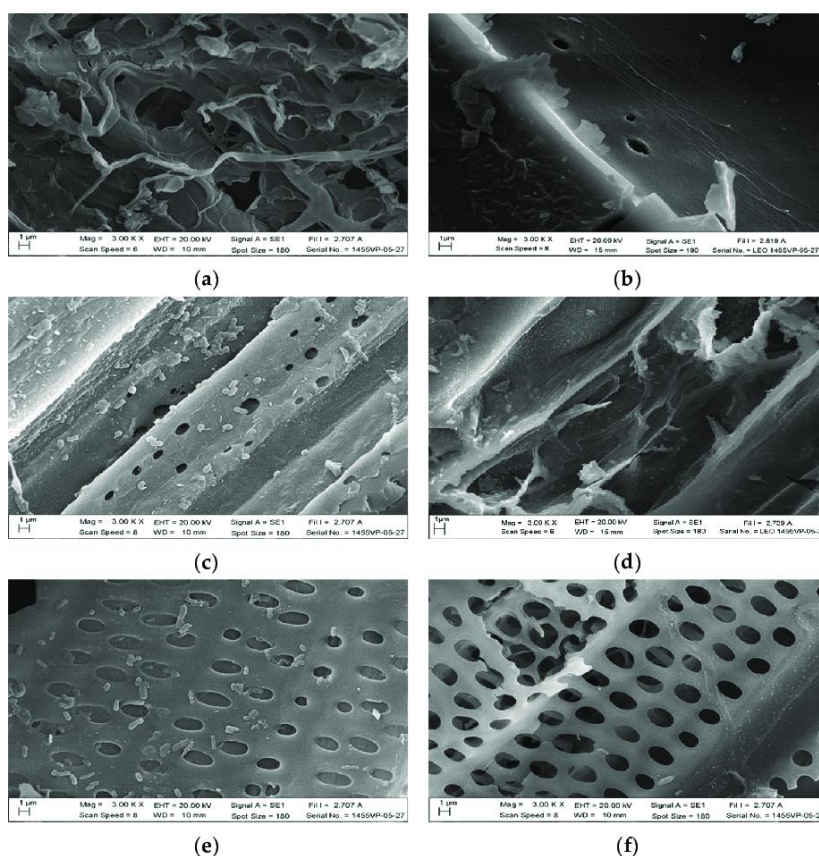


Figure 6. Cont.

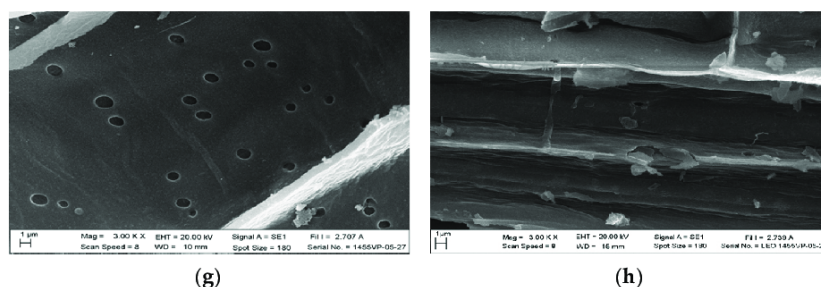


Figure 6. SEM morphologies acquired with a 3000 magnification of (a) activated carbon product pyrolyzed without hydrothermal at 350 °C; (b) activated carbon product made with 0% KMnO_4 pre-hydrothermal treatment and pyrolyzed at 300 °C; (c) activated carbon product made with 0% KMnO_4 pre-hydrothermal treatment and pyrolyzed at 350 °C; (d) activated carbon product made with 0% KMnO_4 pre-hydrothermal treatment and pyrolyzed at 400 °C; (e) activated carbon product made with 1% KMnO_4 pre-hydrothermal treatment and pyrolyzed at 350 °C; (f) activated carbon product made with 3% KMnO_4 treatment and pyrolyzed at 350 °C; (g) activated carbon product made with 5% KMnO_4 pre-hydrothermal treatment and pyrolyzed at 350 °C; (h) and activated carbon product made with 5% KMnO_4 pre-hydrothermal treatment and pyrolyzed at 400 °C.

3.7. Surface Characteristic of Sugarcane Leaf Activated Carbon

The surface areas of pyrolyzed products made with hydrothermal treatment using 0% KMnO_4 are higher than those of products made without hydrothermal treatment. In addition, the surface area increases with the increasing activation temperature from 300 °C to 400 °C for both types of pyrolyzed products (Table 2). The surface areas and micropore volumes of pyrolyzed products made with hydrothermal treatment using 0% KMnO_4 are higher than for samples made without hydrothermal treatment. This is because hydrothermal treatment can remove hemicellulose and some cellulose to generate pores on the pyrolyzed products [3]. In addition, the content of pores increases with the increasing activation temperature from 300 °C to 400 °C for both types of pyrolyzed products (Table 2). This is due to the effect of higher pyrolysis temperatures causing more extensive breakdown of cellulose and lignin present in the initial samples. The addition of KMnO_4 during the hydrothermal pretreatment results in an increased surface area and micropore volume in comparison to samples made without KMnO_4 at all pyrolysis temperatures. In addition, surface area and micropore volume also increase with an increasing temperature and potassium permanganate content. This is due to the ability of potassium permanganate to oxidize components of sugar cane leaves. However, the surface area and micropore volume of pyrolyzed 5% KMnO_4 pre-hydrothermal products decreased below those of pyrolyzed 3% KMnO_4 pre-hydrothermal products at all temperatures. This is due to the presence of excess potassium permanganate, which covers the surface of the pyrolyzed products. Furthermore, the micropore volume of products pyrolyzed at 300 °C made with 3% KMnO_4 pre-hydrothermal treatment is higher in comparison to the products pyrolyzed at 400 °C. However, the surface area of products pyrolyzed at 300 °C made with 3% KMnO_4 pre-hydrothermal treatment is close to products pyrolyzed at 400 °C made with 1% KMnO_4 pre-hydrothermal treatment.

Table 2. Surface area and porosity of sugarcane leaf activated carbon determined by BET.

Temp. (°C)	SLACs * Sample with	BET Surface Area (m ² /g)	Surface Area of Pores between 17 Å and 3000 Å (m ² /g)	Micropore Volume (cm ³ /g)	Volume of Pores between 17 Å and 3000 Å (cm ³ /g)
300	w/t HTP	0.9289	0.1997	0.000698	0.000089
	0%KMnO ₄ ⁻ HTP	2.9560	0.9345	0.006240	0.000921
	1%KMnO ₄ ⁻ HTP	5.9670	3.2251	0.003900	0.004285
	3%KMnO ₄ ⁻ HTP	13.5882	9.2956	0.006700	0.013424
	5%KMnO ₄ ⁻ HTP	7.5572	5.8829	0.002610	0.006508
350	w/t HTP	10.8815	8.8915	0.002647	0.003702
	0%KMnO ₄ ⁻ HTP	12.1574	11.7152	0.007006	0.011131
	1%KMnO ₄ ⁻ HTP	15.1145	13.6461	0.002525	0.071490
	3%KMnO ₄ ⁻ HTP	30.5653	26.0662	0.004230	0.2744
	5%KMnO ₄ ⁻ HTP	24.8480	19.5535	0.001575	0.16119
400	w/t HTP	23.7722	18.1505	0.002759	0.18773
	0%KMnO ₄ ⁻ HTP	24.9388	21.0224	0.005924	0.13548
	1%KMnO ₄ ⁻ HTP	33.3101	31.7505	0.009794	0.14507
	3%KMnO ₄ ⁻ HTP	45.0364	42.4550	0.002290	0.11473
	5%KMnO ₄ ⁻ HTP	34.7107	32.7012	0.002200	0.022678

* SLACs is sugar cane leaves.

3.8. The Results of Water Analysis

The activated carbon made by pyrolysis at 350 °C and with 3% KMnO₄ pre-hydrothermal treatment was used as a filter in an aquaponic system. This material has a high micropore volume, a low content of C-H surface functional groups, and a stable physical and chemical structure, although some of its properties are inferior to products made by pyrolysis at 400 °C. This material was chosen to reduce the energy consumption in the preparation of activated carbon.

3.8.1. pH of Water

The pH of water in pond 1, or aquaculture (control treatment, without connection with plant system and activated carbon), is weakly acidic (Figure 7a), while the pH of water in hydroponic (only plant system), is weakly basic (Figure 7b). After connecting the fishpond to the plant system (pond 2 or aquaponic pond, Figure 7c), the pH of the water in the resulting pond 2 has changed from weakly basic (in the first week) to weakly acidic (2–4 weeks) during the course of the experiment. However, the pH of water in pond 3 (aquaponic pond with activated carbon) remained weakly basic for the whole time (Figure 7d). These phenomena are the result of changing the amount of CO₂ and O₂ present in the water from the processes of respiration and photosynthesis. In the case of pond 1, the respiration of the fish produces CO₂, which can dissolve in water and change into carbonic acid. However, the process of photosynthesis of phytoplankton or microalgae reduces the amount of protons (H⁺) and CO₂ in the water and increases the oxygen content under light conditions, resulting in a gradual increase in the water pH [37]. Nonetheless, it is not sufficient to neutralize the acidity of the water in the conditions of aquaculture alone. Therefore, the water pH increases when the fish farming system is connected to the crop system (pond 2). This is attributed to the absorption of nutrients, metal ions, and other salts and photosynthetic activities (H⁺ uptake) by roots of the plants [38]. Moreover, the water pH increased further in response to the addition of activated carbon to the aquaponic system (pond 3). This is because the activated carbon, which has a negatively charged surface, can adsorb positively charged protons. The water pH of all of the ponds is in the optimal range for the growth of phytoplankton [39].

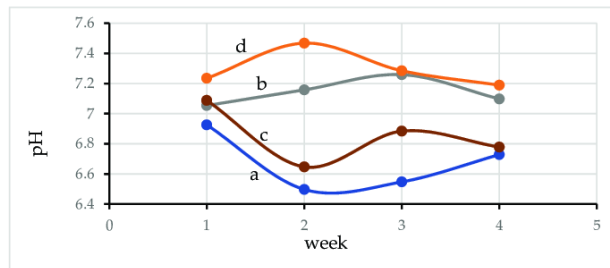


Figure 7. pH values of water of (a) pond 1; (b) the hydroponic system without an aquaculture pond; (c) pond 2; (d) and pond 3.

3.8.2. Dissolved Oxygen in Water

Dissolved oxygen (DO) in water is the basic requirement for survival for aquatic animals [40]. It can be seen that the DO of water in pond 1 (Figure 8a) is low in comparison to other ponds (pond 2–3). The DO value of water is higher in the aquaponic system (pond 2) (Figure 8c). This increase in DO content is even higher for the pond with the activated carbon filter system (pond 3) (Figure 8d). This is due to the effects of both photosynthesis and respiration. Oxygen is used in the respiration of fish, plant roots, phytoplankton, microbes, and during the nitrification of NH_4^+ [39,41]. On the other hand, the photosynthesis performed by microalgae increases the dissolved oxygen content [38]. In addition, the amount of dissolved oxygen can also be increased by gas exchange between atmosphere and water in the circulation system or by a mechanical aeration of the pond. Therefore, DO increases in the aquaponic system (pond 2, Figure 8c), which is due to water circulation and aerenchyma of plant root zones in the pond [39]. Furthermore, DO is further increased after inclusion of activated carbon (pond 3, Figure 8d), which can increase water pH and oxidation of manganese oxide present in activated carbon. It can be seen that the amount of DO in the water for all ponds increases with an increasing of the time of raising the fish. This is due to the presence of an induction phase for microorganism growth in water during which minimal increases in cell density occurs, or when the physiological adaptation of the cell metabolism to growth in the first week takes place [42]. In addition, this also resulted in the presence of more plant roots over the experimental time, which helps to add oxygen to the water. Different rates of oxygen exchange from aerial tissue into the root zone primarily contribute to the differences in DO levels among the plant cultures [38]. This is also related to having more plant roots over time, which helps to add more oxygen to the water.

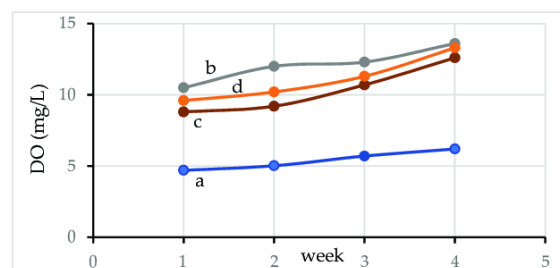


Figure 8. DO values of the water of (a) pond 1 (b) hydroponic system without an aquaculture pond (c); pond 2; and (d) pond 3.

Turbidity of water is an important indicator of the amount of suspended materials and microorganisms in water, which can have many negative effects on aquatic life [38]. Turbidity can prevent light penetration through the water and can consequently decrease the photosynthetic activity of phytoplankton [43]. It can be seen that the turbidity of water is quite high in pond 1 (Figure 9a) and is low in the hydroponic system (Figure 9b). Furthermore, it is lower in the aquaponic system (pond 2, Figure 9c) and the aquaponic system supplemented with activated carbon (pond 3, Figure 9d). In the case of pond 1, metabolic wastes from fish after feeding are not filtered and adsorbed by any material. Therefore, the turbidity value is quite high and increases over time. For aquaponic culture (pond 2), the turbidity value is highly reduced by the adsorption and filtration of suspended organic matters through plant roots during water circulation and this decreases over time. This is because plant roots grow more over time. Furthermore, the turbidity is more extensively reduced for the aquaponic cultures supplemented with activated carbon by filtration and adsorption through plant roots and activated carbon.

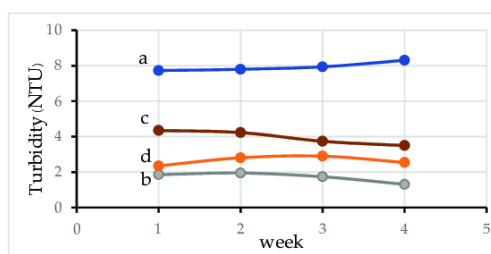


Figure 9. Turbidity values of the water in (a) pond 1; (b) the hydroponic system without aquaculture pond; (c) pond 2; (d) and pond 3.

The removal and relative removal rate of $\text{NH}_3\text{-N}$ (expressed in the form of total ammonia, $\text{NH}_3 + \text{NH}_4^+$), $\text{NO}_2^- \text{-N}$, and orthophosphate from water in ponds 1–4 at week 4 are shown in Table 3. The results show that the concentrations of all the species decreased in the aquaponic system (pond 2) and the aquaponic system, supplemented with activated carbon (pond 3), in comparison to control pond 1. In the case of $\text{NH}_3\text{-N}$, the content was lower than the recommended values in production pond management practices, which is below 2 mg/L for all ponds [44]. However, the value was quite high for pond 1 as it is formed as a waste product of protein metabolism. Furthermore, it was oxidized and transformed to nitrate, via nitrite, under aerobic conditions by nitrification through the actions of ammonia-oxidizing and nitrite-oxidizing bacteria [45]. It also accumulates in the reducing environment of the pond bottom and is released continuously into the water [46]. Its value was lowered for the aquaponic system (pond 2) with a 70.39% relative removal rate and with a 86.84% relative removal rate for aquaponic culture supplemented with activated carbon (pond 3), which is the result of having a high DO content. High dissolved oxygen concentration promotes ammonia oxidation by nitrification and decreases the toxicity of NH_3 to fish. In addition, nitrogen compounds such as NO , N_2O , and N_2 [45], which form from nitrification as well as denitrification, were absorbed by plant roots for growth. Another way of NH_3 removal, which exists for both ionized (NH_4^+) and unionized (NH_3) ammonia [40], is the removal by NH_4^+ adsorption of KMnO_4 -treated pre-hydrothermal activated carbon. As a result, more ammonia was removed in pond 3. Nitrite, which forms by oxidation of NH_3 and is subsequently transformed into NO_3^- by nitrification bacteria, is removed in the same way as ammonia. However, it is still higher than the appropriate content in aquaculture water, which should be less than 0.1 mg/L [35], except in the hydroponic system. The relative removal rates are 41.46% and 73.17% for pond 2 and pond 3, respectively. It can be seen that nitrite content of pond 3 is close to the appropriate

level, which is the result of high DO values. In the case of orthophosphate (PO_4^{3-}), it is also reduced with relative removal rates of 44.44% and 53.33% for pond 2 and pond 3, respectively. This is mainly the result of absorption by plant roots for plant growth.

Table 3. The removal and percent relative removal rate of NH_3 , NO_2^- , and orthophosphate.

Pond Number	Removal of					
	NH_3		NO_2^-		PO_4^{3-} mg/L	
	mg/L	Removal Rate %	mg/L	Removal Rate %	mg/L	Removal Rate %
1	1.52	-	0.41	-	0.45	-
Hydroponic	0.04	-	0.02	-	0.02	-
2	0.45	70.39	0.24	41.46	0.25	44.44
3	0.20	86.84	0.11	73.17	0.21	53.33

3.9. Growth of Fish and Plants

The growth of fish weight in ponds 1, 2, and 3 are presented in Figure 10. It can be seen that fish growth is higher for the aquaponic system (pond 2, Figure 10b) and the aquaponic system supplemented with activated carbon (pond 3, Figure 10c) as compared to the aquatic culture (pond 1, Figure 10a) only in the first week. The fish growth in pond 2 and pond 3 continued to be higher than that of pond 1 until the 4th week. Moreover, the growth of fish in pond 3 is higher than in pond 2 over the course of 4 weeks. These results indicate that pH, DO content, turbidity, NH_3 content level, and NO_2^- content levels in pond 2 and pond 3 are suitable for improved fish growth. The plant growth data for all crop panels collected in the 4th week are shown in Table 4. It can be seen that among all of the growth parameters, plant crop tube panel 2 (aquaponic) and plant crop tube panel 3 (aquaponic system supplemented with activated carbon) tend to be slightly higher than crops in tube panel 1 (hydroponic system). A higher plant growth also resulted in a higher removal efficiency of NH_3 , NO_2^- , and other species. This is especially the case with the growth of plant roots, which has a great effect on the adsorption of various chemicals and DO, since the plant roots have an important function in reducing nitrogen and increasing DO. The roots form habitats for microbes, which cause nitrification/denitrification and also nutrient absorption in the hydroponic plant [47]. Thus, it can be expected that the level of ammonia, nitrite, and turbidity would be substantially lower in an efficient aquaponic system and an aquaponic system supplemented with activated carbon due to the continual uptake or adsorption and in filtering by the plant roots and activated carbon.

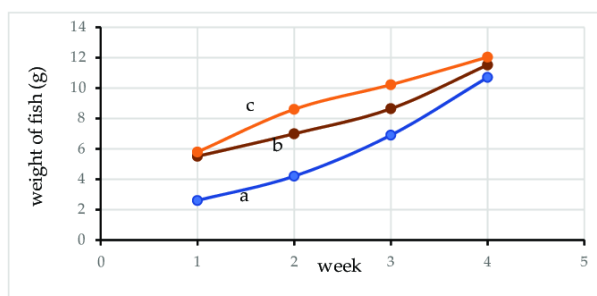


Figure 10. The fish growth observed in (a) pond 1; (b) pond 2; (c) and pond 3.

Table 4. The growth parameters of red oak in the 4th week.

Crop Tube Panel Number	Stem Height (cm)	Dried Stem Weight (g/stem)	Root Length (cm)	Dried Root Weight (g/stem)	Number of Leaves/Stem	Dried Leaf Weight (g)	Trunk Diameter (cm)
1	15.63	1.12	9.32	0.24	9.2	0.14	16.4
2	16.87	1.26	10.22	0.26	9.3	0.15	16.4
3	16.89	1.47	11.22	0.29	9.3	0.17	17.75

4. Conclusions

Hydrothermal treatment, potassium permanganate content, and pyrolysis temperature all had a significant effect on the properties of activated carbon prepared from sugar cane leaves. The percent yields of all activated carbons decrease with the increase in the activation temperature from 300 °C to 400 °C. The percent yield of hydrothermal-activated carbon was higher than non-hydrothermal-activated carbon prepared using the same conditions and increased with the potassium permanganate concentration used. Likewise, the carbon content of activated carbon increases with hydrothermal processing and increasing pyrolysis temperature, while the oxygen content exhibits the opposite trend. However, the O/C ratio of pyrolyzed activated carbons increased as the potassium permanganate content increased. The surface functional groups of activated carbon have been eliminated as a result of the effects of hydrothermal pretreatment and increasing pyrolysis temperature, while the content of aromatics has increased. On the other hand, the addition of potassium permanganate increased the presence of C-O, Mn-OH, O-Mn-O, and Mn-O bonds as surface functional groups on pyrolyzed KMnO₄-treated pre-hydrothermal products. The XRD results also confirm that the pyrolyzed KMnO₄-treated pre-hydrothermal products were amorphous and contained oxides of K and Mn. In addition, the zeta potential values of pre-hydrothermal activated carbons are negative throughout the pH range from 3 to 11 and are more negative for materials made with added potassium permanganate. Likewise, the addition of potassium permanganate and hydrothermal treatment have a significant effect on the breakdown and degradation of surface particles in pyrolyzed products. These results indicate that the surface area and porosity of the KMnO₄-treated pre-hydrothermal-activated carbon materials increased. The activated carbon made with 3% KMnO₄ pre-hydrothermal treatment and pyrolyzed at 350 °C was used as a filter material in an aquaponic system. The results from these experiments have shown that the water was weakly alkaline (pH (7.2–7.4)), had a DO value suitable for fish farming (9.6–13.3 mg/L), and that its turbidity was significantly reduced (reduced from 7.73–8.31 NTU to 2.35–2.90 NTU). It has also been found that pyrolyzed activated carbon made with KMnO₄ pre-hydrothermal treatment can significantly reduce ammonia (relative removal rate = 86.84%), nitrites (relative removal rate = 73.17%), and phosphates (relative removal rate = 53.33%), as a result of adsorption and filtration on activated carbon and plant roots and that these species are used for plant growth. The water properties found in the aquaponic system supplemented with activated carbon appear to be suitable for fish growth, as the fish showed good growth for 4 weeks. The results of this research indicate that the hydrothermal treatment at the low temperature of 120 °C at 15 bar with 1–3% KMnO₄ content and pyrolysis at 350 °C are suitable for activated carbon production from sugar cane leaves to be used in aquaponic systems of catfish and red oak. The combined process can decompose surface functional groups of sugarcane leaves more easily during pyrolysis. In addition, the process also results in the formation of aromatics in the pyrolysis products, with a high yield at only 350 °C. Furthermore, KMnO₄ causes partial oxidation, which induces a greater amorphousness and negative zeta-potential in the activated carbon throughout the pH range from 3 to 11. This in turn increases the affinity between the activated carbon and positively charged adsorbates. These results imply a reduced energy consumption for activated carbon production and improved adsorption properties of the activated carbon.

Author Contributions: S.M. wrote the manuscript and prepared all the tables and figures. K.T. performed the experiments and analyzed the data. All authors have read and agreed to the published version of the manuscript.

Funding: This research was funded by the Science Achievement Scholarship of Thailand (Number: NU 004/2558) and the APC was funded by Naresuan University.

Institutional Review Board Statement: The animal study protocol was approved by the Institutional Review Board of the Committee on Animal Execution for Science, Naresuan University (protocol code 61 01 007 and date of approval; 20 November 2018).

Informed Consent Statement: Not applicable.

Data Availability Statement: Data sharing not applicable.

Acknowledgments: The authors acknowledge Chemistry Department and Science Lab Center, Faculty of Science, Naresuan University, for all of the analyses.

Conflicts of Interest: The authors declare no conflict of interest.

References

- Benstoem, F.; Becker, G.; Firk, J.; Kaless, M.; Wuest, D.; Pinnekamp, J.; Kruse, A. Elimination of micropollutants by activated carbon produced from fibers taken from wastewater screenings using hydrothermal carbonization. *J. Environ. Manag.* **2018**, *211*, 278–286. [[CrossRef](#)] [[PubMed](#)]
- Mbarki, F.; Selmi, T.; Kesraoui, A.; Seffen, M.; Gadonneix, P.; Celzard, A.; Fierro, V. Hydrothermal pre-treatment, an efficient tool to improve activated carbon performances. *Ind. Crops Prod.* **2019**, *140*, 111717. [[CrossRef](#)]
- Sun, G.; Qiu, L.; Zhu, M.; Kang, K.; Guo, X. Activated carbons prepared by hydrothermal pretreatment and chemical activation of *Eucommia ulmoides* wood for supercapacitors application. *Ind. Crops Prod.* **2018**, *125*, 41–49. [[CrossRef](#)]
- Khan, T.A.; Saud, A.S.; Jamari, S.S.; Rahim, M.H.A.; Park, J.-W.; Kim, H.-J. Hydrothermal carbonization of lignocellulosic biomass for carbon rich material preparation: A review. *Biomass Bioenergy* **2019**, *130*, 105384. [[CrossRef](#)]
- Wilk, M.; Magdziarz, A.; Kalembe-Rec, I.; Szymańska-Chargot, M. Upgrading of green waste into carbon-rich solid biofuel by hydrothermal carbonization: The effect of process parameters on hydrochar derived from acacia. *Energy* **2020**, *202*, 117717. [[CrossRef](#)]
- Wang, B.; Zhai, Y.; Wang, T.; Li, S.; Peng, C.; Wang, Z.; Li, C.; Xu, B. Fabrication of bean dreg-derived carbon with high adsorption for methylene blue: Effect of hydrothermal pretreatment and pyrolysis process. *Bioresour. Technol.* **2019**, *274*, 525–532. [[CrossRef](#)] [[PubMed](#)]
- Pari, G.; Darmawan, S.; Prihandoko, B. Porous carbon spheres from hydrothermal carbonization and KOH activation on cassava and tapioca flour raw material. *Procedia Environ. Sci.* **2014**, *20*, 342–351. [[CrossRef](#)]
- Selmi, T.; Sanchez, A.; Gadonneix, P.; Jagiello, J.; Seffen, M.; Sammouda, H.; Celzard, A.; Fierro, V. Tetracycline removal with activated carbons produced by hydrothermal carbonisation of *Agave americana* fibres and mimosa tannin. *Ind. Crops Prod.* **2018**, *115*, 146–157. [[CrossRef](#)]
- Su, Y.; Liu, L.; Xu, D.; Du, H.; Xie, Y.; Xiong, Y.; Zhang, S. Syngas production at low temperature via the combination of hydrothermal pretreatment and activated carbon catalyst along with value-added utilization of tar and bio-char. *Energy Convers. Manag.* **2020**, *205*, 112382. [[CrossRef](#)]
- Aguilar, A.; Milessi, T.S.; Mulinari, D.R.; Lopes, M.S.; Costa, S.M.; Candido, R.G. Sugarcane straw as a potential second generation feedstock for biorefinery and white biotechnology applications. *Biomass Bioenergy* **2021**, *144*, 105896. [[CrossRef](#)]
- Arumugam, A.; Sankaranarayanan, P. Biodiesel production and parameter optimization: An approach to utilize residual ash from sugarcane leaf, a novel heterogeneous catalyst, from *Calophyllum inophyllum* oil. *Renew Energy* **2020**, *153*, 1272–1282. [[CrossRef](#)]
- Yadav, S.K.J.; Vedrtam, A.; Gunwant, D. Experimental and numerical study on mechanical behavior and resistance to natural weathering of sugarcane leaf reinforced polymer composite. *Constr. Build. Mater.* **2020**, *262*, 120785. [[CrossRef](#)]
- Kyaw, T.Y.; Ng, A.K. Smart aquaponics system for urban farming. *Energy Procedia* **2017**, *143*, 342–347. [[CrossRef](#)]
- Khiari, Z.; Alka, K.; Kelloway, S.; Mason, B.; Savidov, N. Integration of Biochar Filtration into Aquaponics: Effects on Particle Size Distribution and Turbidity Removal. *Agric. Water Manag.* **2020**, *229*, 105874. [[CrossRef](#)]
- Pous, N.; Korth, B.; Alvarez, M.O.; Balaguer, M.D.; Harnisch, E.; Puig, S. Electrifying biotrickling filters for the treatment of aquaponics wastewater. *Bioresour. Technol.* **2021**, *319*, 124221. [[CrossRef](#)]
- Bhakar, V.; Kaur, K.; Singh, H. Analyzing the Environmental Burden of an Aquaponics System using LCA. *Procedia CIRP* **2021**, *98*, 223–228. [[CrossRef](#)]
- Pérez-Urrestarazu, L.; Lobillo-Eguibar, J.; Fernández-Cañero, R.; Fernández-Cabanás, V.M. Suitability and optimization of FAO's small-scale aquaponics systems for joint production of lettuce (*Lactuca sativa*) and fish (*Carassius auratus*). *Aquac. Eng.* **2019**, *85*, 129–137. [[CrossRef](#)]
- Tůmová, V.; Klímová, A.; Kalous, L. Status quo of commercial aquaculture in Czechia: A misleading public image? *Aquac. Rep.* **2020**, *18*, 100508. [[CrossRef](#)]

19. Mori, J.; Smith, R. Transmission of waterborne fish and plant pathogens in aquaponics and their control with physical disinfection and filtration: A systematized review. *Aquaculture* **2019**, *504*, 380–395. [[CrossRef](#)]
20. Suhl, J.; Dannehl, D.; Baganz, D.; Schmidt, U.; Kloas, W. An innovative suction filter device reduces nitrogen loss in double recirculating aquaponic systems. *Aquac. Eng.* **2018**, *82*, 63–72. [[CrossRef](#)]
21. Tejido-Núñez, Y.; Aymerich, E.; Sancho, L.; Refard, D. Co-cultivation of microalgae in aquaculture water: Interactions, growth and nutrient removal efficiency at laboratory- and pilot-scale. *Ecol. Eng.* **2019**, *136*, 1–9. [[CrossRef](#)]
22. Yena, H.Y.; Chou, J.H. Water purification by oyster shell bio-medium in a recirculating aquaponic system. *Ecol. Eng.* **2016**, *95*, 229–236. [[CrossRef](#)]
23. Li, G.; Tao, L.; Li, X.; Peng, L.; Song, C.; Dai, L.; Wu, Y.; Xie, L. Design and performance of a novel rice hydroponic biofilter in a pond-scale aquaponic recirculating system. *Ecol. Eng.* **2018**, *125*, 1–10. [[CrossRef](#)]
24. Effendi, H.; Widyatmoko; Utomo, B.A.; Pratiwi, N.T.M. Ammonia and orthophosphate removal of tilapia cultivation wastewater with *Vetiveria zizanioides*. *J. King Saud Univ. Sci.* **2020**, *32*, 207–212. [[CrossRef](#)]
25. Mahat, N.A.; Aisyah Shamsudin, S.A. Transformation of oil palm biomass to optical carbon quantum dots by carbonisation-activation and low temperature hydrothermal processes. *Diam. Relat. Mater.* **2020**, *102*, 107660. [[CrossRef](#)]
26. Carpenter, J.H. The Chesapeake bay institute technique for the Winkler dissolved oxygen method. *Limnol. Oceanogr.* **1965**, *10*, 141–143. [[CrossRef](#)]
27. Iradukunda, Y.; Wang, G.; Li, X.; Shi, G.; Hu, Y.; Luo, F.; Yi, K.; Ismail, A.; Albashir, M.; Niu, X.; et al. High performance of activated carbons prepared from mangosteen (*Garcinia mangostana*) peels using the hydrothermal process. *J. Energy Storage* **2021**, *39*, 102577. [[CrossRef](#)]
28. Dessie, Y.; Tadesse, S.; Eswaramoorthy, R. Physicochemical parameter influences and their optimization on the biosynthesis of MnO₂ nanoparticles using Vernonia amygdalina leaf extract. *Arab. J. Chem.* **2020**, *13*, 6472–6492. [[CrossRef](#)]
29. Pan, Z.; Li, Y.; Wang, B.; Sun, F.; Xu, F.; Zhang, X. Mild fractionation of poplar into reactive lignin via lignin-first strategy and its enhancement on cellulose saccharification. *Bioresour. Technol.* **2022**, *343*, 126122. [[CrossRef](#)]
30. Goydaragh, M.G.; Taghizadeh-Mehrjardi, R.; Golchin, A.; Jafarzadeh, A.A.; Lado, M. Predicting weathering indices in soils using FTIR spectra and random forest models. *Catena* **2021**, *204*, 105437. [[CrossRef](#)]
31. Ying, D.; Hong, P.; Jiali, F.; Qinjin, T.; Yuhui, L.; Youqun, W.; Zhibin, Z.; Xiaohong, C.; Yunhai, L. Removal of uranium using MnO₂/orange peel biochar composite prepared by activation and in-situ deposit in a single step. *Biomass Bioenergy* **2020**, *142*, 105772. [[CrossRef](#)]
32. Li, C.; Sun, Y.; Yi, Z.; Zhang, L.; Zhang, S.; Hu, X. Co-pyrolysis of coke bottle wastes with cellulose, lignin and sawdust: Impacts of the mixed feedstock on char properties. *Renew Energy* **2022**, *181*, 1126–1139. [[CrossRef](#)]
33. Istadi, I.; Prasetyo, S.A.; Nugroho, T.S. Characterization of K₂O/CaO-ZnO catalyst for transesterification of soybean oil to biodiesel. *Procedia Environ. Sci.* **2015**, *23*, 394–399. [[CrossRef](#)]
34. Mařálek, R.; Švidmoch, M. The adsorption of amitriptyline and nortriptyline on activated carbon, diosmectite and titanium dioxide. *Environ. Chall.* **2020**, *1*, 100005. [[CrossRef](#)]
35. Li, L.; Li, Y.; Tan, C.; Zhang, T.; Xin, X.; Li, W.; Li, J.; Lu, R. Study of the interaction mechanism between GO/rGO and trypsin. *J. Hazard. Mater. Adv.* **2021**, *3*, 100011. [[CrossRef](#)]
36. Zhuang, Y.; Liu, J.; Chen, J.; Fei, P. Modified pineapple bran cellulose by potassium permanganate as a copper ion adsorbent and its adsorption kinetic and adsorption thermodynamic. *Food Bioprod. Process.* **2020**, *122*, 82–88. [[CrossRef](#)]
37. Zerveas, S.; Mente, M.S.; Tsakiri, D.; Kotzabasis, K. Microalgal photosynthesis induces alkalization of aquatic environment as a result of H⁺ uptake independently from CO₂ concentration—New perspectives for environmental applications. *J. Environ. Manag.* **2021**, *289*, 112546. [[CrossRef](#)] [[PubMed](#)]
38. Nahar, K.; Hoque, S. Phytoremediation to improve eutrophic ecosystem by the floating aquatic macrophyte, water lettuce (*Pistia stratiotes* L.) at lab scale. *Egypt. J. Aquat. Res.* **2021**, *47*, 231–237. [[CrossRef](#)]
39. Li, F.; Sun, Z.; Qi, H.; Zhou, X.; Xu, C.; Wu, D.; Fang, F.; Feng, J.; Zhang, N. Effects of rice-fish co-culture on oxygen consumption in intensive aquaculture pond. *Rice Sci.* **2019**, *26*, 50–59. [[CrossRef](#)]
40. Hossain, M.A.; Hossain, M.A.; Haque, M.A.; Mondol, M.M.R.; Harun-Ur-Rashid, M.; Das, S.K. Determination of suitable stocking density for good aquaculture practice-based carp fattening in ponds under drought-prone areas of Bangladesh. *Aquaculture* **2022**, *547*, 737485. [[CrossRef](#)]
41. Schuijt, L.M.; van Bergen, T.J.H.M.; Lamers, L.P.M.; Smolders, A.J.P.; Verdonchot, P.F.M. Aquatic worms (*Tubificidae*) facilitate productivity of macrophyte *Azolla filiculoides* in a wastewater biocascade system. *Sci. Total Environ.* **2021**, *787*, 147538. [[CrossRef](#)]
42. Belaïdi, F.S.; Salvagnac, L.; Souleille, S.A.; Blatché, M.C.; Bedel-Pereira, E.; Séguy, I.; Launay, J. Accurate physiological monitoring using lab-on-a-chip platform for aquatic micro-organisms growth and optimized culture. *Sens. Actuators B Chem.* **2020**, *321*, 128492. [[CrossRef](#)]
43. Cunha, M.E.; Quental-Ferreira, H.; Parejo, A.; Gamito, S.; Ribeiro, L.; Moreira, M.; Monteiro, I.; Soares, F.; Pousão-Ferreira, P. Understanding the individual role of fish, oyster, phytoplankton and macroalgae in the ecology of integrated production in earthen ponds. *Aquaculture* **2019**, *512*, 734297. [[CrossRef](#)]
44. Rawles, S.D.; Green, B.W.; McEntire, M.E.; Gibson Gaylord, T.G.; Barrows, F.T. Reducing dietary protein in pond production of hybrid striped bass (*Morone chrysops* × *M. saxatilis*): Effects on fish performance and water quality dynamics. *Aquaculture* **2018**, *490*, 217–227. [[CrossRef](#)]

45. Liu, H.; Li, H.; Wei, H.; Zhu, X.; Han, D.; Jin, J.; Yang, Y.; Xie, S. Biofloc formation improves water quality and fish yield in a freshwater pond aquaculture system. *Aquaculture* **2019**, *506*, 256–269. [[CrossRef](#)]
46. Hoess, R.; Geist, J. Nutrient and fine sediment loading from fish pond drainage to pearl mussel streams—Management implications for highly valuable stream ecosystems. *J. Environ. Manag. Part A* **2022**, *302*, 113987. [[CrossRef](#)]
47. Paudel, S.R. Nitrogen transformation in engineered aquaponics with water celery (*Oenanthe javanica*) and koi carp (*Cyprinus carpio*): Effects of plant to fish biomass ratio. *Aquaculture* **2020**, *520*, 734971. [[CrossRef](#)]